MR3252: Tropical Meteorology

Tropical Cyclone Forecasting

Main Topics:

- Models used
- NHC Model Verification
- Some resources for forecasting

Module 3.1

Dynamic models (https://www.nhc.noaa.gov/modelsummary.shtml)

ATCF ID	Global/Regional Model Name	Horizontal Resolution	Vertical Levels and Coordinates	Data Assimilation	Convective Scheme	Cycle/Run Frequency	NHC Forecast Paramter(s)
NVGM/NVGI	Navy Global Environmental Model	Spectral (~31km)	60 Hybrid Sigma-pressure	NAVDAS-AR 4D-VAR	Simplified Arakawa Schubert	6 hr (144 hr) 00/06/12/18 UTC	Track and intensity
AVNO/AVNI GFSO/GFSI	Global Forecast System (FV3-GFS)	Finite Volume Cube Sphere (~13km)	64 Hybrid Sigma-pressure	GSI/4D-VAR EnKF hybrid	Simplified Arakawa Schubert	6 hr (240 hr) 00/06/12/18 UTC	Track and intensity
*EMX/EMXI/EMX2	European Centre for Medium-Range Weather Forecasts	Spectral (~9km)	137 Hybrid Sigma-pressure	4D-VAR	Tiedke mass flux	12 hr (240 hr) 00/12 UTC	Track and intensity
EGRR/EGRI/EGR2	U.K. Met Office Global Model	Grid point (~10 km)	70 Hybrid Sigma-pressure	4D-VAR Ensemble Hybrid	UKMET	12 hr (144 hr) 00/12 UTC	Track and intensity
CMC/CMCI	Canadian Deterministic Prediction System	Grid point (~25 km)	80 Hybrid Sigma-pressure	4D-VAR Ensemble Hybrid	Kain-Fritsch	12 hr (240 hr) 00/12 UTC	Track and intensity
HWRF/HWFI	Hurricane Weather Research and Forecast system	Nested Grid point (13.5-4.5-1.5km)	75 Hybrid Sigma-pressure	4D-VAR Hybrid GDAS GFS IC/BC	Simplified Arakawa Schubert + GFS shallow convection (6 and 18km) 1.5km nest - none	6 hr (126 hr) 00/06/12/18 UTC *Runs on request from NHC/JTWC*	Track and intensity
CTCX/CTCI	NRL COAMPS-TC w/ GFS initial and boundary conditions	Nested Grid point (45-15-5 km)	42 Hybrid Sigma-pressure	3D-VAR (NAVDAS) EnKF DART	Kain-Fritsch	6 hr (126 hr) 00/06/12/18 UTC *Runs commence on 1st NHC/JTWC advisory*	Track and intensity
HMON/HMNI	Hurricane Multi-scale Ocean-coupled Non-hydrostatic model	Nested Grid point (18-6-2km)	51 Hybrid Sigma-pressure	GFS IC/BC	Simplified Arakawa Schubert + GFS shallow convection (6 and 18km) 2km nest - none	6 hr (126 hr) 00/06/12/18 UTC *Runs on request from NHC/JTWC*	Track and intensity

Consensus models/ensembles (https://www.nhc.noaa.gov/modelsummary.shtml)

ATCF ID	Model Name or Type	Horizontal Resolution	Vertical Levels and Coordinates	Data Assimilation	Pertubation or Consensus Methods	Cycle/Run Frequency	Ensemble Members	NHC Forecast Paramter(s)
AEMN/AEMI	Global Ensemble Forecast System	~33 km for 1st 192 hr ~55 km for 192-384 hr	64 Hybrid Sigma-pressure	GSI/3D-VAR EnKF hybrid	20 of 80 6 hr DA system hybrid EnKF members per cycle	6 hr (384 hr) 00/06/12/18 UTC	20	Track
*UEMN/UEMI	U.K. Met Office MOGREPS	~20 km	70 Hybrid Sigma-pressure	4D-VAR EnKF hybrid	44 member EnKF	12 hr (168 hr) 00/12 UTC	11	Track
*EEMN/EMN2	ECMWF EPS	~18 km	91 Hybrid Sigma-pressure	4D-VAR	Leading singluar vectors based initial pertubations	12 hr (360 hr) 00/12 UTC	50	Track
*FSSE	Florida State Super Ensemble				Corrected consensus	6 hr (120 hr) 00/06/12/18 UTC		Track and Intensity
*HCCA	HFIP Corrected Consensus Approach				Corrected consensus	6 hr (120 hr) 00/06/12/18 UTC	AEMI AVNI CTCI DSHP EGRI EMN2 EMXI HWFI LGEM	Track and Intensity
*GFEX	2 model consensus				Simple consensus	6 hr (120 hr) 00/06/12/18 UTC	AVNI EMXI	Track
TVCN (Atlantic) (TVCA)	Variable consensus				Simple consensus, minimum 2 members	6 hr (120 hr) 00/06/12/18 UTC	AVNI, EGRI, HWFI EMHI, CTCI, EMNI	Track
TVCN (E. Pacific) (TVCE)	Variable consensus				Simple consensus, minimum 2 members	6 hr (120 hr) 00/06/12/18 UTC	AVNI, EGRI, HWFI, EMHI CTCI, EMNI, HMNI	Track
TVCX	Variable consensus				Simple consensus, minimum 2 members, double-weighted EMXI	6 hr (120 hr) 00/06/12/18 UTC	AVNI EMXI HWFI CTCI EGRI	Track
RVCN	Wind Radii Consensus				Multi-model wind radii, bias corrected initial wind	6 hr (120 hr) 00/06/12/18 UTC	AHNI, HHFI, EHHI, CHCI (FV3GFS, HWRF, ECMWF, COAMPS-TC)	34-kt wind radii
ICON	Intensity consensus				Simple consensus, all 4 must be present	6 hr (120 hr) 00/06/12/18 UTC	DSHP, LGEM, HWFI, HMNI	Intensity
IVCN	Intensity variable consensus				Simple consensus, minimum 2 members	6 hr (120 hr) 00/06/12/18 UTC	DSHP, LGEM, HWFI, HMNI, CTCI	Intensity

Statistical models (https://www.nhc.noaa.gov/modelsummary.shtml)

ATCF ID	Model Name or Type	Comments	Prediction Methodology	Cycle/Run Frequency	NHC Forecast Paramter(s)
CLP5 (OCD5)	CLIPER5 Climatology and Persistence	Used to measure skill in a set of track forecasts	Multiple regression technique. Inputs are current and past TC motion (previous 12-24hr), forward motion, date, latitude/longitude, and initial intensity	6 hr (120 hr) 00/06/12/18 UTC	Track
SHF5/DSF5 (OCD5)	Decay-SHIFOR5 Statistical Hurricane Intensity Forecast	Used to measure skill in a set of intensity forecasts, includes land decay rate component	Multiple regression technique using climatology and persistence predictors	6 hr (120 hr) 00/06/12/18 UTC	Intensity
TCLP	Trajectory-CLIPER	Used to measure skill in a set of track or intensity forecasts	Substitute for CLIPER and SHIFOR; similar predictors but uses trajectories based on reanalysis fields instead of linear regression	6 hr (168 hr) 00/06/12/18 UTC	Track and intensity
DRCL	Wind Radii CLIPER	Statistical parametric vortex model	Employs climatology with the paramaters determined from 13 coefficients and persistence to produce 34-kt, 50-kt, 64-kt wind radii estimates	6 hr (168 hr) 00/06/12/18 UTC	Wind radii
SHIP	Statistical Hurricane Intensity Prediction Scheme	Statistical-dynamical model based on standard multiple regression techniques	Climatology, persistence, environmental atmosphere parameters, and an ocean component	6 hr (168 hr) 00/06/12/18 UTC	Intensity
DSHP	Decay-Statistical Hurricane Intensity Prediction Scheme	Statistical-dynamical model based on standard multiple regression techniques	Climatology, persistence, environmental atmosphere parameters, oceanic input, and an inland decay component	6 hr (168 hr) 00/06/12/18 UTC	Intensity
LGEM	Logistic Growth Equation Model	Statistical intensity model based on a simplified dynamical prediction framework	A subset of SHIPS predictors, ocean heat content, and variability of the environment used to determine growth rate maximum wind coefficient	6 hr (168 hr) 00/06/12/18 UTC	Intensity

Model ID	Forecast Period (h)						
	12	24	36	48	72	96	120
OFCL	23.1	36.3	52.7	70.9	97.6	108.0	119.1
OCD5	39.1	80.4	138.2	197.0	314.4	414.8	514.9
GFSI	25.5	44.5	70.1	101.7	143.6	129.8	166.0
HMNI	27.0	47.5	72.0	104.1	145.1	147.2	177.9
HWFI	26.9	47.7	70.0	101.6	146.8	159.5	208.2
EMXI	23.4	**34.4**	**47.1**	**63.8**	100.9	121.7	142.5
EGRI	24.0	40.9	58.0	73.6	102.7	130.4	156.1
NVGI	29.7	46.0	63.8	82.0	132.7	156.4	195.1
CTCI	24.2	41.8	62.2	81.1	112.7	132.6	190.4
AEMI	26.1	42.6	62.0	82.0	115.1	136.1	180.1
FSSE	**21.5**	**33.8**	**48.2**	**63.3**	**83.3**	**105.6**	136.5
TVCA	**21.8**	**35.2**	**51.2**	**68.6**	98.5	**104.0**	123.1
HCCA	**22.6**	36.5	52.7	72.7	103.6	**102.8**	120.4
TABD	31.4	65.4	111.5	165.8	276.2	372.6	535.5
TABM	28.1	46.8	70.3	91.6	151.2	196.7	246.1
TABS	40.9	82.9	126.1	165.4	248.7	264.0	337.0
# Cases	134	121	108	100	79	58	43

ATL track errors (2019)

https://www.nhc.noaa.gov/verification/pdfs/Verification_2019.pdf

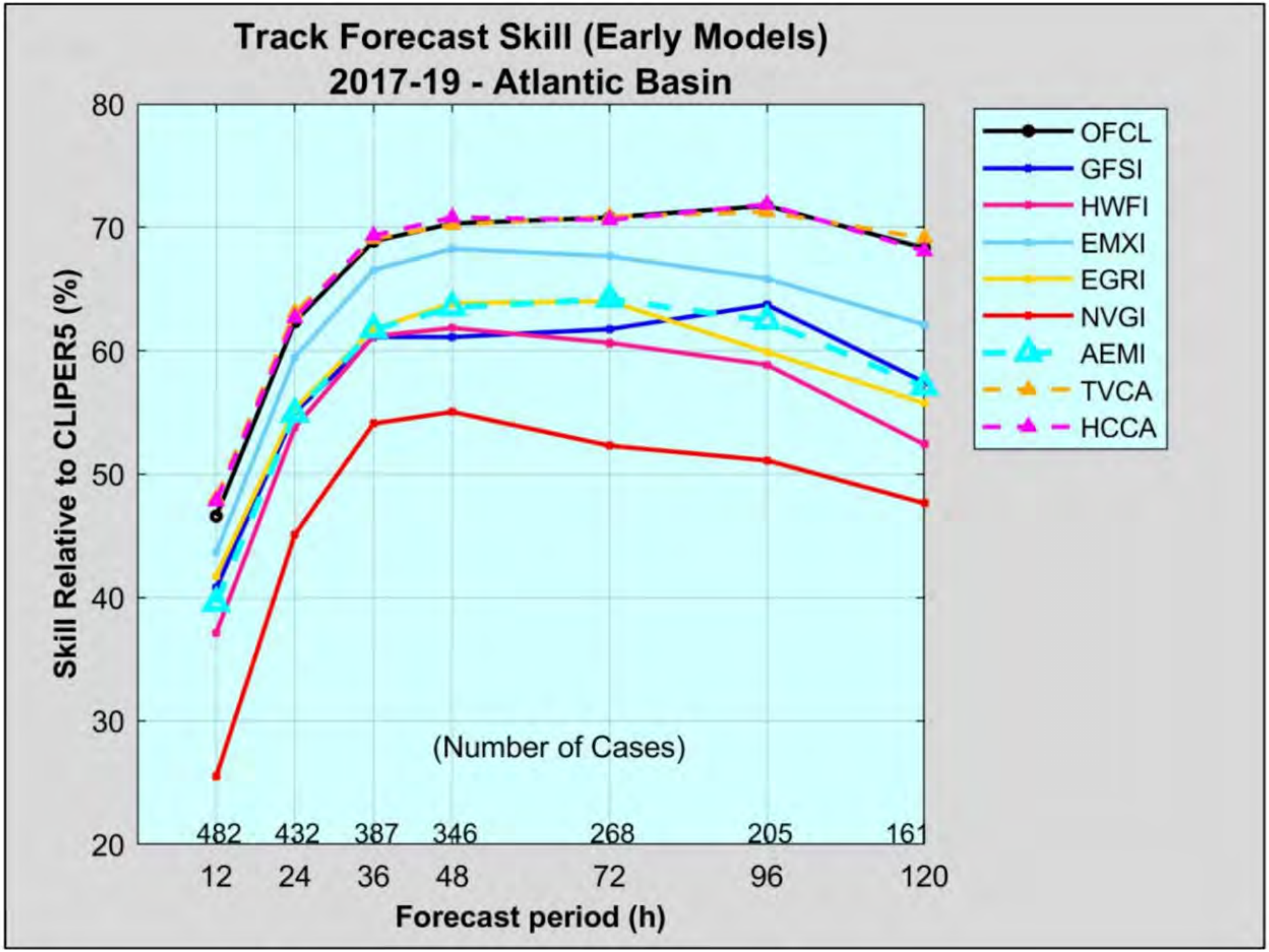

ATL intensity errors (2019)

Model ID	Forecast Period (h)						
	12	24	36	48	72	96	120
OFCL	5.6	8.7	10.0	10.2	13.8	15.7	20.1
OCD5	7.4	11.9	15.7	17.8	22.9	31.3	37.4
HWFI	7.4	10.4	13.1	14.2	15.9	20.7	25.1
HMNI	7.2	10.2	12.3	13.7	20.3	25.8	29.1
CTCI	7.3	10.7	13.1	12.9	15.3	15.9	**17.4**
DSHP	7.1	10.8	13.2	14.5	17.6	19.2	28.6
LGEM	7.2	10.7	12.9	14.5	16.9	16.0	25.5
IVCN	6.5	9.1	10.8	11.3	**13.4**	**14.6**	21.1
FSSE	6.4	9.2	10.5	10.8	**12.8**	**14.5**	**18.3**
HCCA	6.2	9.1	10.4	10.5	**13.3**	16.2	**20.0**
GFSI	7.2	10.5	14.6	17.0	23.3	23.8	30.7
EMXI	8.1	10.9	14.0	16.2	20.9	23.7	29.2
# Cases	143	130	115	107	83	62	47

https://www.nhc.noaa.gov/verification/pdfs/Verification_2019.pdf

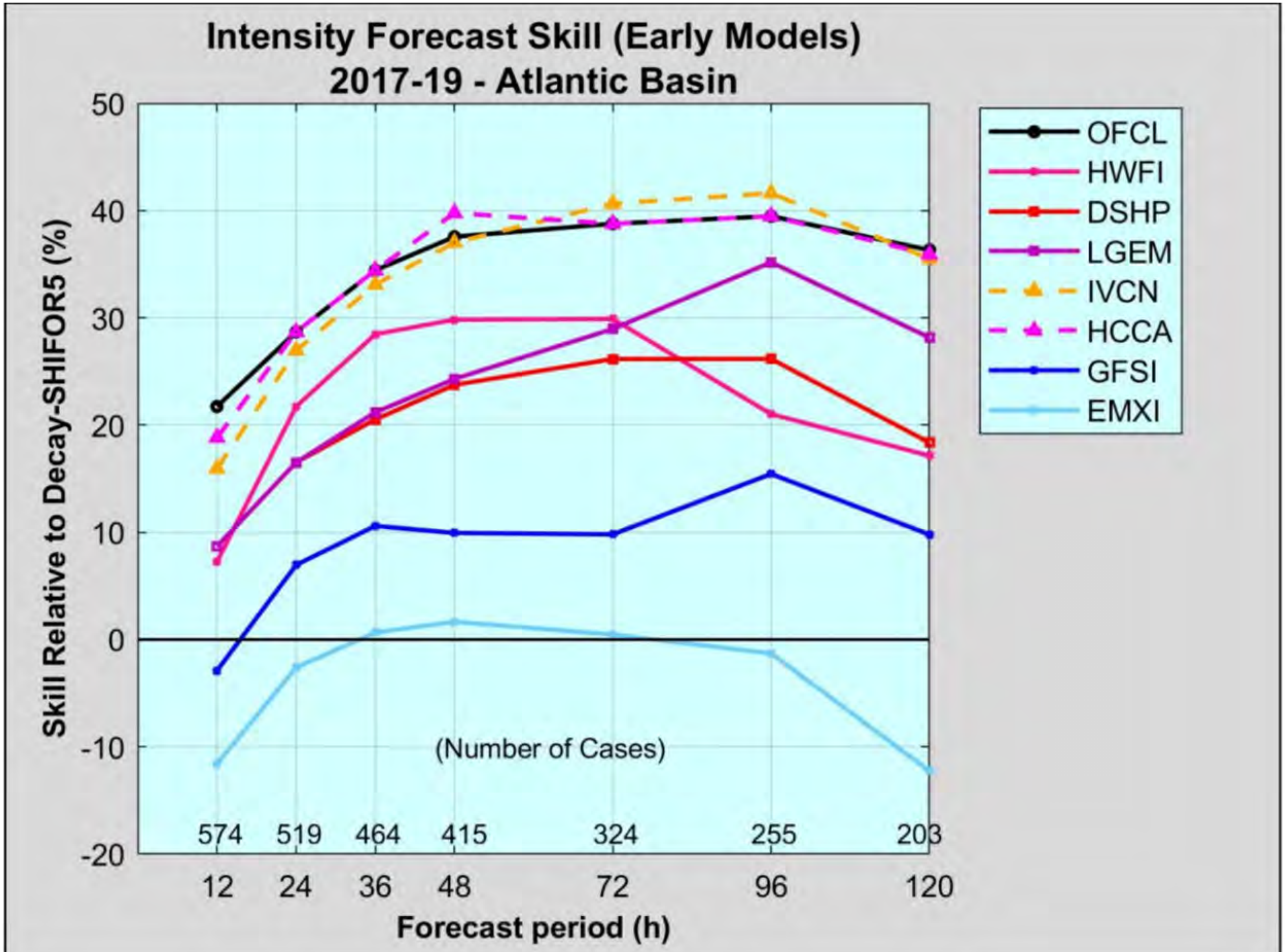

Model ID	Forecast Period (h)						
	12	24	36	48	72	96	120
OFCL	22.2	35.3	49.2	63.1	86.9	104.1	114.7
OCD5	37.8	75.0	113.5	150.3	191.6	218.9	260.8
GFSI	25.9	40.1	57.2	78.1	124.9	161.9	188.3
HWFI	26.0	43.6	61.7	78.0	115.5	143.8	167.0
HMNI	25.8	41.3	59.5	78.6	121.0	157.6	183.5
EMXI	23.7	38.8	52.4	65.6	92.3	120.8	130.1
EGRI	24.7	40.6	55.3	69.4	92.7	121.7	177.5
NVGI	35.1	60.2	84.0	105.8	154.2	188.2	235.0
AEMI	24.7	39.7	55.9	70.9	101.9	124.6	148.6
FSSE	**21.6**	**33.0**	**46.8**	**60.6**	88.1	115.0	139.4
TVCE	**21.3**	**33.5**	**47.3**	**60.4**	**86.6**	107.0	121.8
HCCA	**20.8**	**31.5**	**43.7**	**55.8**	**80.0**	**102.7**	125.3
TABD	33.9	66.0	99.3	127.1	193.1	267.2	380.1
TABM	27.9	46.6	70.7	89.8	135.4	178.4	217.0
TABS	34.2	65.4	97.9	123.1	161.4	206.0	231.0
# Cases	148	131	116	100	78	59	44

EPAC track errors (2019)

https://www.nhc.noaa.gov/verification/pdfs/Verification_2019.pdf

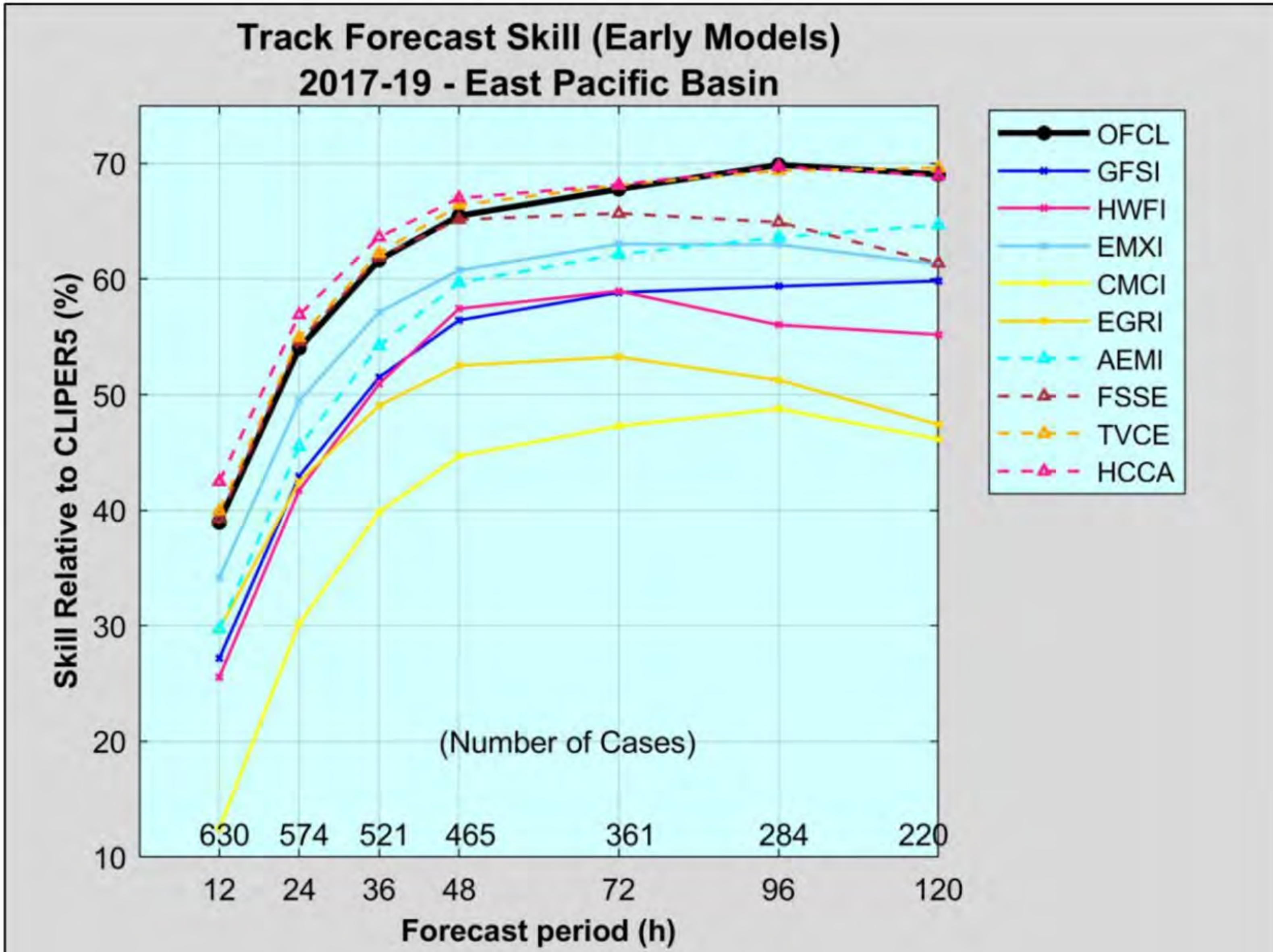

EPAC intensity errors (2019)

Model ID	Forecast Period (h)						
	12	24	36	48	72	96	120
OFCL	5.5	9.8	12.0	14.1	16.5	18.3	16.6
OCD5	7.1	12.5	16.3	18.7	17.8	**14.8**	**12.0**
HWFI	7.0	10.1	12.1	14.6	19.5	23.3	23.1
HMNI	7.3	11.1	14.1	17.1	21.0	22.0	19.6
DSHP	6.4	10.4	12.8	14.4	**14.6**	**11.1**	**9.1**
LGEM	6.8	11.2	14.0	15.7	**15.1**	**13.0**	**10.1**
IVCN	6.0	**9.2**	**11.3**	**13.2**	**14.7**	**15.2**	**15.0**
HCCA	6.0	**9.2**	**11.2**	**12.9**	**15.5**	**17.4**	**16.4**
FSSE	6.0	**9.4**	**11.7**	**13.8**	**15.8**	**16.2**	**16.0**
GFSI	7.5	11.8	14.7	16.2	16.8	**14.2**	**11.9**
EMXI	8.7	14.3	17.4	18.8	16.9	**12.9**	**11.3**
# Cases	171	151	133	112	86	66	48

https://www.nhc.noaa.gov/verification/pdfs/Verification_2019.pdf

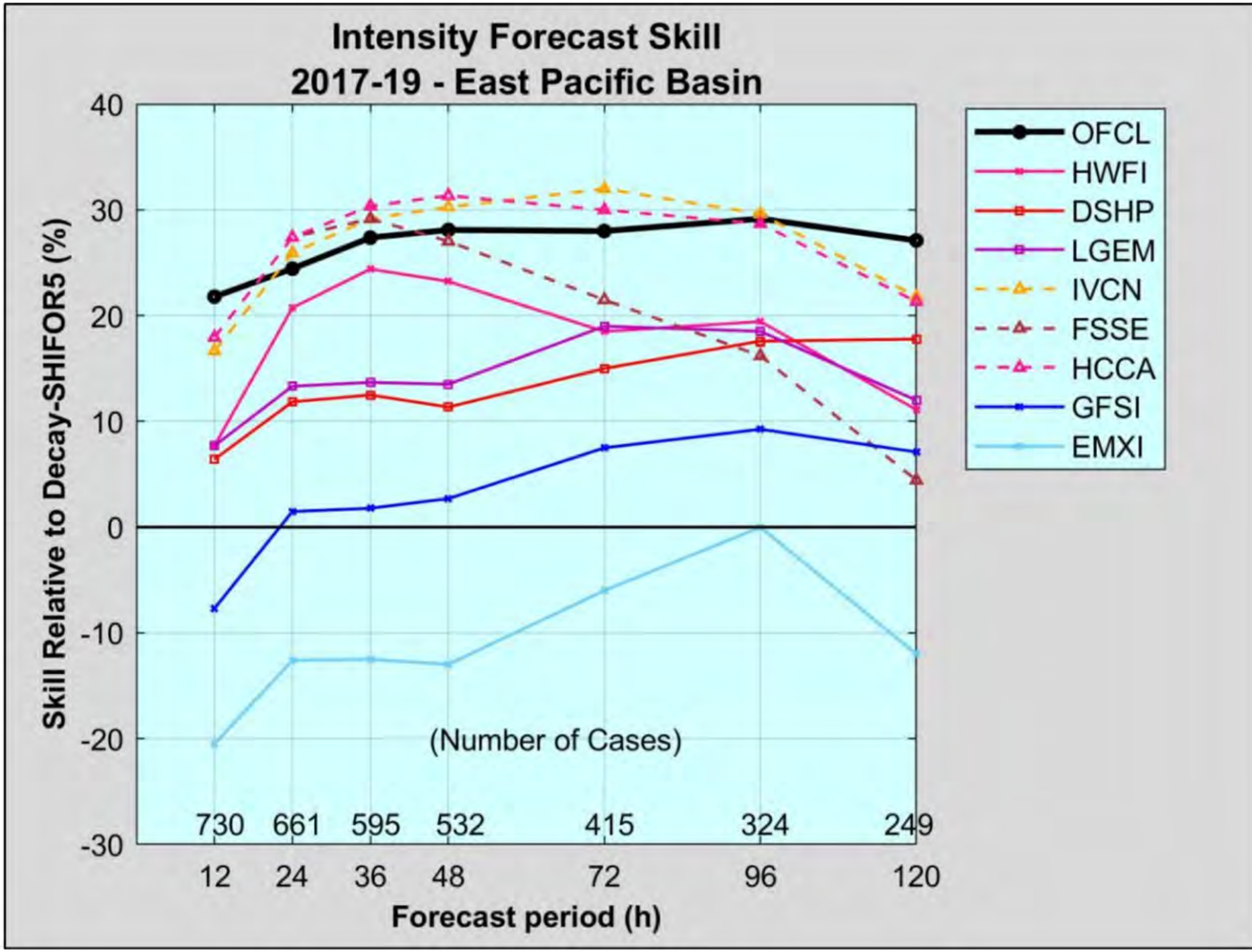

Some useful information online

NRL TC Page:	https://www.nrlmry.navy.mil/tc_pages/tc_home.html
Univ. of Wisconsin CIMSS (contains satellite-derived wind and objective intensity estimates):	http://tropic.ssec.wisc.edu/
NOAA Tracker (often out of date):	https://ruc.noaa.gov/tracks/
NHC ATCF server (includes SHIPS output and model forecast information):	https://ftp.nhc.noaa.gov/atcf/
Tropical Tidbits (a useful student-run web model-visualization suite):	https://www.tropicaltidbits.com/analysis/models/
NHC Aircraft Reconnaissance Archive:	https://www.nhc.noaa.gov/archive/recon/2020/
Scatterometer Data:	https://manati.star.nesdis.noaa.gov/products.php
GEO Satellite Imagery:	https://rammb-slider.cira.colostate.edu/

MR3252: Tropical Meteorology

Tropical Cyclone Structure

<u>Main Topics</u>:

- Eye, eyewall, and rainbands
- Distribution of TCs
- Mean flow in TCs

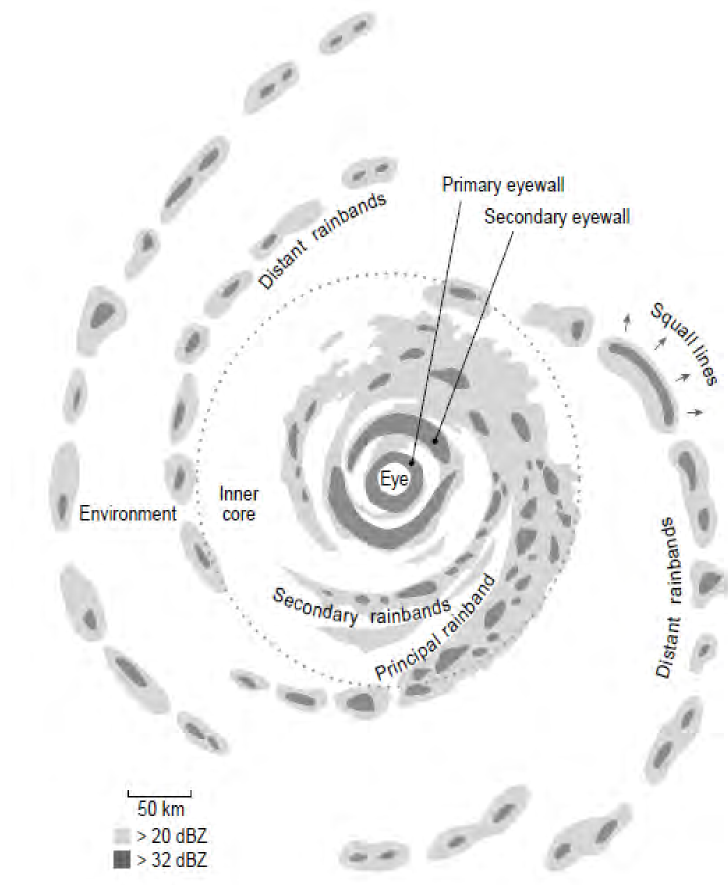

Module 3.2

Tracks of Tropical Cyclones

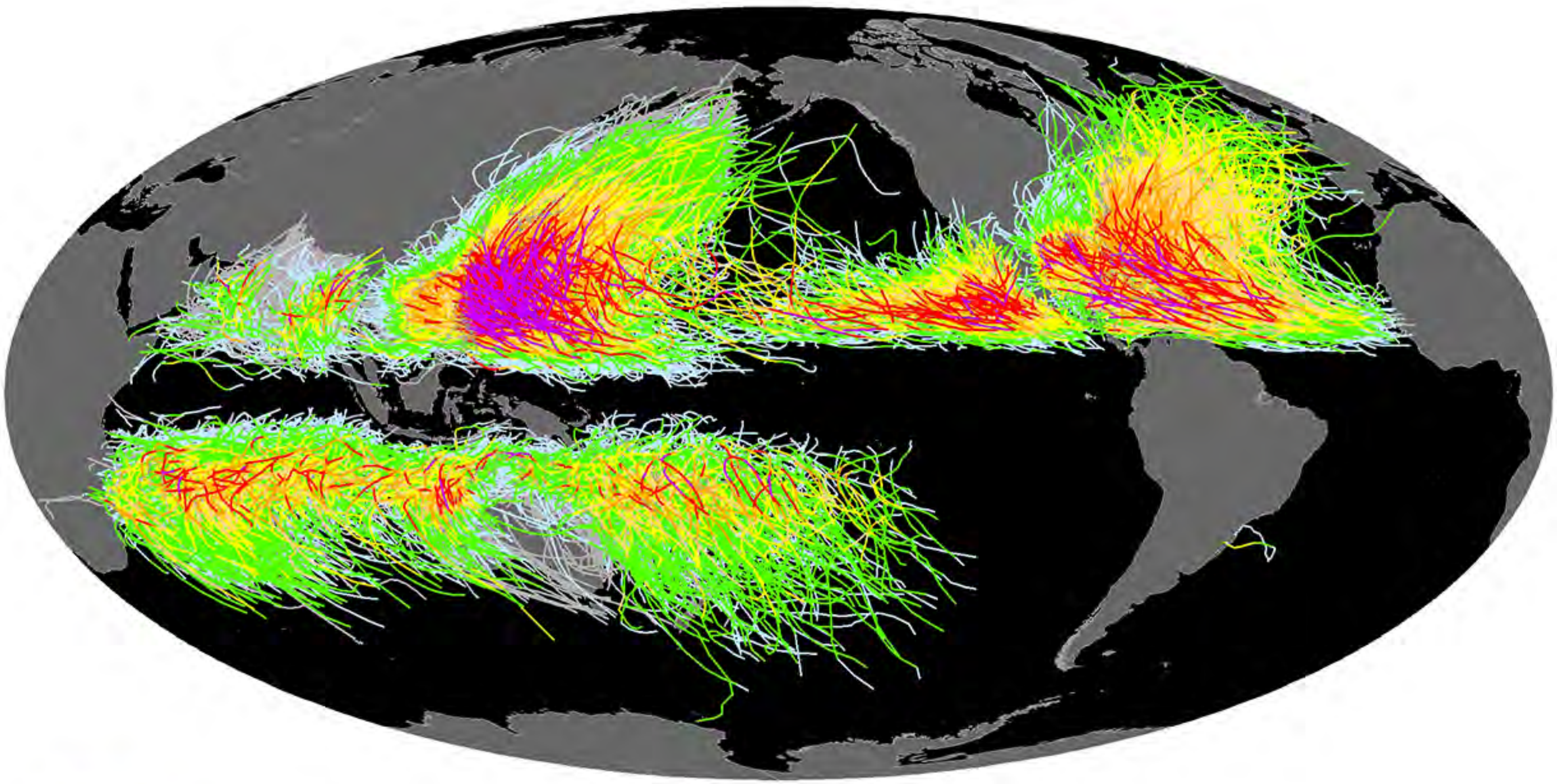

The International Best Track Archive for Climate Stewardship (IBTrACS) stores global tropical cyclone information.

Saffir-Simpson Hurricane Wind Scale

Intensity Missing
Tropical Depression
Tropical Storm
Category 1
Category 2
Category 3
Category 4
Category 5

TC Origin and Tracks with SST > 26.5°C

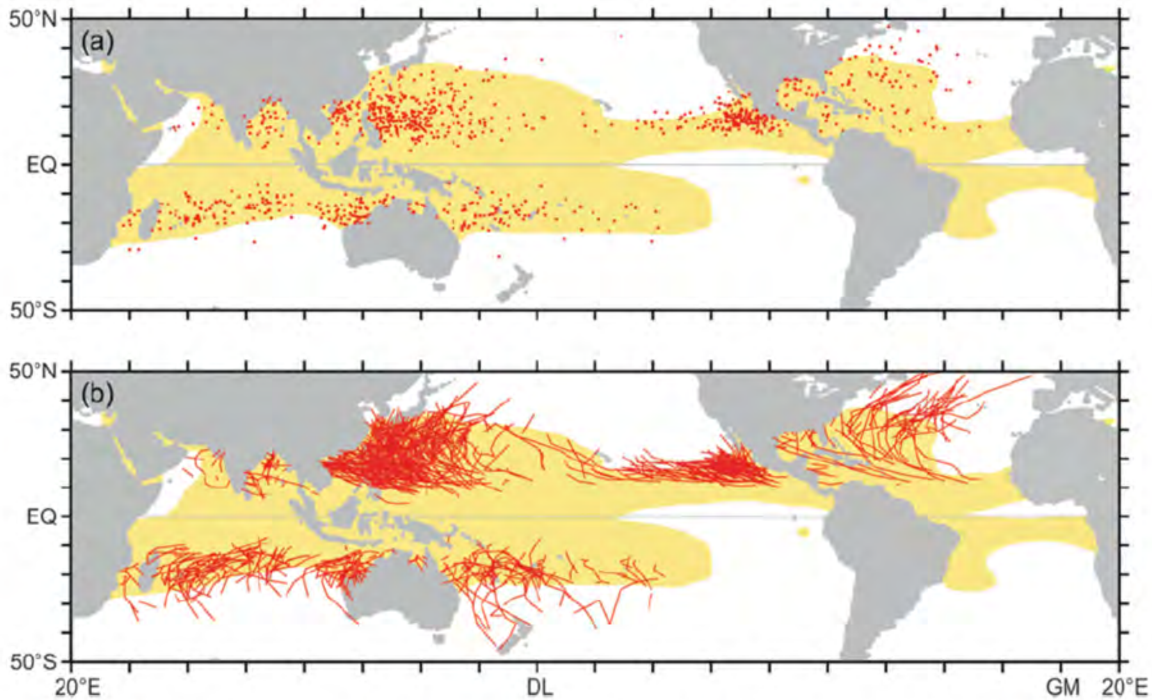

FIG. 1. Locations and tracks of tropical cyclones for 1970–89 relative to the global surface temperature analysis of Legates and Willmott (1990): (a) locations of hurricanes on the first day with hurricane-force winds (>32 m s^{-1}), and (b) tracks of hurricanes. The shaded oceanic regions are where SST exceeds 26.5°C in summertime, represented by August in the Northern Hemisphere and February in the Southern Hemisphere. (Provided through the courtesy of T. Mitchell, University of Washington.)

Ingredients for Tropical Cyclogenesis

- Question:
  - How is disorganized convection transformed into a weak surface-based vortex that can self-amplify?

- Gray (1968) necessary (**but not independently sufficient**) conditions:
  - (i) sufficient ocean thermal energy [SST > 26°C to a depth of 60 m]
  - (ii) enhanced mid-troposphere (e.g. 700 hPa) RH
  - (iii) conditional instability
  - (iv) enhanced lower troposphere relative vorticity
  - (v) "weak" vertical shear of the horizontal winds
  - (vi) displacement by at least 5° latitude away from the equator

Ingredients we listed for deep moist tropical convection in general. [(i)–(iii)]

A rotating vortex has additional requirements. [(iv)–(vi)]

- Genesis is a multi-scale problem
  - Large scale influences: ITCZ, equatorial waves, MJO, monsoon trough, African easterly waves
  - Mesoscale and convective-scale influences: mesoscale convective systems, hot towers, vortex mergers

Precipitation Banding Structure of a Mature Tropical Cyclone

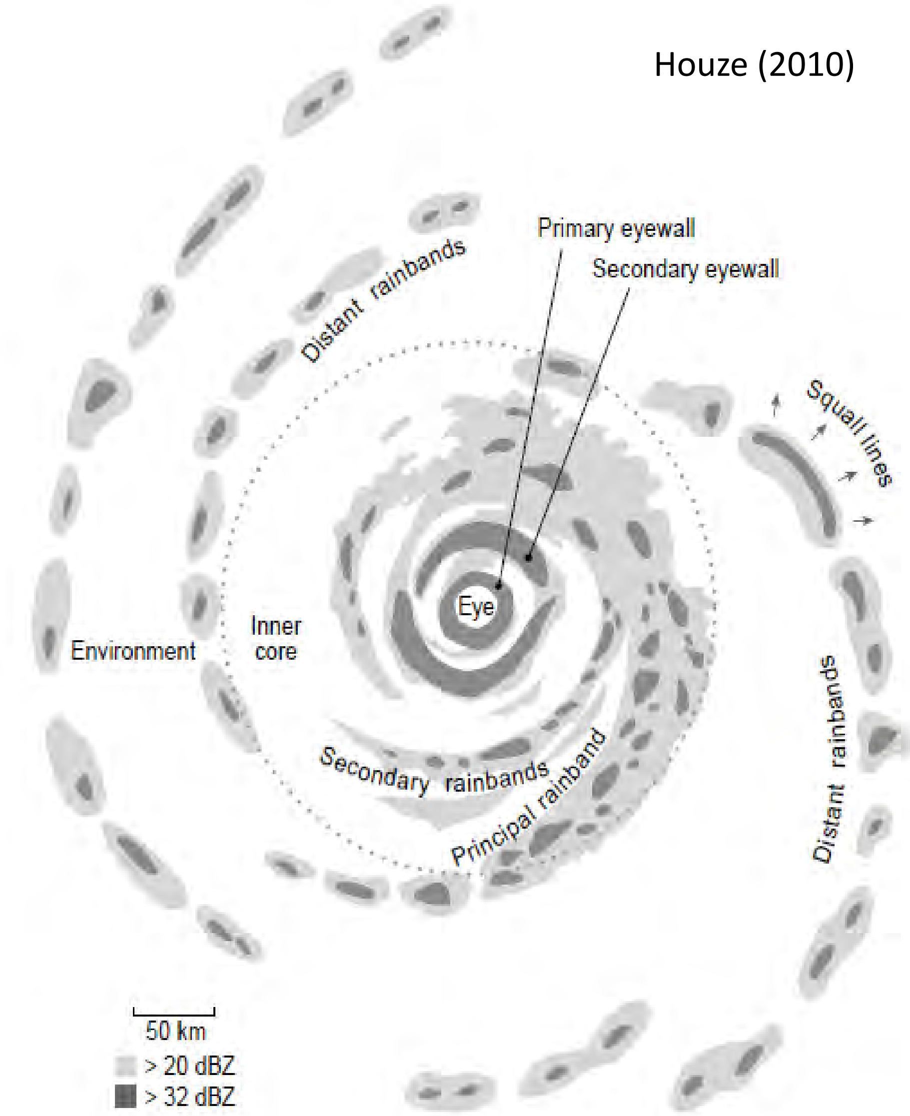

These features can be detected via radar or passive microwave, but not with IR or visible wavelengths.

Hurricane Michael 10 October 2018

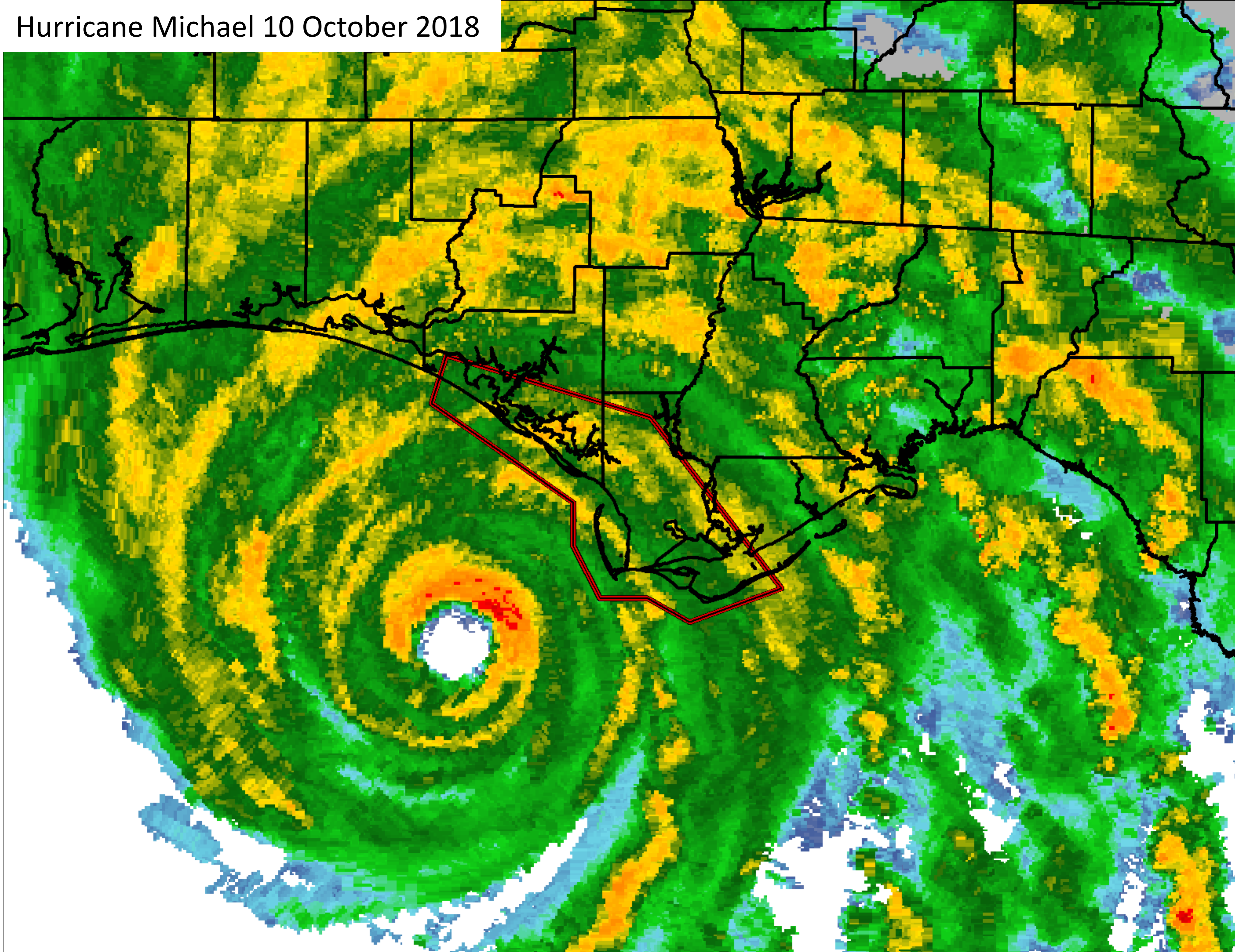

Hurricane Michael 10 October 2018

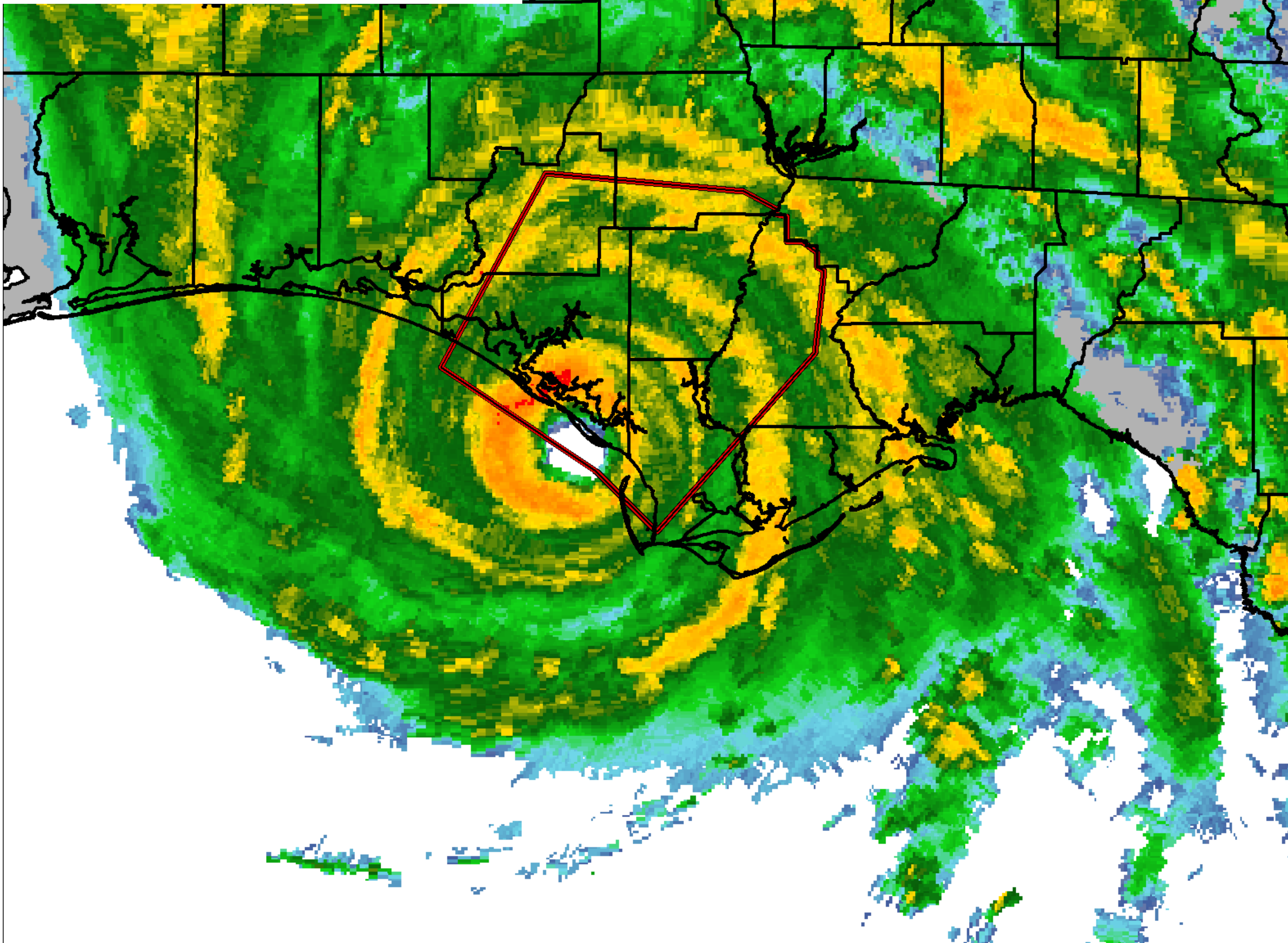

Hurricane
Katrina (2005)

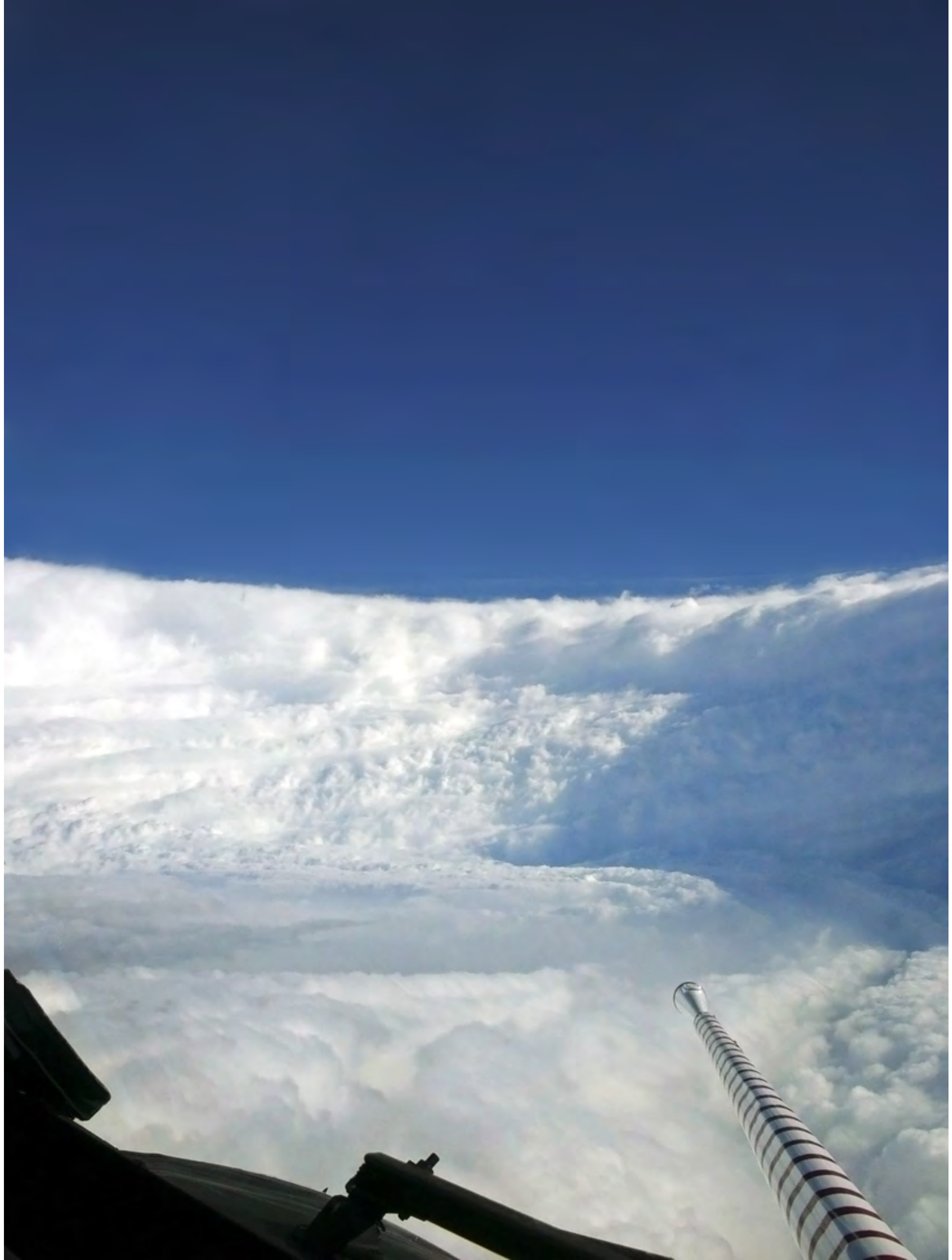

Image:
NOAA/Wikipedia

WC-130J USAF, 53rd Weather Reconnaissance Squadron, 403rd Wing

NOAA WP-3D Orion

Willoughby (1988)

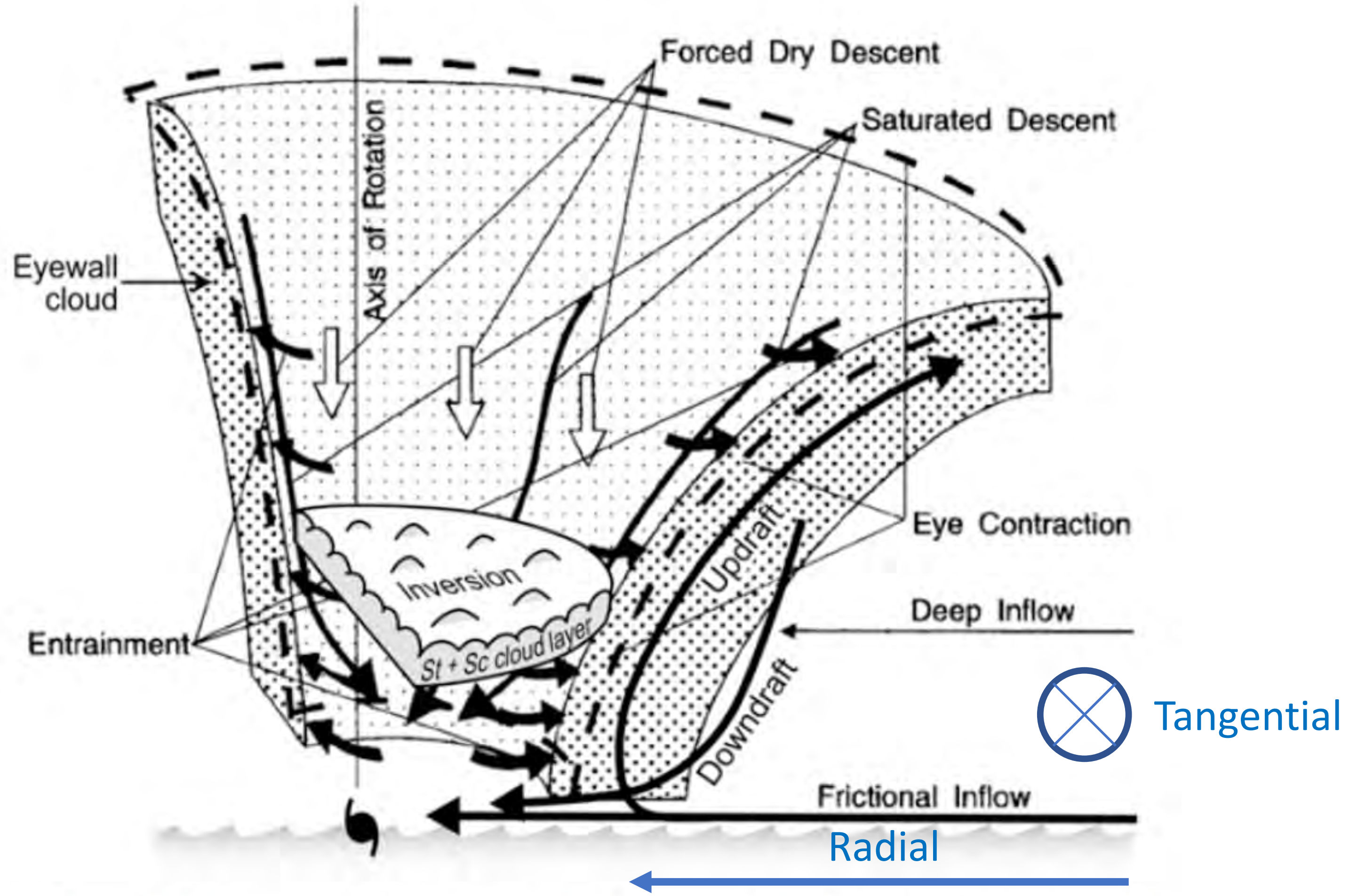

FIG. 9. Schematic illustration of the secondary flow in the eye and eyewall of a hurricane. Dashed lines show an earlier location of the contracting eyewall. [Adapted from Willoughby (1998).]

Mean radial and tangential wind

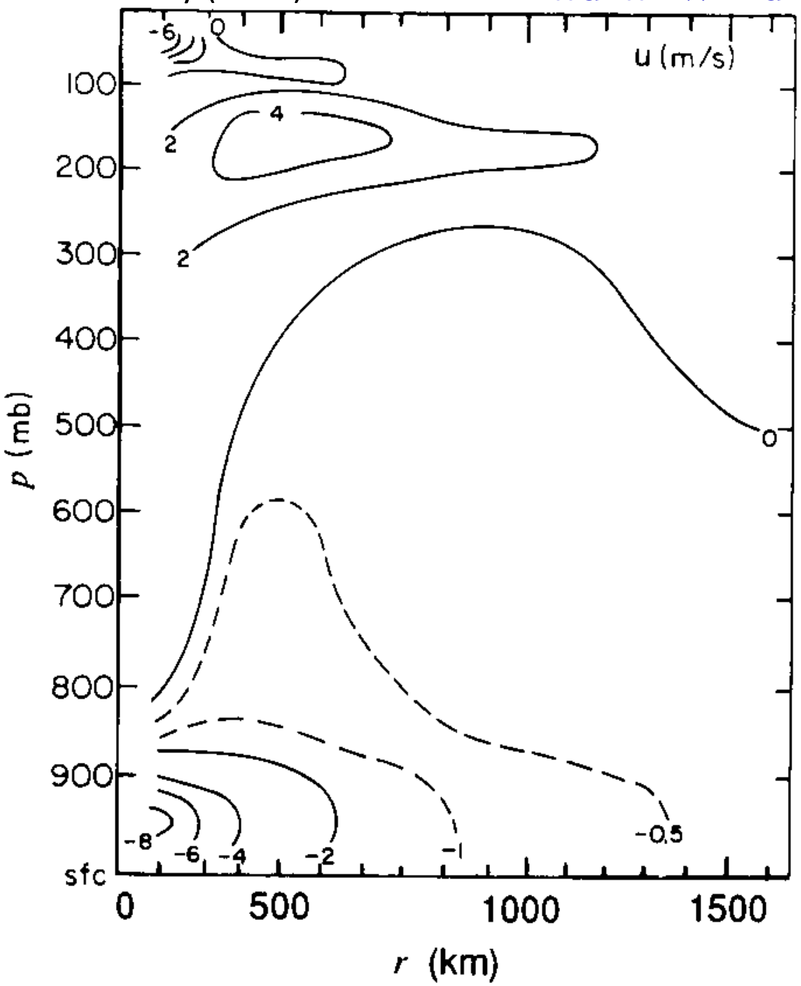

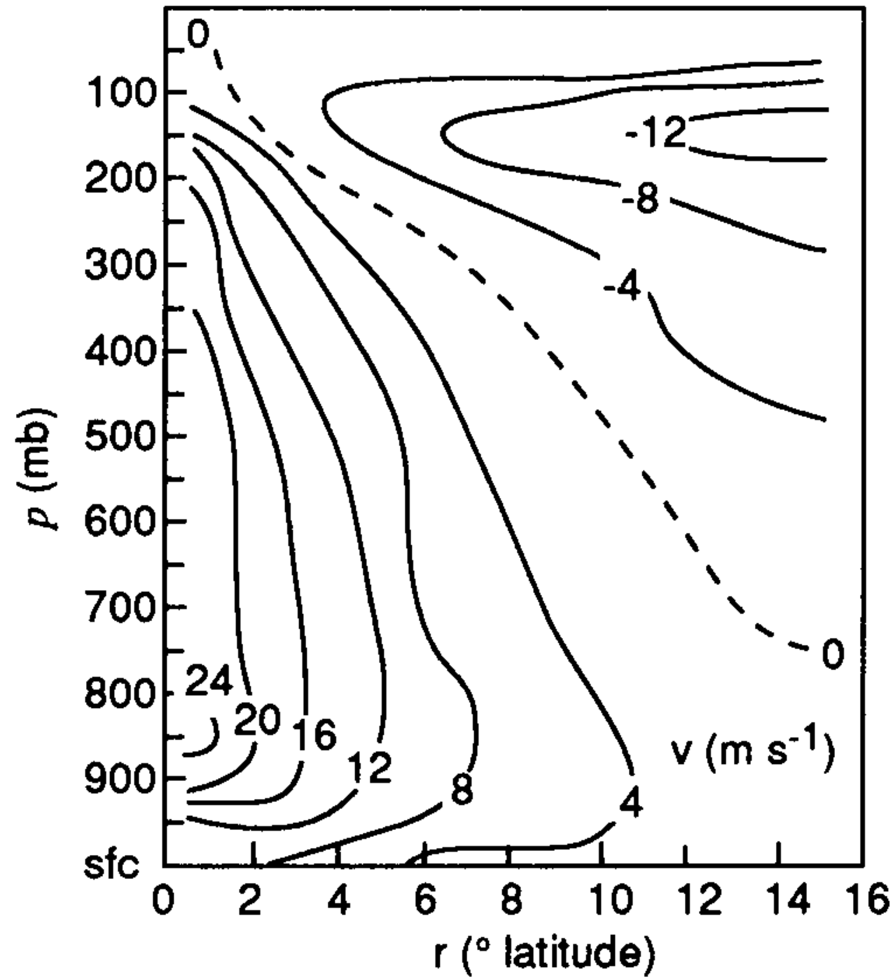

Atlantic hurricanes

Pacific typhoons

Gradient wind balance: $\frac{1}{\rho}\frac{\partial p}{\partial r} = fV_{gr} + \frac{V_{gr}^2}{r}$

Angular momentum: $m = rV_{gr} + \frac{fr^2}{2}$

Strength of warm core decreases with height

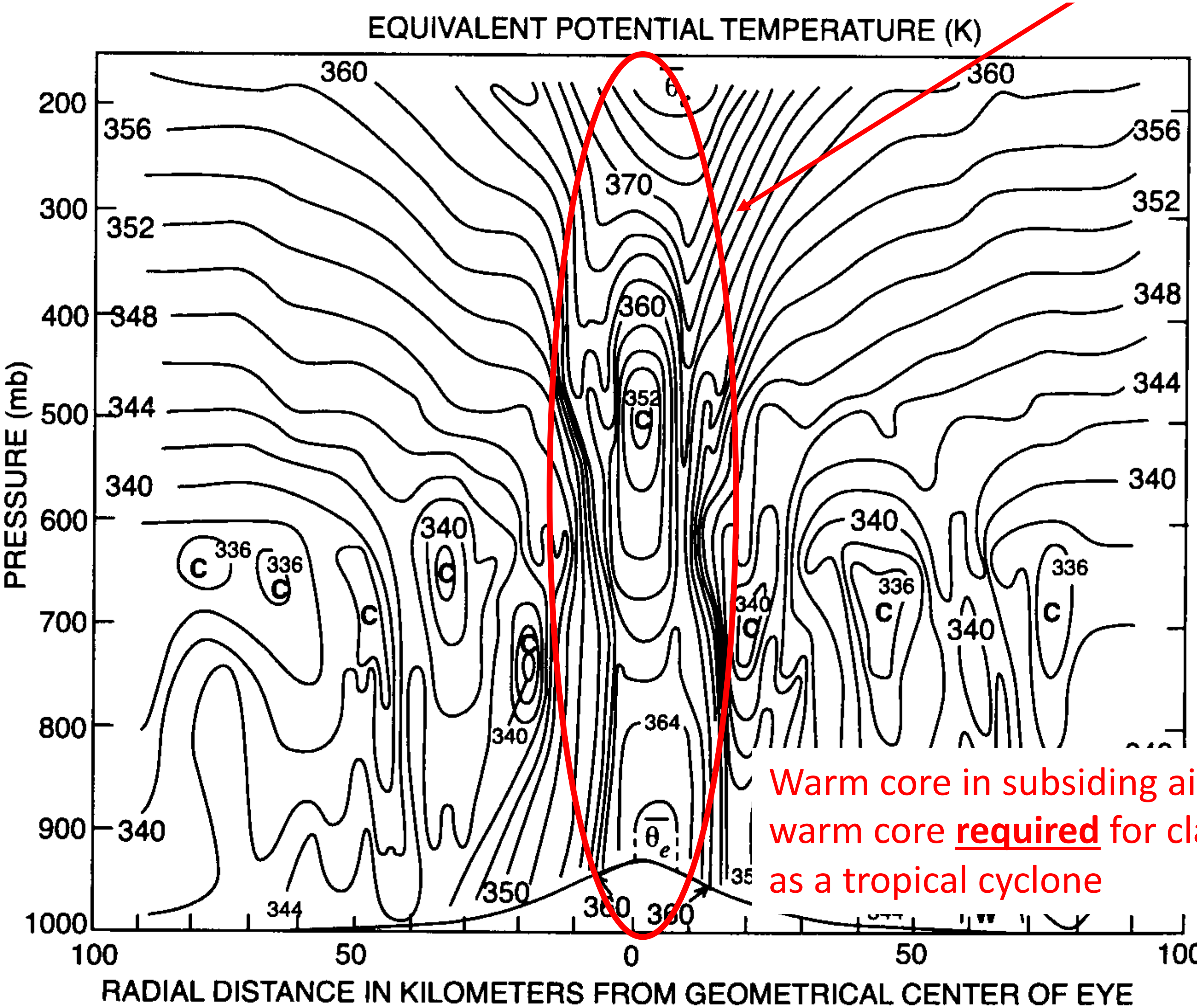

Warm core in subsiding air in eye; warm core **required** for classification as a tropical cyclone

Hawkins and Imbembo (1976)

Cyclone Phase Space Diagram (Florida State University, described in Evans and Hart 2003)

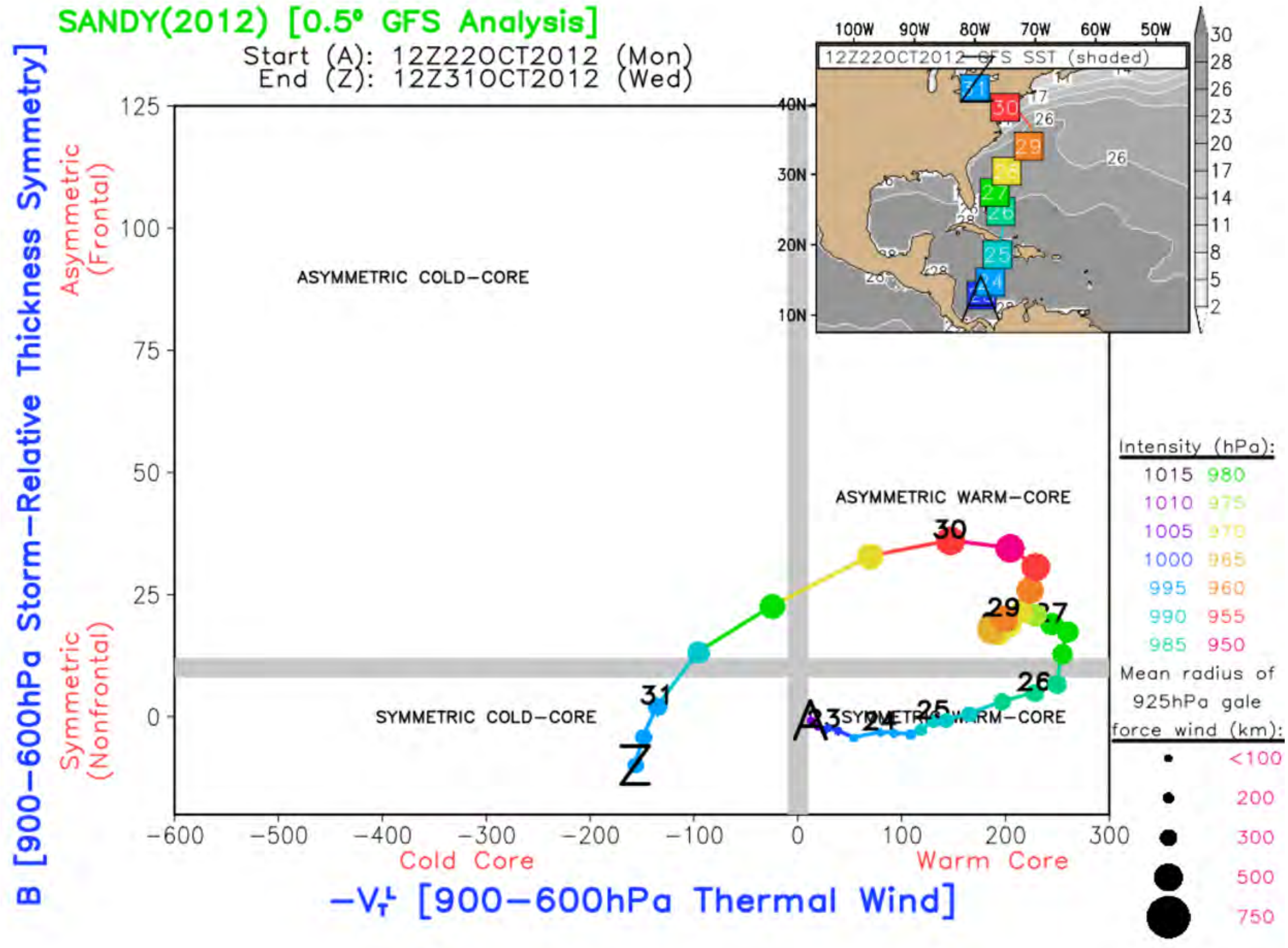

Cyclone Phase Space Diagram (Florida State University, described in Evans and Hart 2003)

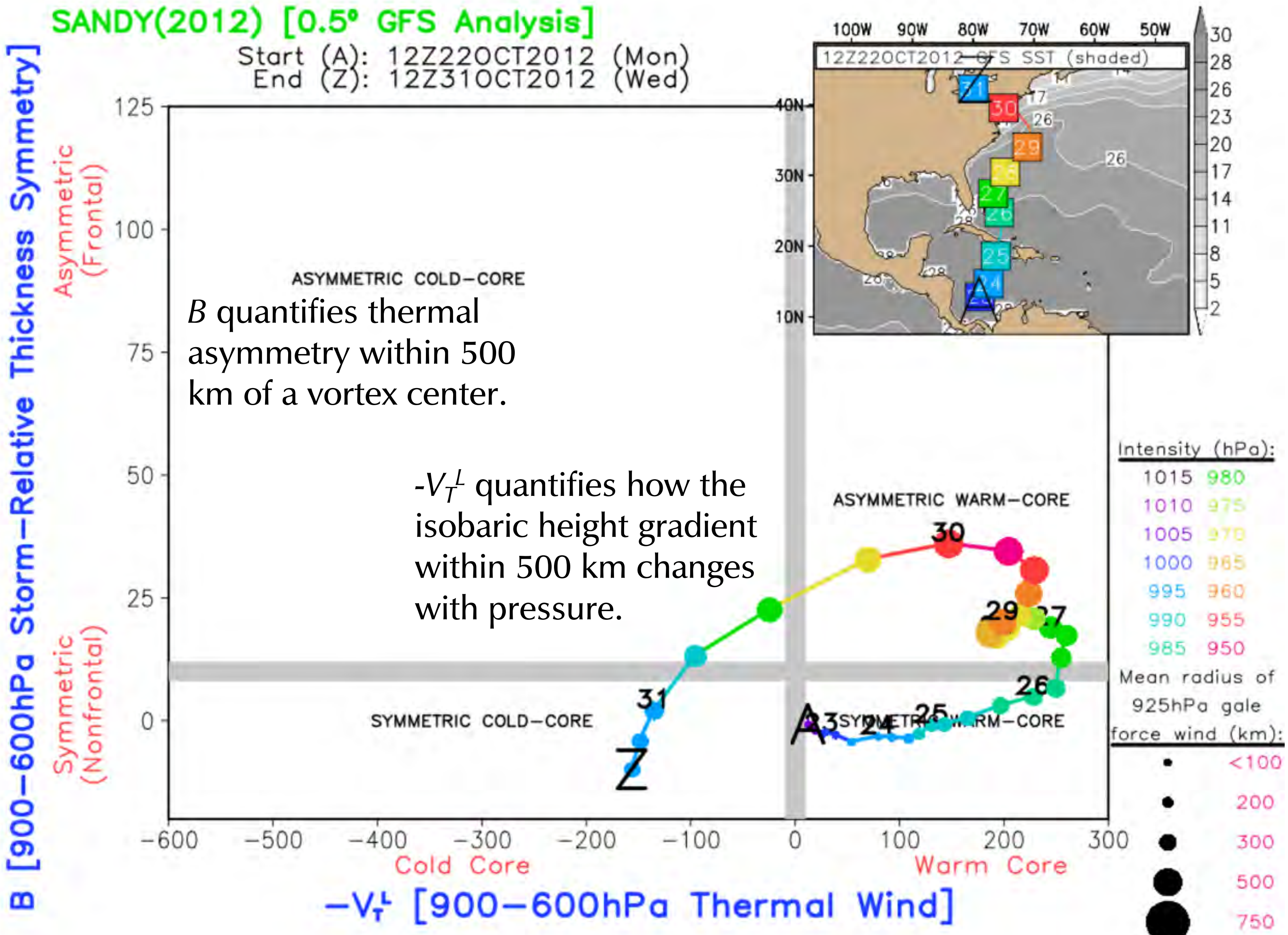

B quantifies thermal asymmetry within 500 km of a vortex center.

-V_T^L quantifies how the isobaric height gradient within 500 km changes with pressure.

Thermal wind: $$-\mathbf{V}_T^L = \frac{R}{f}\int_{900}^{600} (\mathbf{k} \times \nabla_p T)\, d\ln p$$

Sloped θ_e contours are parallel to m contours.

Magnitude of tangential wind

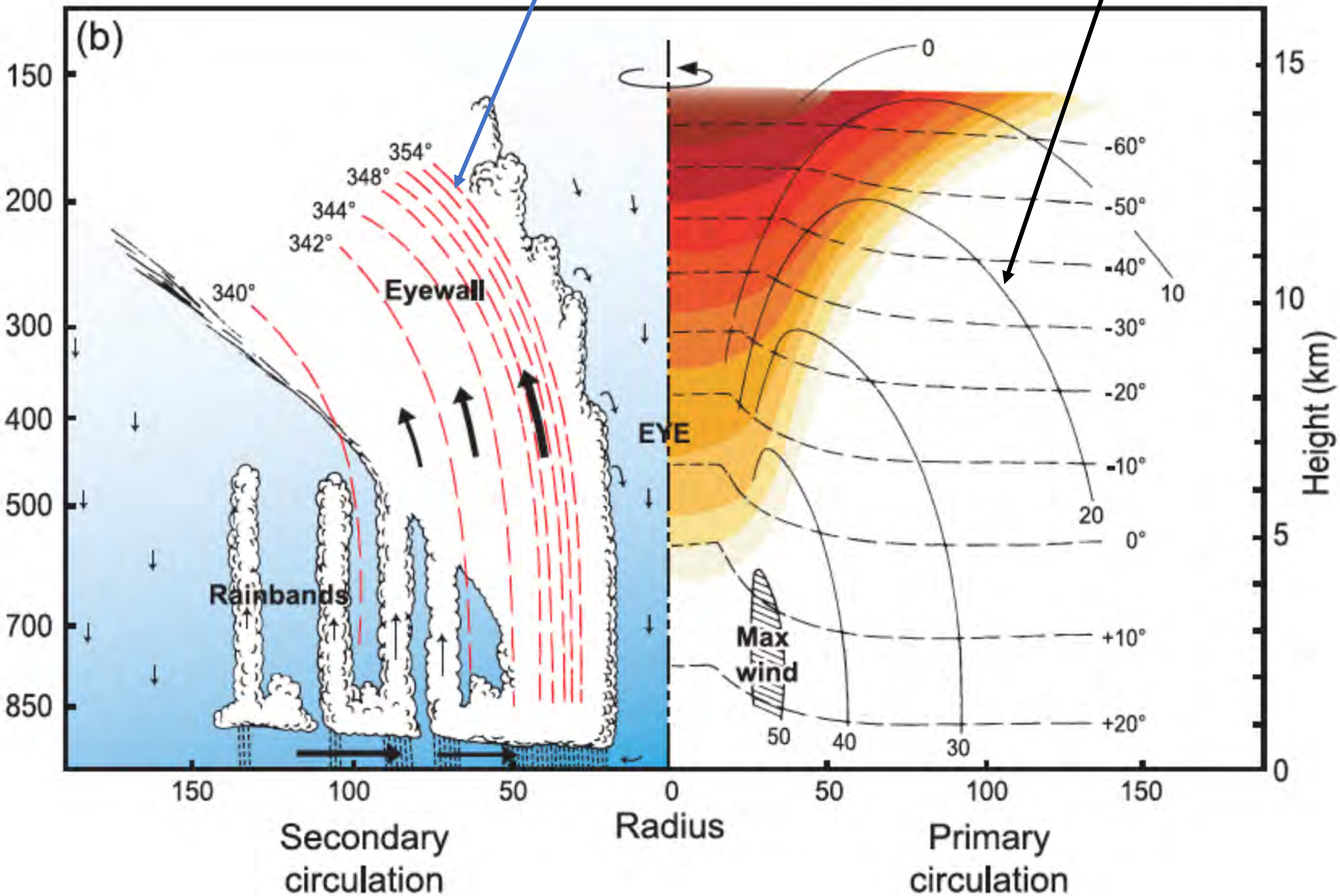

Wallace and Hobbs (2006)

Magnitude of tangential wind

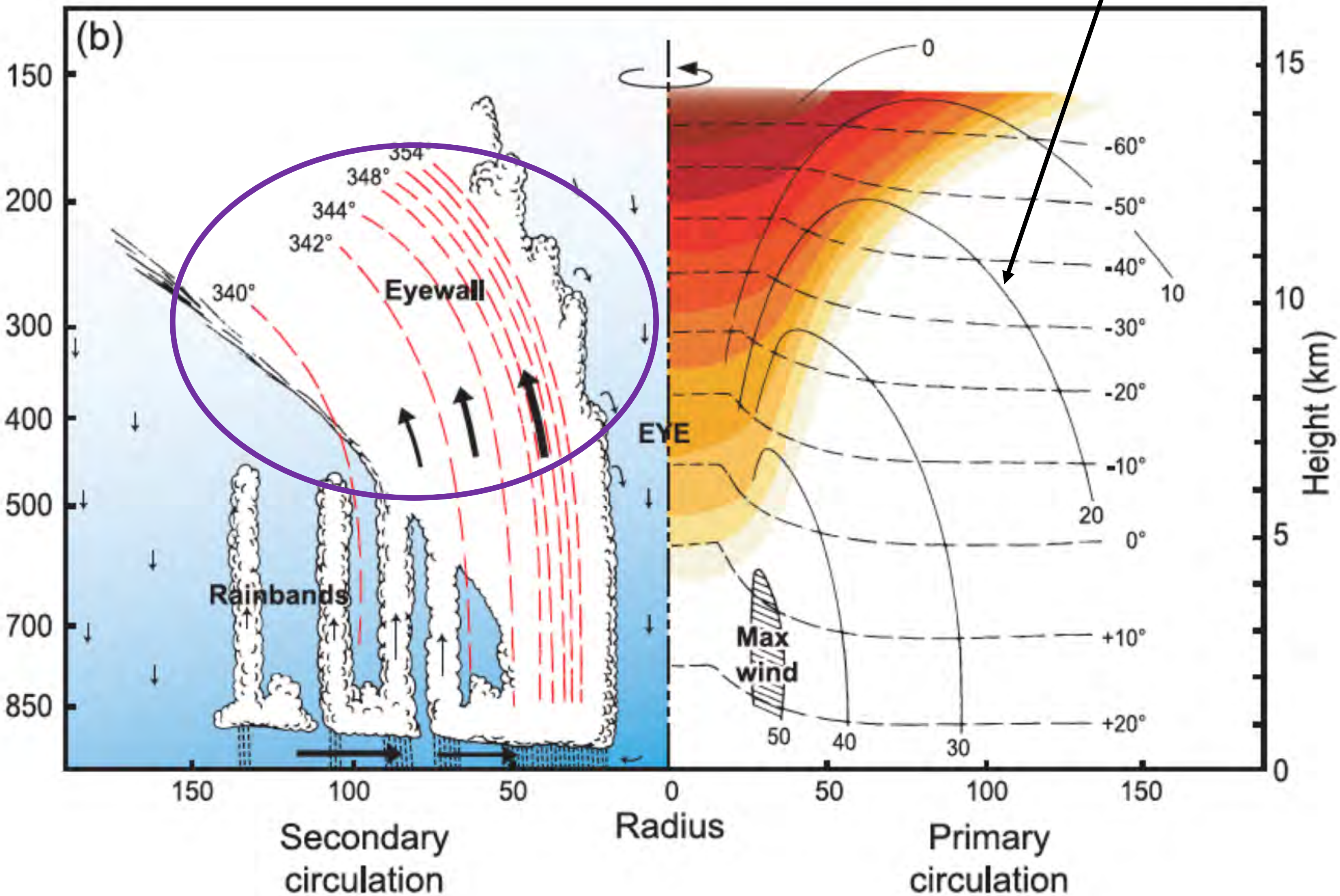

Wallace and Hobbs (2006)

Why is the eyewall sloped?

Homework problem 1

DeHart et al. (2014)

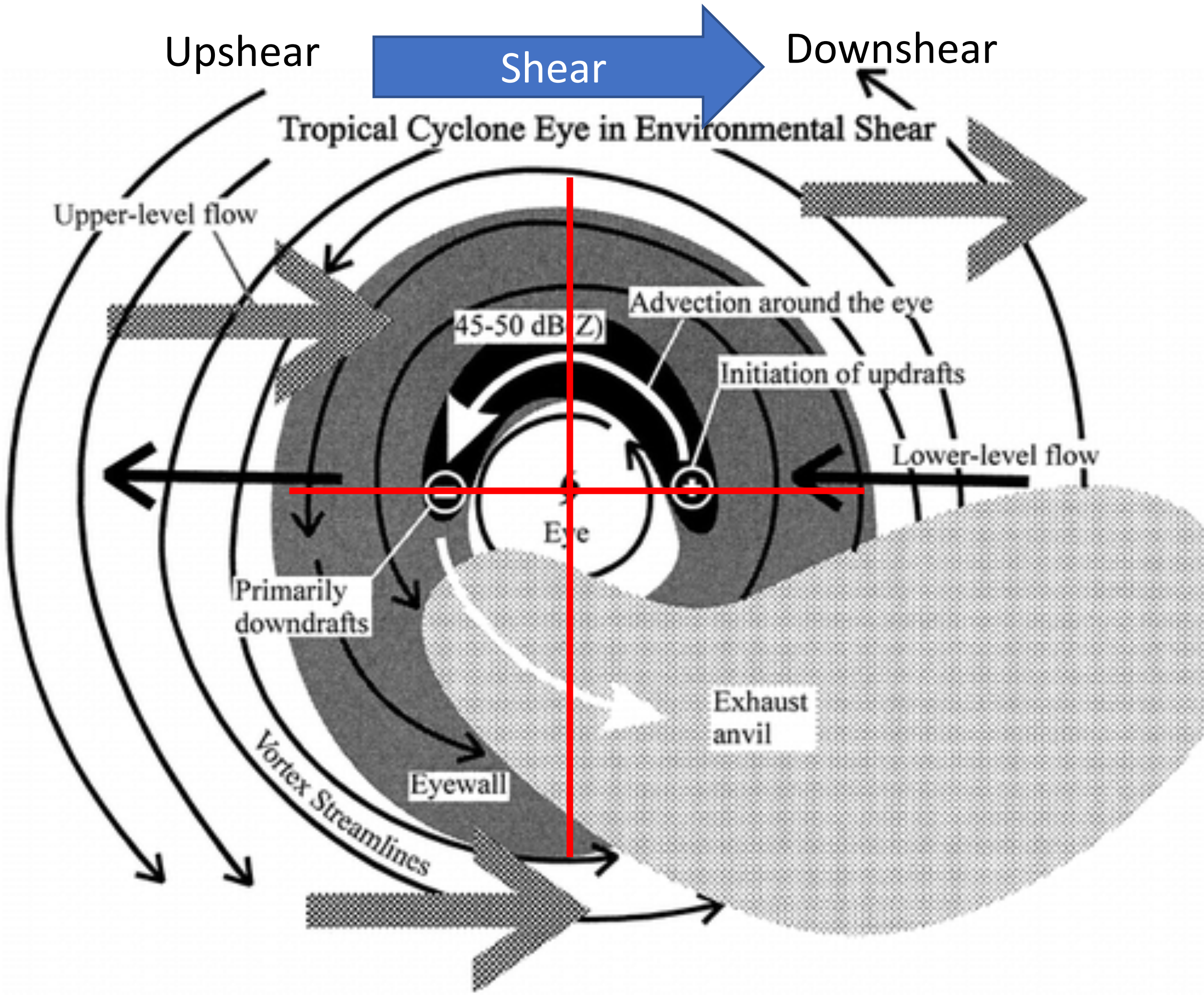

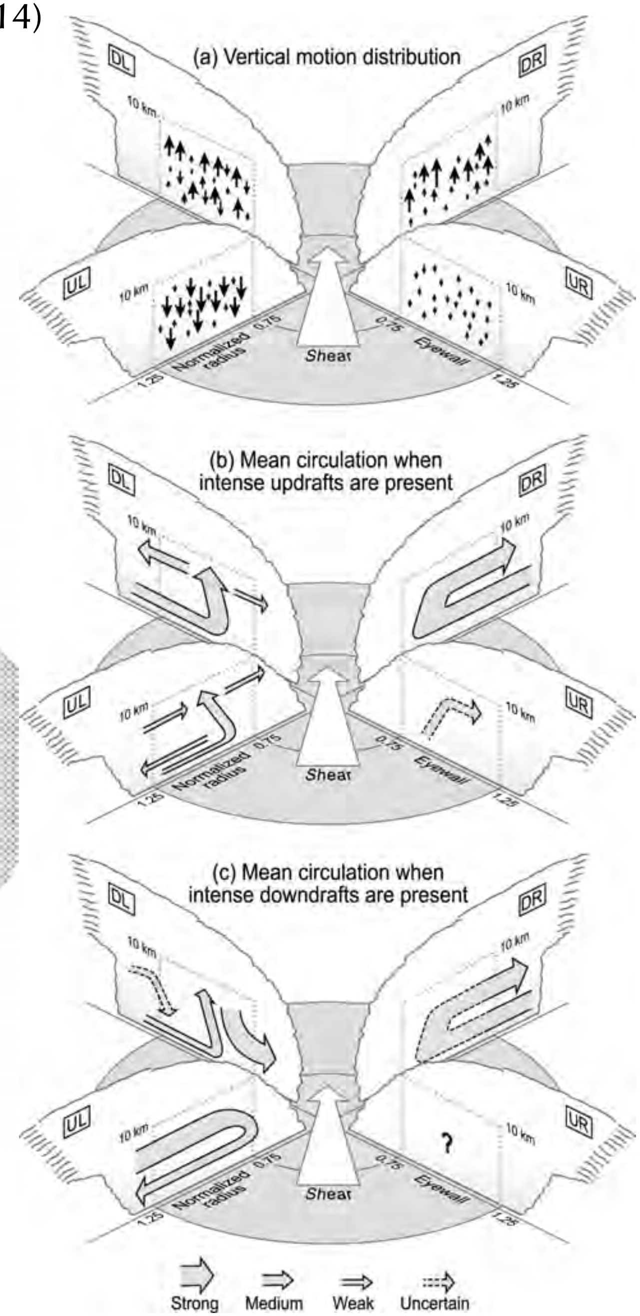

Black et al. (2002)

Hurricane Michael 10 October 2018

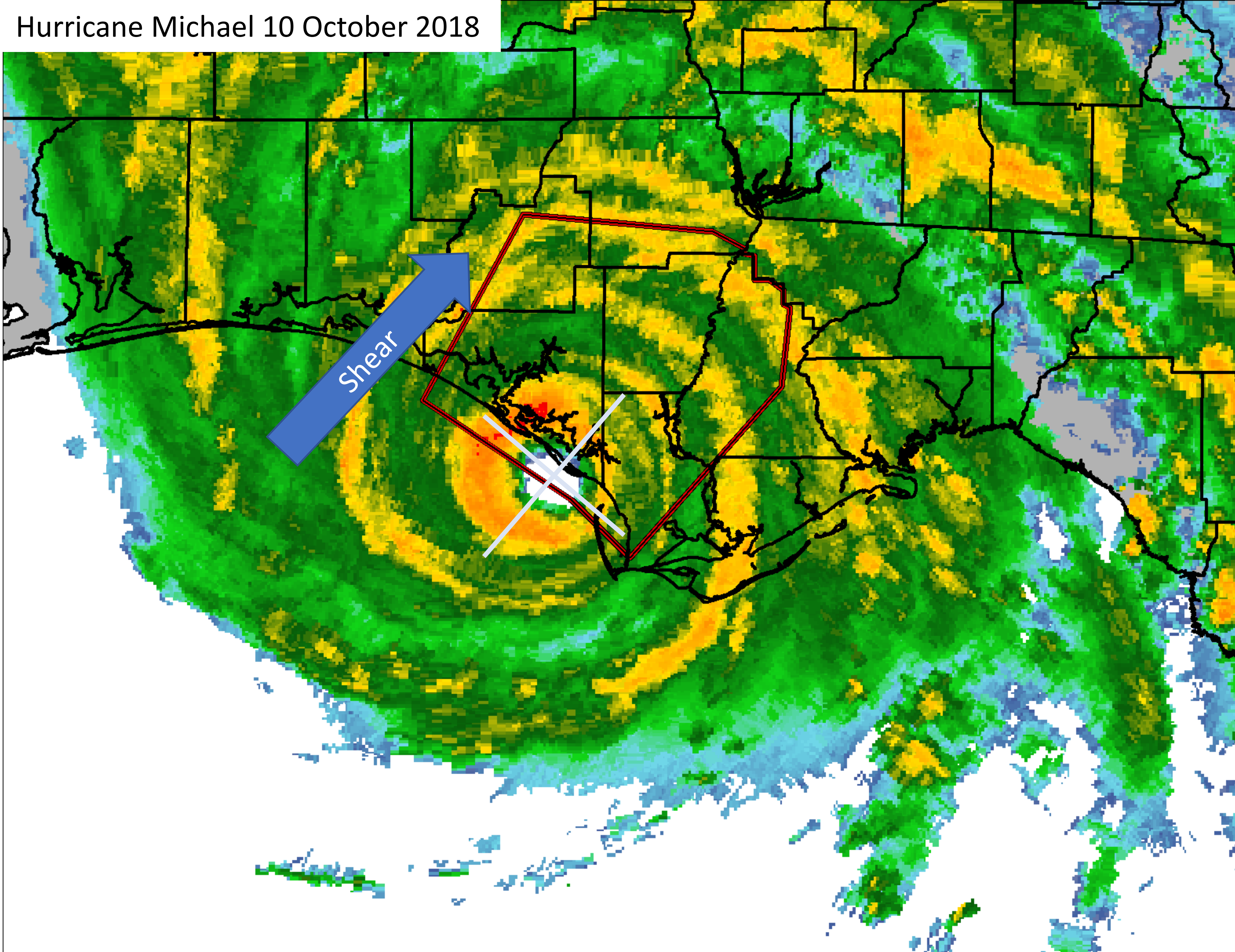

MR3252: Tropical Meteorology

Concentric Eyewalls in Tropical Cyclones

Main Topics:

- Observations of concentric eyewalls
- Eyewall replacement cycles

Module 3.3

Kossin and Sitkowski (2008)

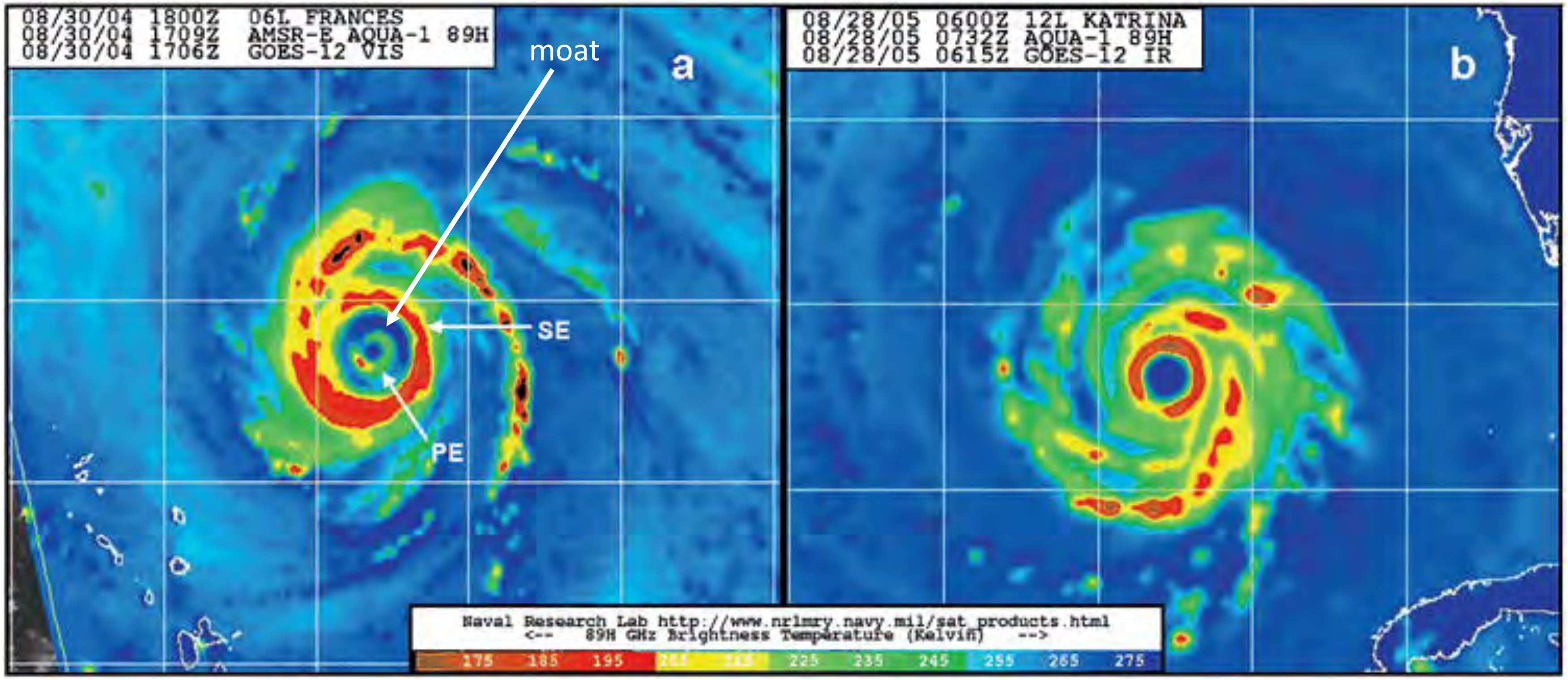

Theorized Mechanisms for Concentric Eyewall Formation (in no particular order)

- Vortex Rossby waves (Terwey and Montgomery 2003)
- Supergradient wind near top of boundary layer drive convergence (Huang et al. 2012)
- Development of radial vorticity gradients (Kepert 2013); Heating-convergence feedback driven by Ekman pumping and rotational flow (Miyamoto et al. 2018)
- Latent heat release in rainbands (Zhu and Zhu 2014)
- Outflow-jet interactions promote growth of convection in stratiform regions outside primary eyewall (Dai et al. 2017)
- External forcing (e.g. humidity of TC environment, flux of angular momentum to environment) (Ortt and Chen 2006, Nong and Emanuel 2003)
- Beta skirt outside primary eyewall (Terwey and Montgomery 2008)

Bell et al. (2012)

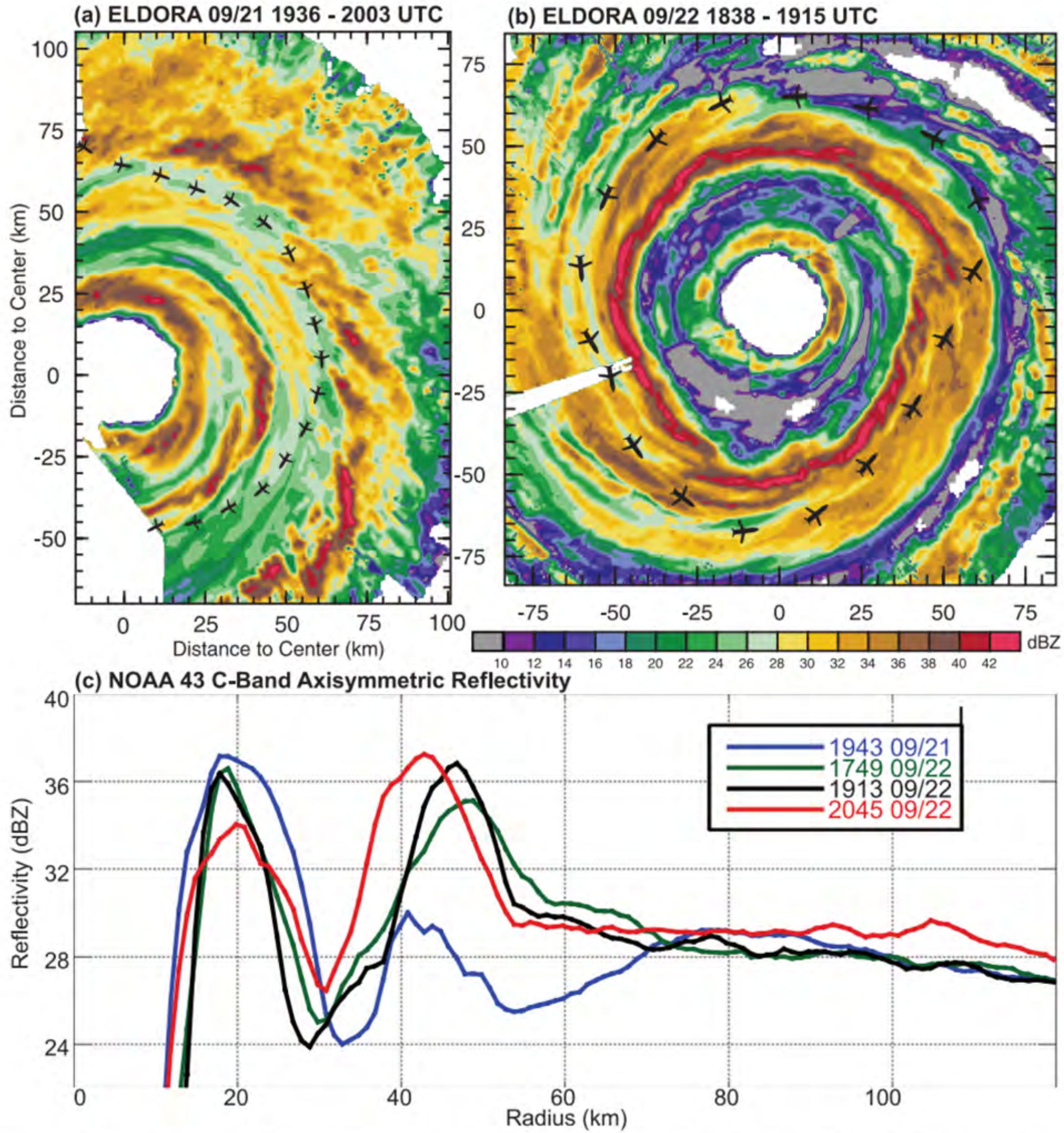

FIG. 3. Radar reflectivity from ELDORA X-band at 3-km altitude during (a) 1936–2003 UTC 21 September and (b) 1838–1915 UTC 22 September, and (c) axisymmetric reflectivity from NOAA C-band at ~3 km at four consecutive times shown in inset.

Concentric Eyewall Cycles

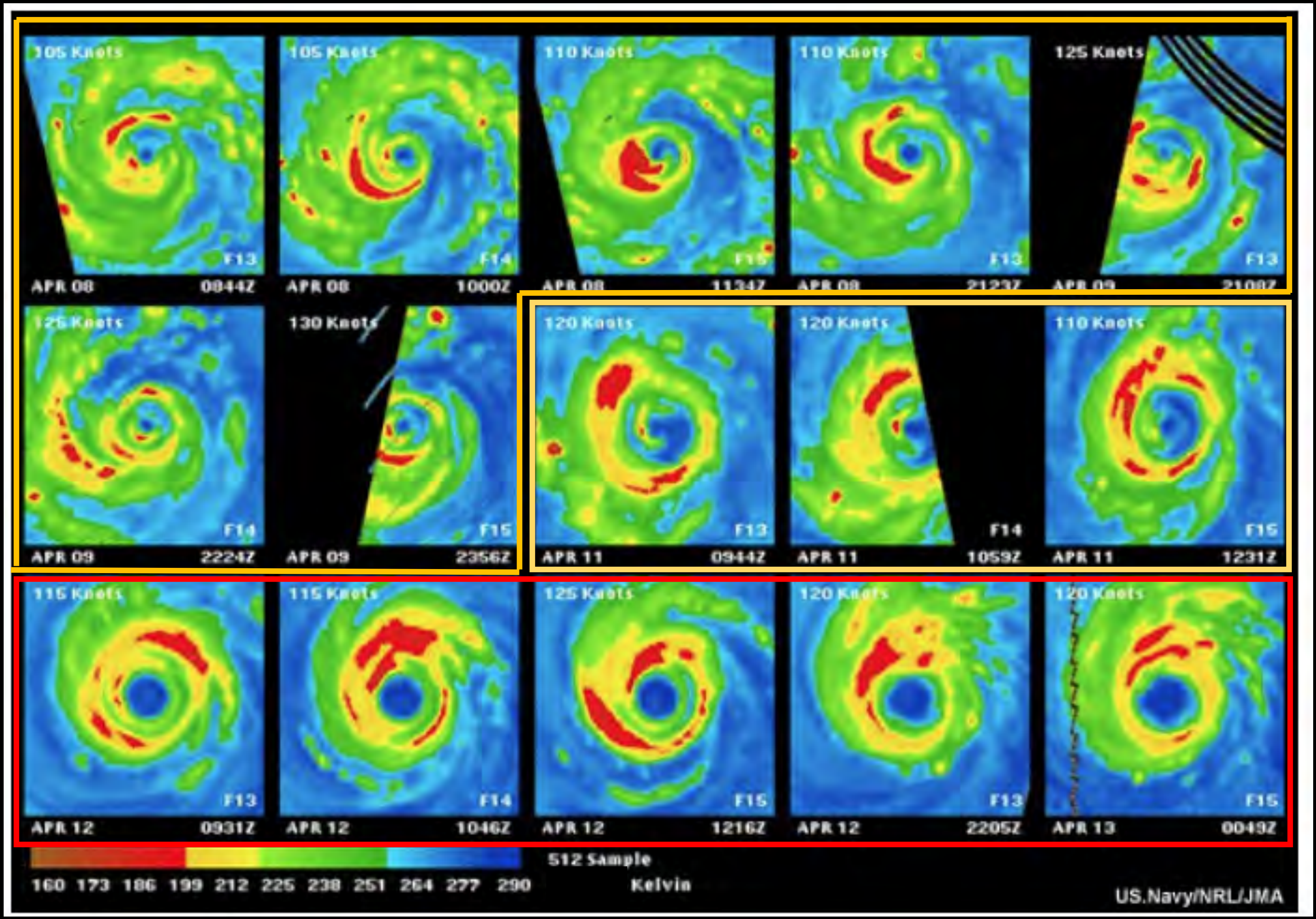

Hurricane Gilbert (1988)

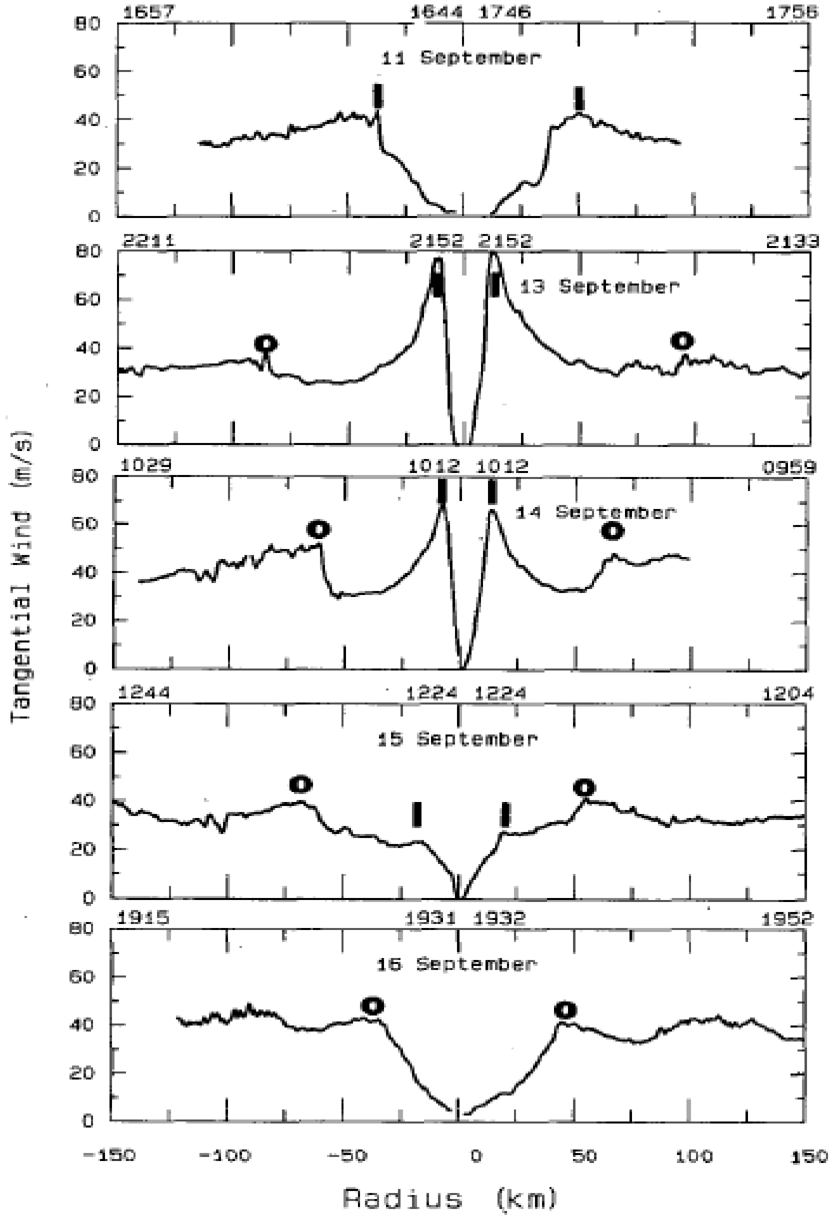

FIG. 7. Flight-level tangential wind speed from south–north traverses through the center of Hurricane Gilbert for five of the six reconnaissance flights listed in Table 1. Bold *I*'s and *O*'s denote the location of the inner- and outer-eyewall wind maxima, respectively. Times at the beginning and end of each radial pass are plotted at the top of the panels.

One wide eye

2 days later; Small eye

12 hours later; outer wind max obvious; inner wind max still intense

1 day later; inner wind maximum decaying; outer becoming primary

1 day later; eyewall replacement complete

Sitkowski et al. (2011) evolution

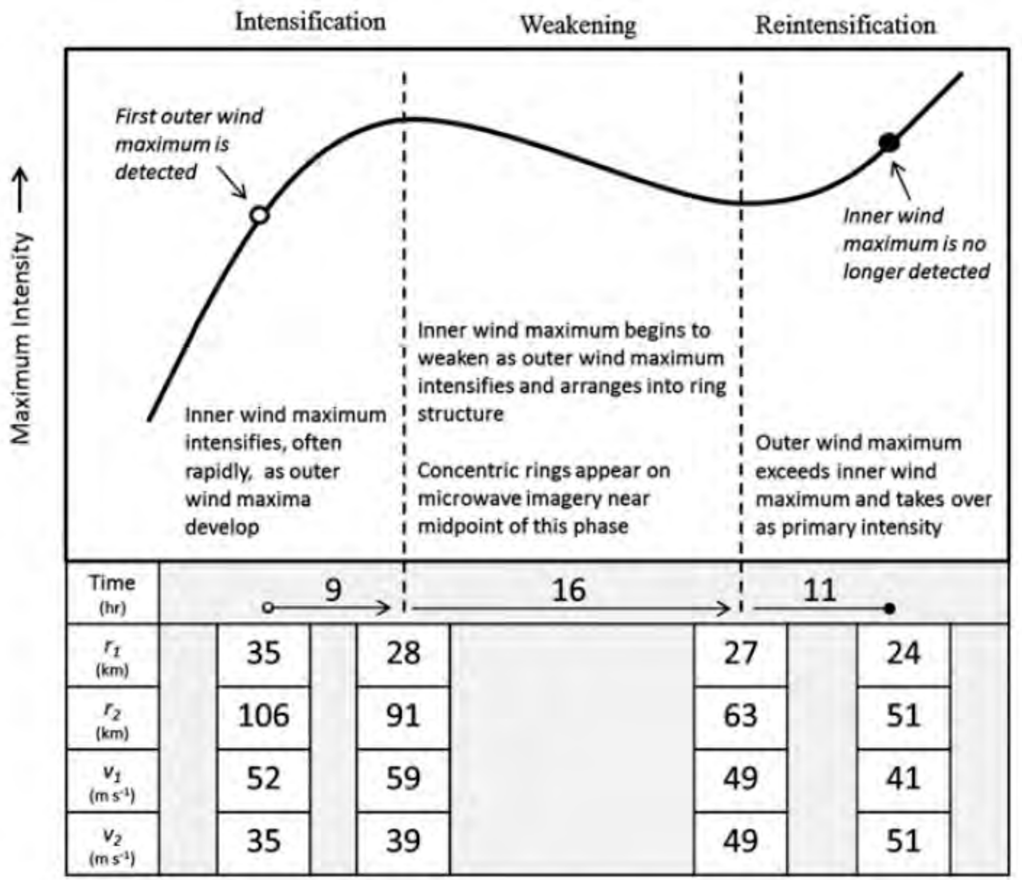

FIG. 8. Schematic of the maximum intensity evolution during three phases of an ERC. The average amount of time to complete each phase, along with the average values of the Rankine parameters, as determined from the third-order polynomial fits, are listed for the start and end of the ERC, as well as the transition of phases.

MR3252: Tropical Meteorology

Extratropical Transition of Tropical Cyclones

Main Topics:

- Predecessor rain events
- Baroclinic conversion of energy
- Frontogenesis and instability in transitioning cyclones

Module 3.4

Klein et al. (2000)

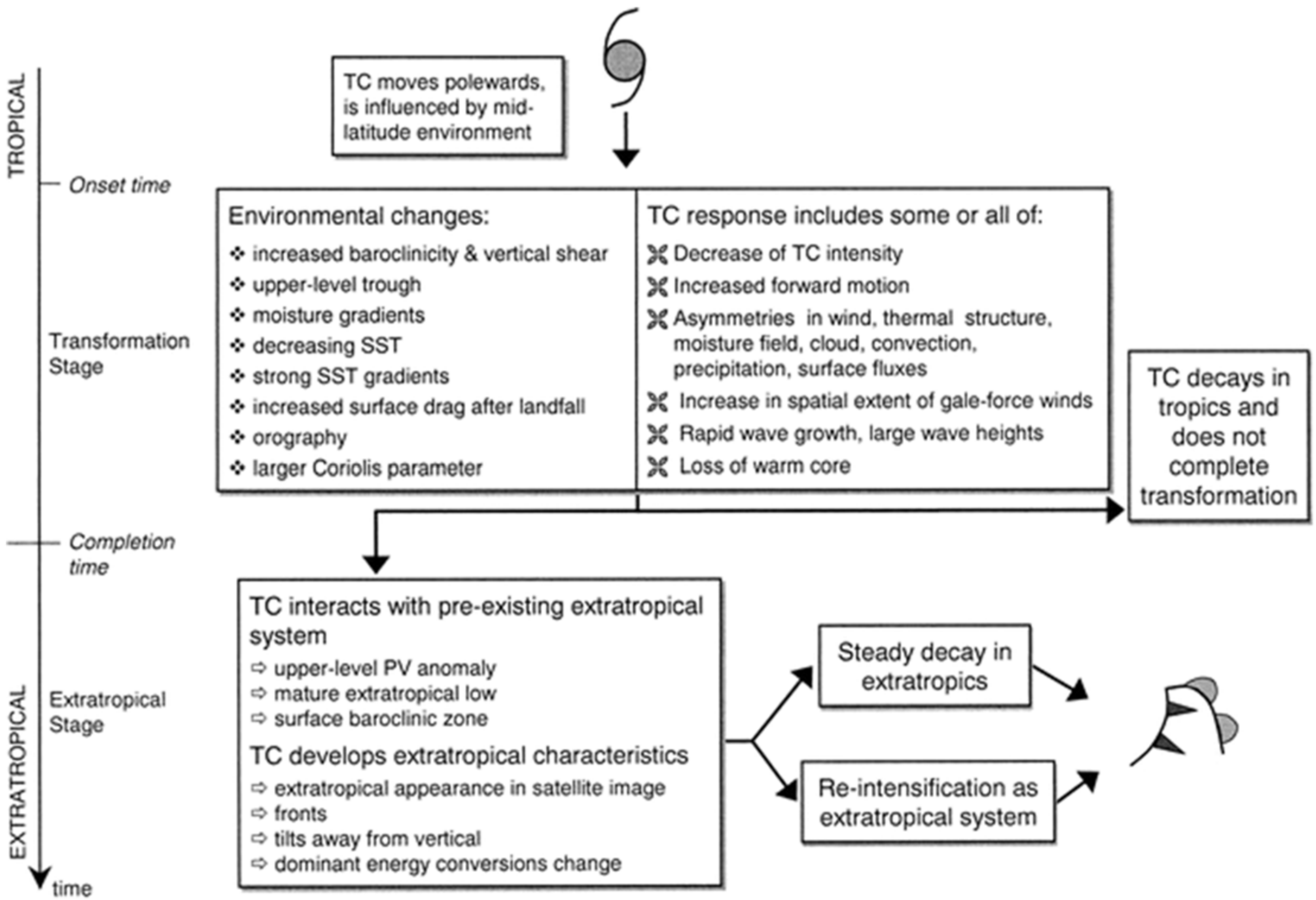

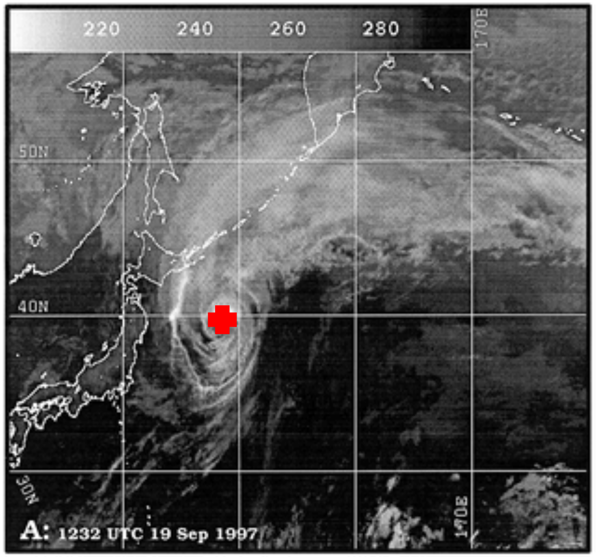

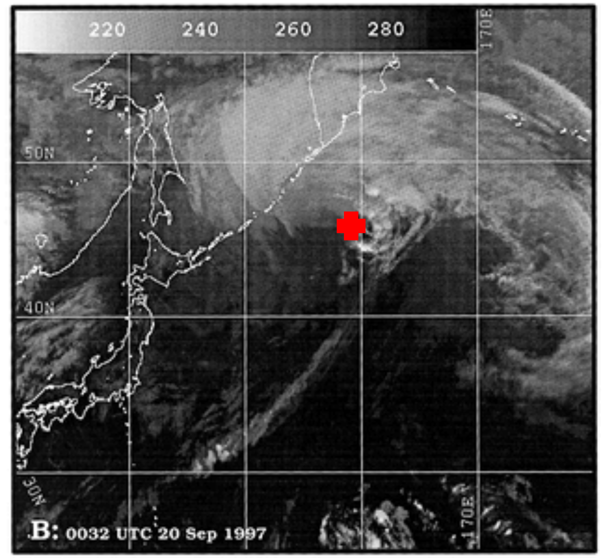

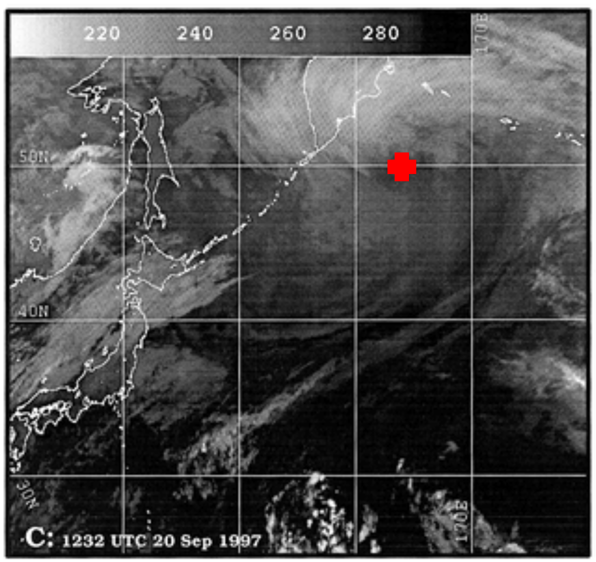

Harr and Elsberry (2000); ET of Typhoon David over 24 hours

Quinting and Jones (2016); Keller et al. (2019)

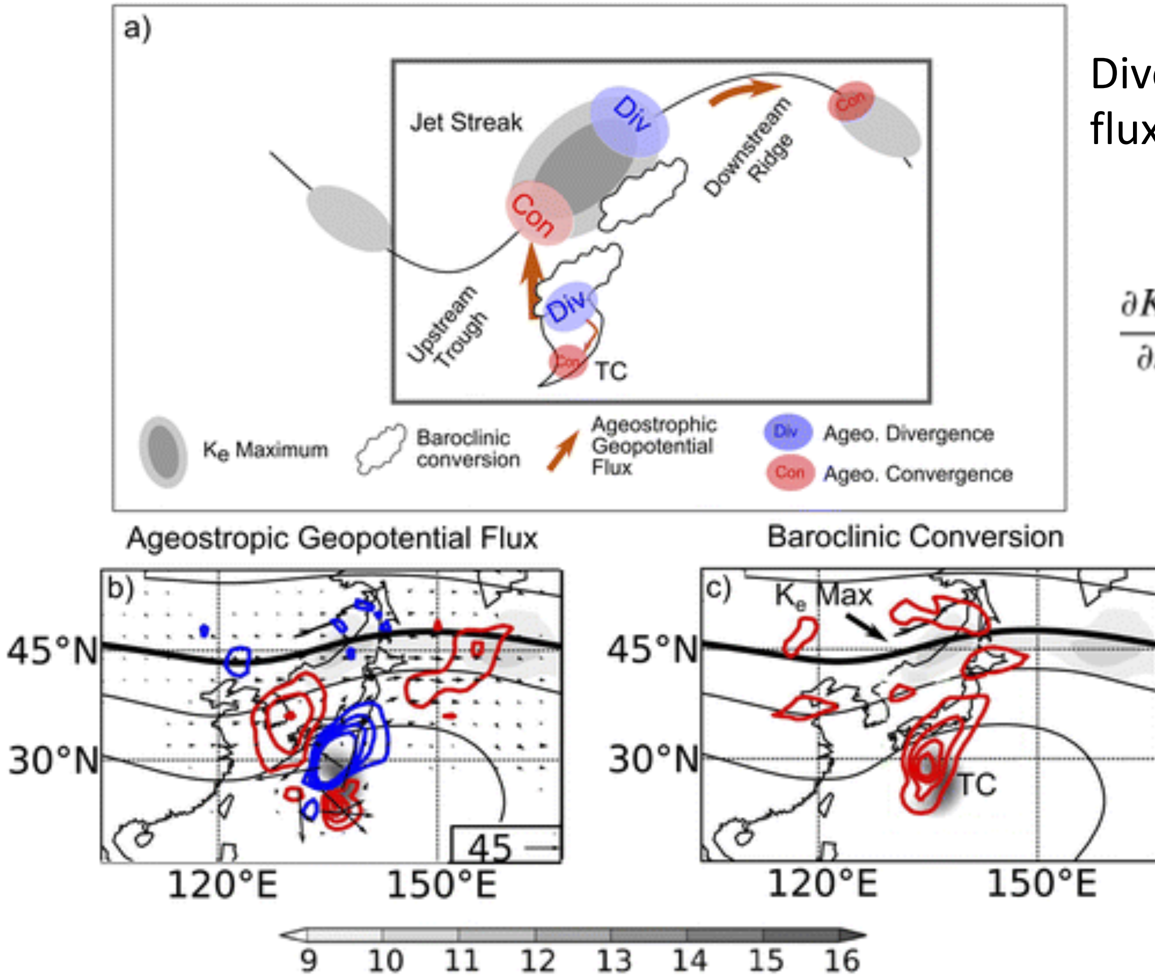

Divergence of ageostrophic flux of geopotential

$$\frac{\partial K_e}{\partial t} = -\nabla_p \cdot (\mathbf{v}\phi)_a - \omega\alpha - \frac{\partial(\omega\phi)}{\partial p} - \nabla_p \cdot (\mathbf{V}K_e) - \frac{\partial(\omega K_e)}{\partial p} - \mathbf{v} \cdot (\mathbf{v} \cdot \nabla_p \mathbf{V}_m) + \text{residue},$$

$$\alpha = \frac{1}{\rho}, \mathbf{V}_m = \text{mean flow}$$

Jet streak formation during ET from an energetics perspective. (a) Schematic representation, showing midlatitude jet (black line), developing K_e maxima (jet streak; gray ellipses), baroclinic conversion of K_e (clouds), ageostrophic geopotential flux (orange arrow), and its divergence (blue ellipses) and convergence (red ellipses). (b),(c) TC-relative composite of K_e budget for western North Pacific ETs, based on ERA-Interim for 1980–2010 [after Quinting and Jones (2016), their Figs. 12a,b]: vertically integrated K_e (shaded in 10^5 J m^{-2}), 200-hPa geopotential (contours every 200 m^2 s^{-2}; thick black contour illustrates 11 800 m^2 s^{-2}), and (b) ageostrophic geopotential flux (vectors, reference vector in 10^6 W m^{-1}; divergence as colored contours every 8 W m^{-2}, divergence in blue, 0 W m^{-2} omitted) and (c) vertically integrated baroclinic conversion of K_e (red contours every 8 W m^{-2}). The black box approximates the area that is captured by (b),(c). Composites are shown relative to the mean TC position.

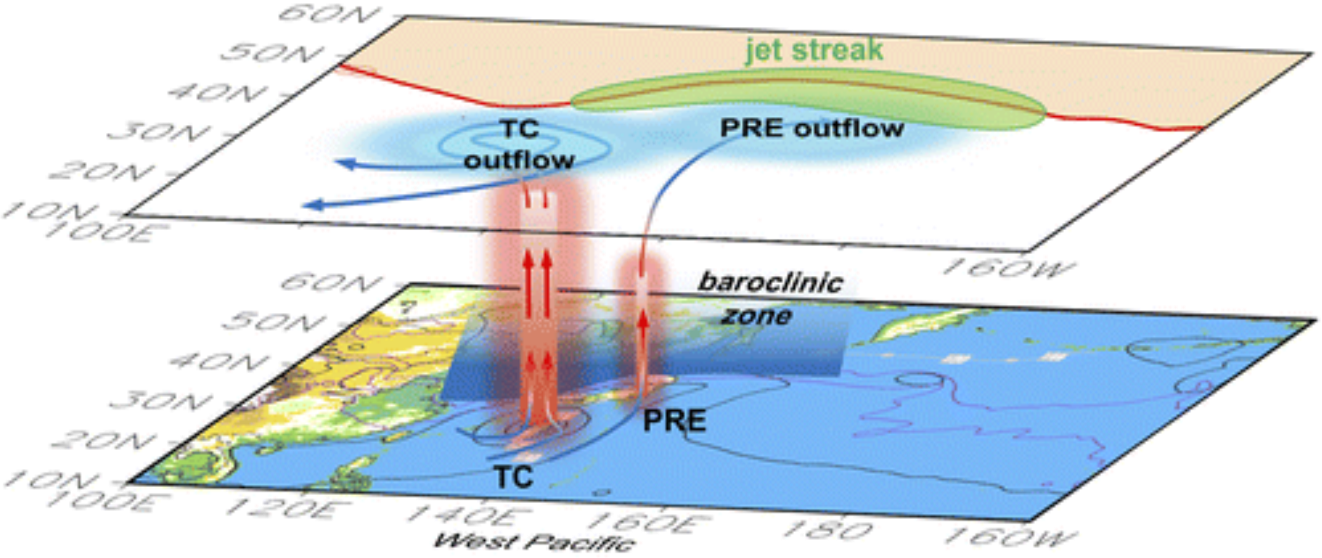

Predecessor Rain Events (PREs)

Keller et al. (2019)

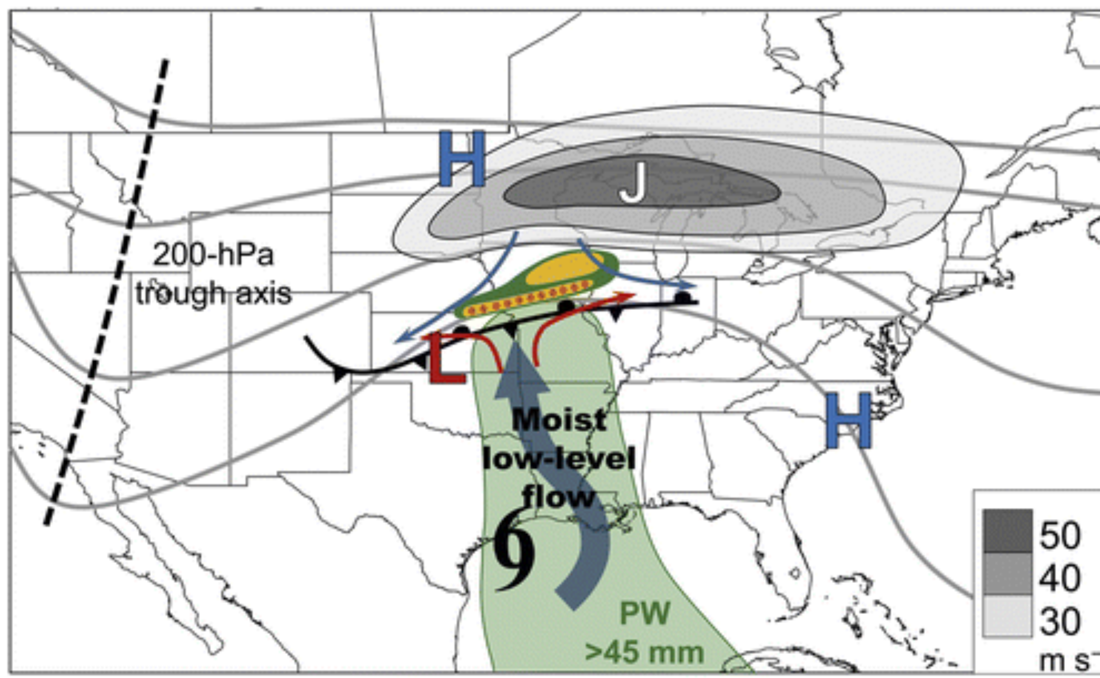

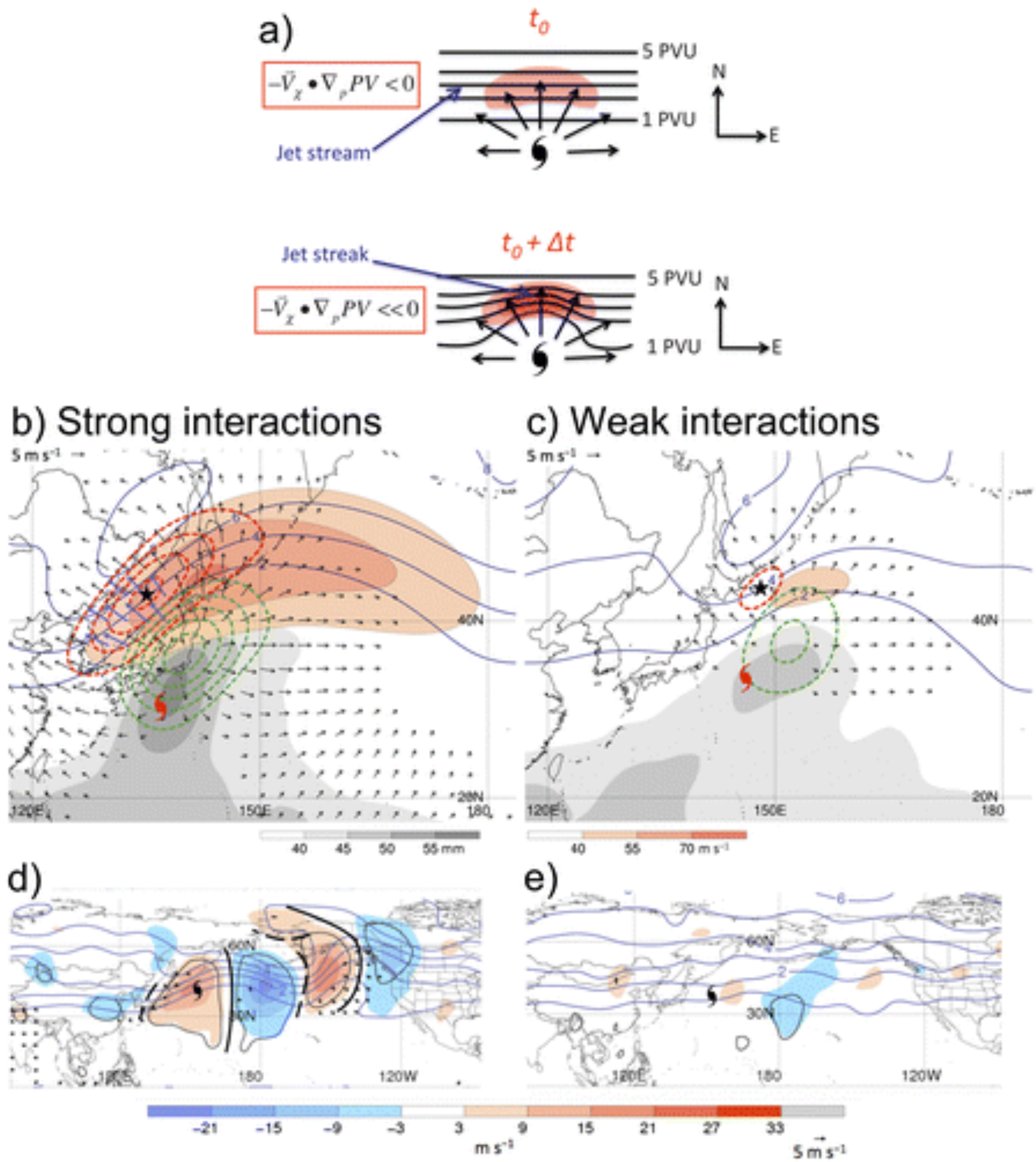

Keller et al. (2019)

Powell and Bell (2019)
ET of 2016 Hurricane
Matthew in NC/SC/VA

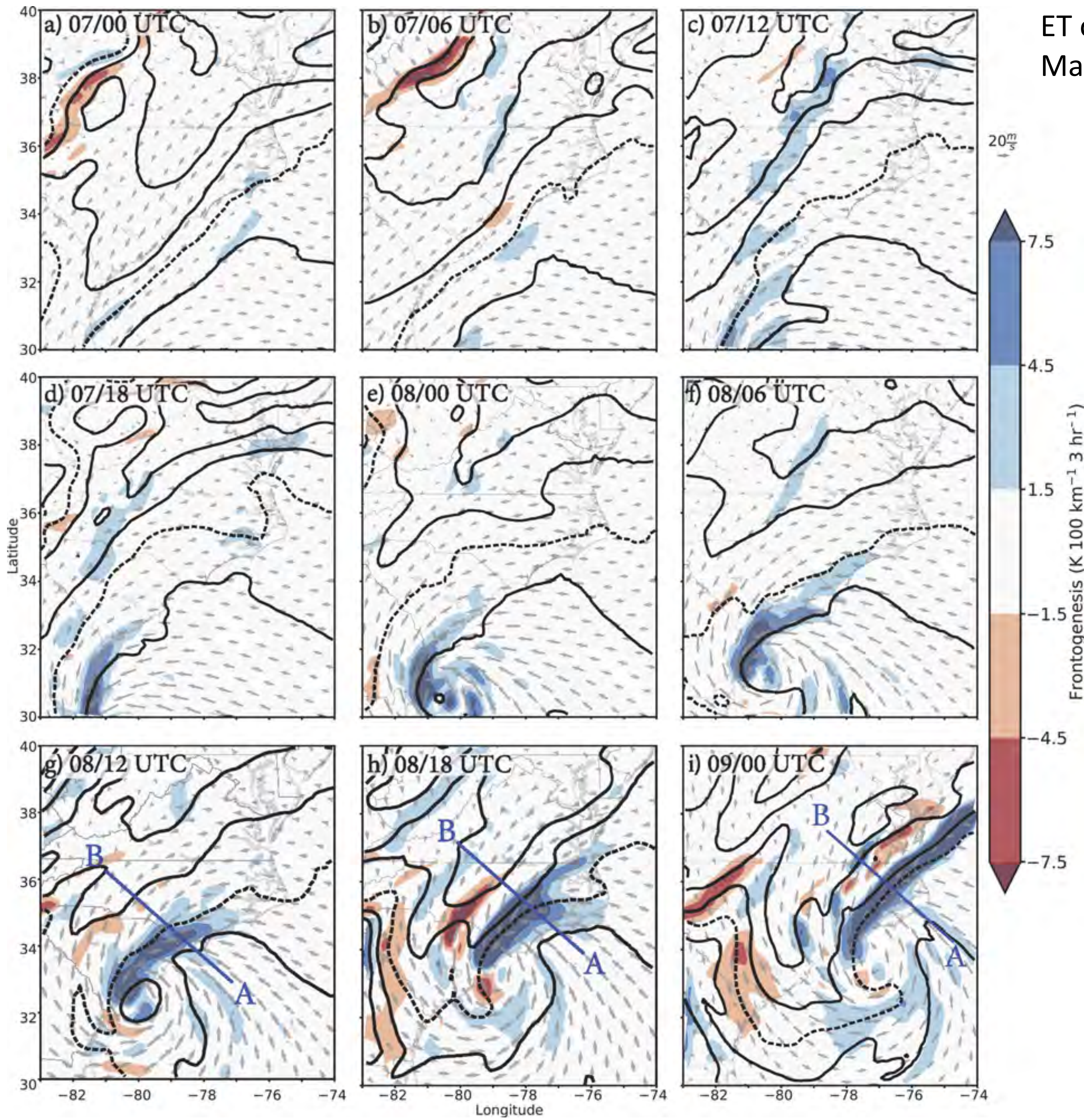

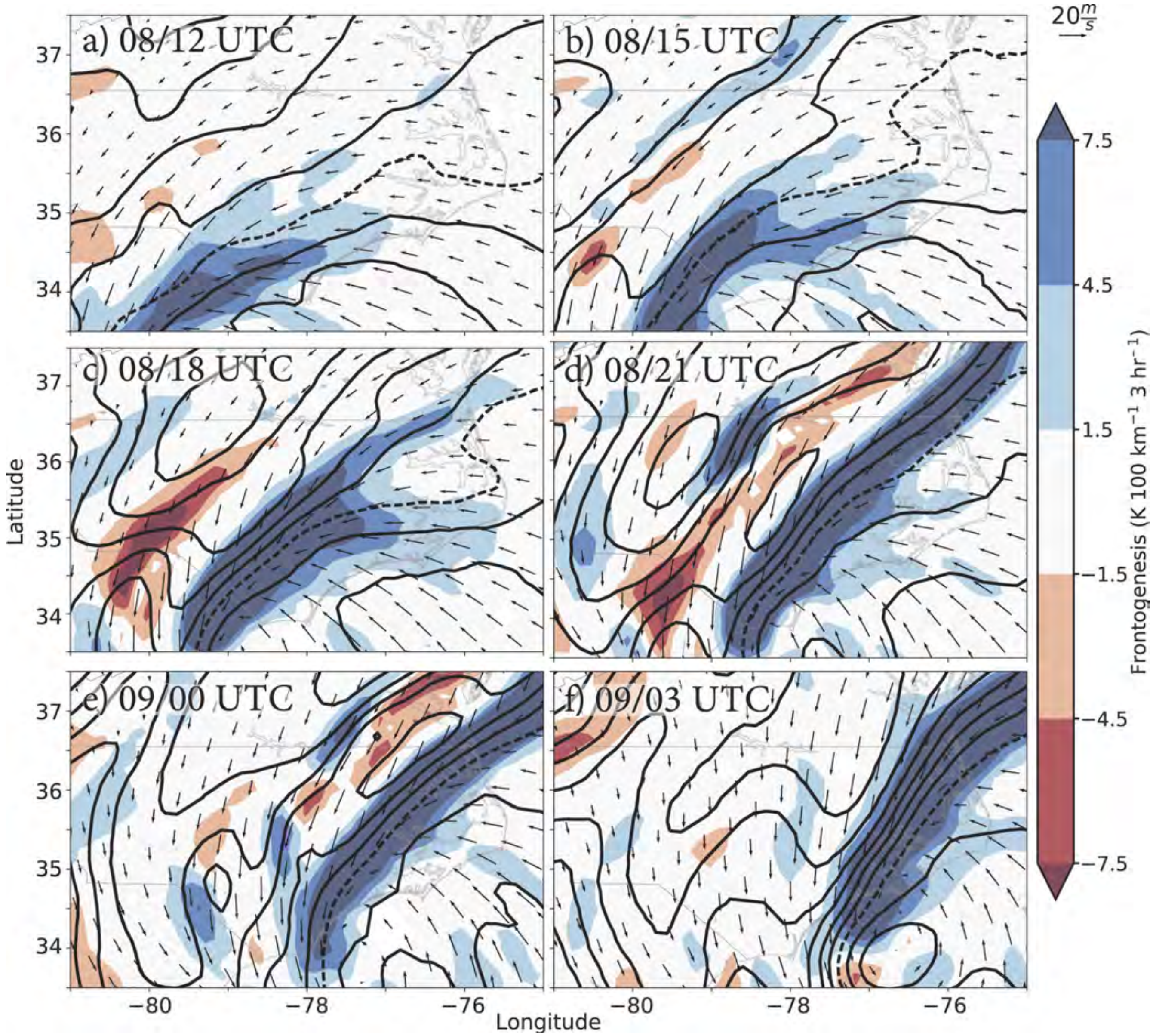

$$F = \frac{d}{dt}|\nabla_h \theta| \approx \frac{1}{|\nabla_h \theta|}\left\{\left[\left(\frac{\partial \theta}{\partial x}\right)^2 \frac{\partial u}{\partial x} + \left(\frac{\partial \theta}{\partial y}\right)^2 \frac{\partial v}{\partial y}\right] + \left[\frac{\partial \theta}{\partial x}\frac{\partial \theta}{\partial y}\left(\frac{\partial v}{\partial x} + \frac{\partial u}{\partial y}\right)\right]\right\}$$

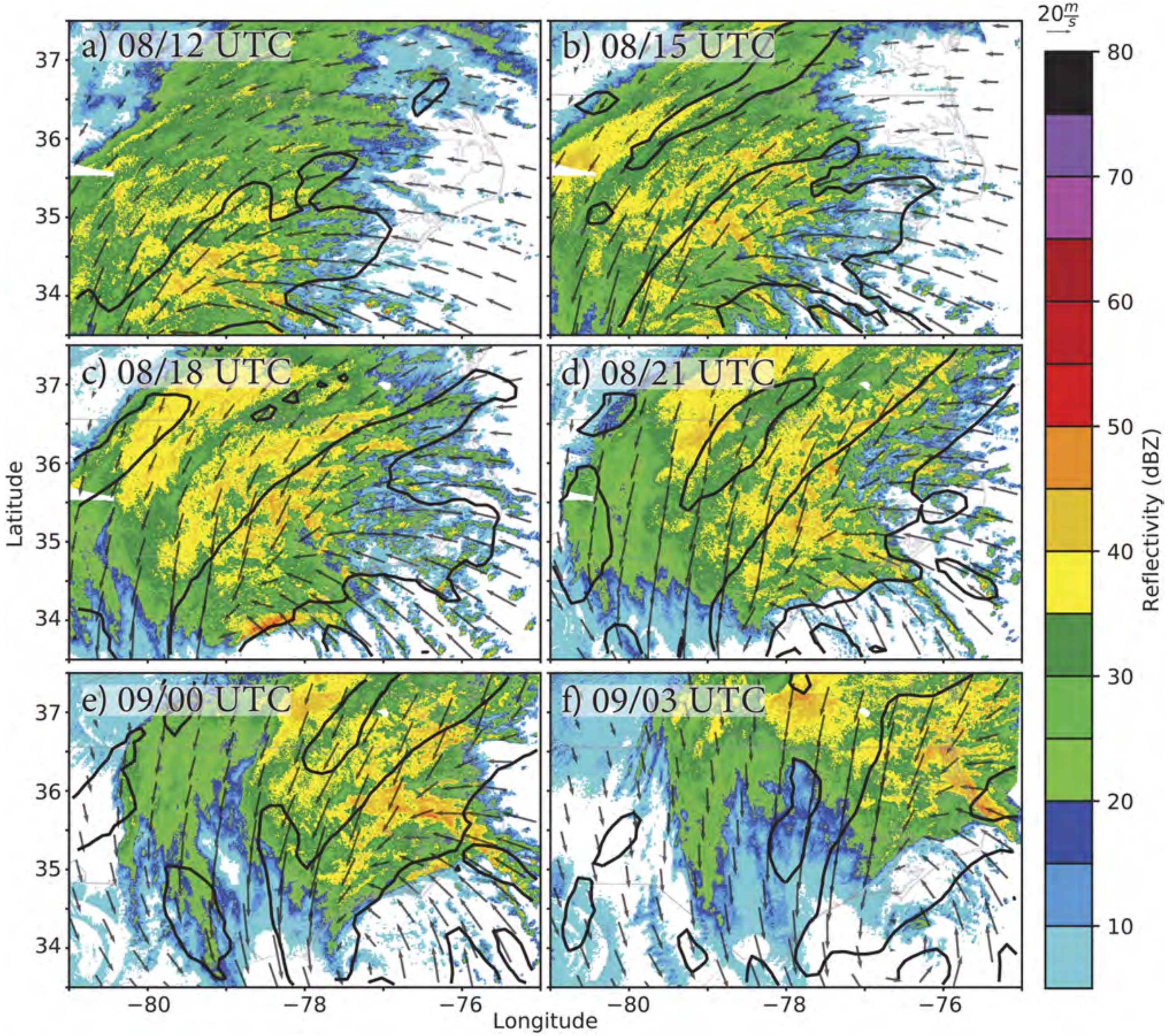

a) 08/12 UTC
b) 08/15 UTC
c) 08/18 UTC
d) 08/21 UTC
e) 09/00 UTC
f) 09/03 UTC
Latitude
Longitude
Reflectivity (dBZ)
$20\frac{m}{s}$

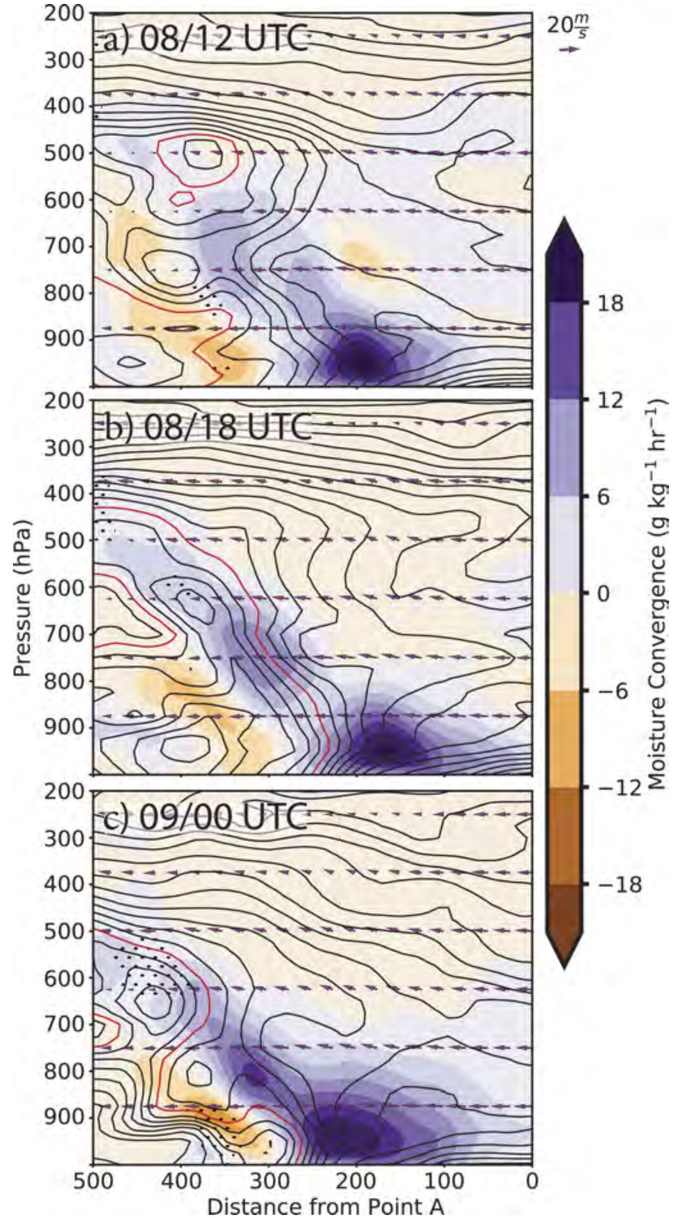

a) 08/12 UTC
b) 08/18 UTC
c) 09/00 UTC
Pressure (hPa)
Distance from Point A
$20\frac{m}{s}$
Moisture Convergence (g kg^{-1} hr^{-1})

MR3252: Tropical Meteorology

Tropical Cyclone Energetics

<u>Main Topics</u>:

- CISK and WISHE
- Maximum Potential Intensity
- TC idealized as a Carnot engine
- Radar observation of vortical hot tower

Module 3.5

Angular momentum in a tropical cyclone

- **Basic principle controlling tangential wind velocity - Conservation of absolute angular momentum:**

$$m = rv + \frac{fr^2}{2}$$

f = **Coriolis parameter**
= 2Ω sin(latitude)

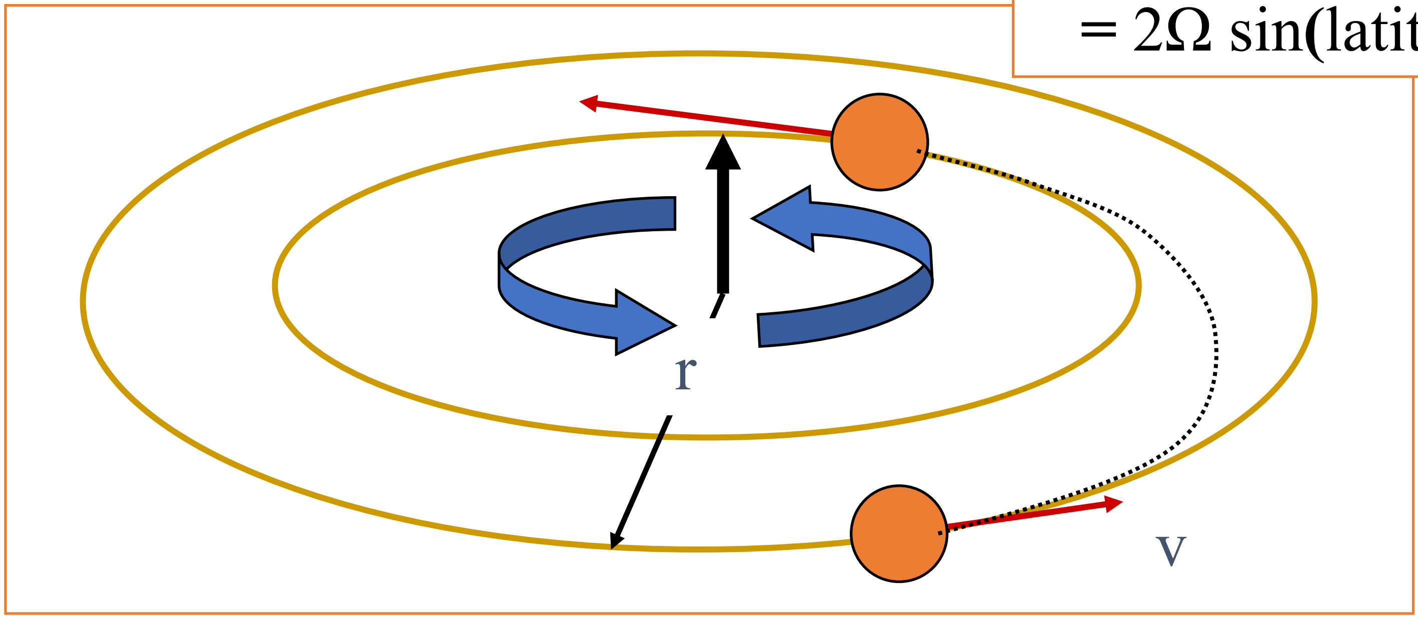

$$v = \frac{m}{r} - \frac{fr}{2}$$

If r **decreases,** v **increases!**

Spin up requires inflowing m surfaces

Montgomery and Smith (2014)

Conditional Instability of the Second Kind (CISK)

Conventional view of intensification

(Charney & Eliassen (CISK), Ooyama, Carrier)

Montgomery and Smith (2014)

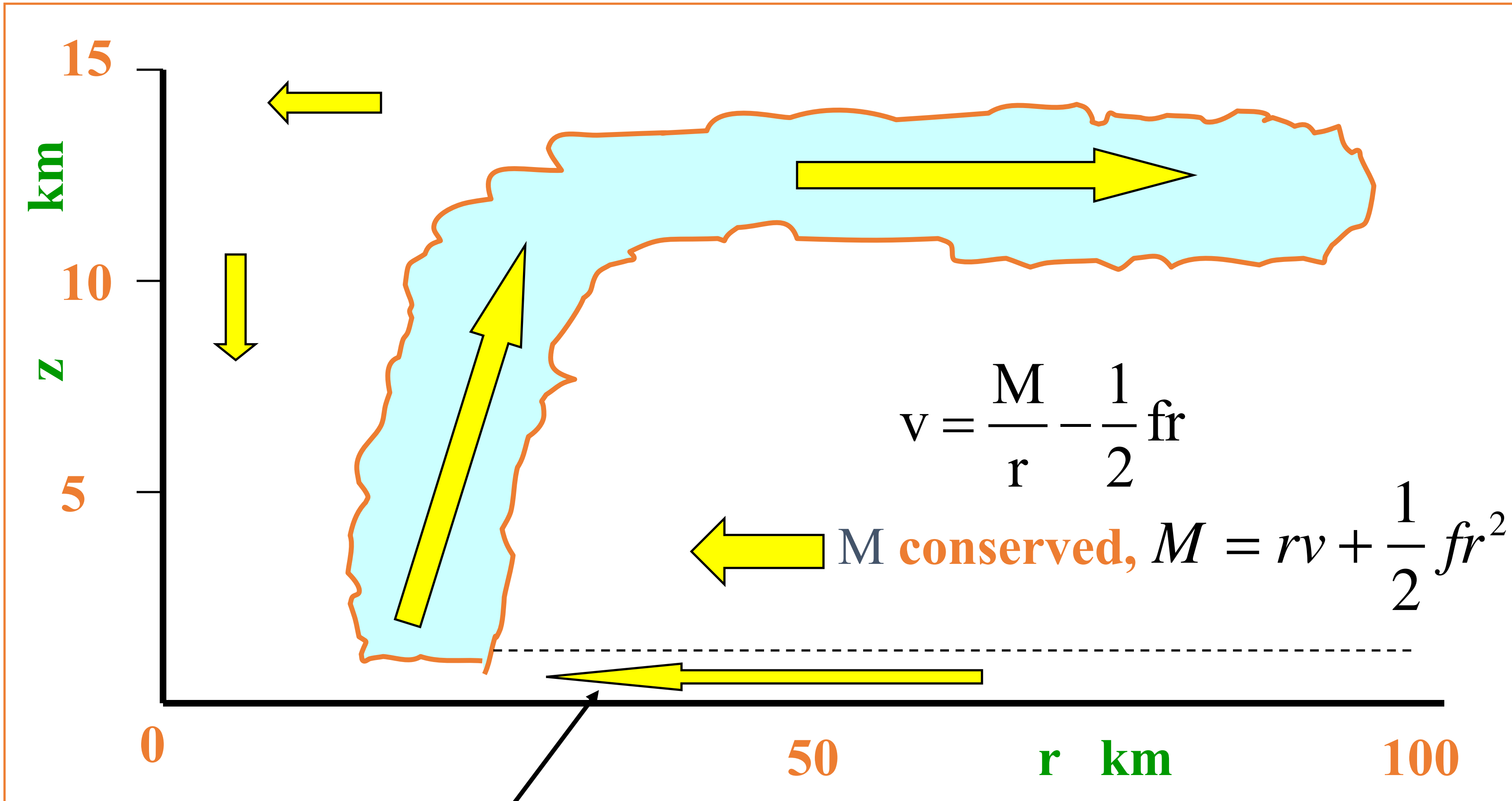

M not materially conserved,
boundary layer supplies clouds with moisture

Conventional view of intensification

(Charney & Eliassen (CISK), Ooyama, Carrier)

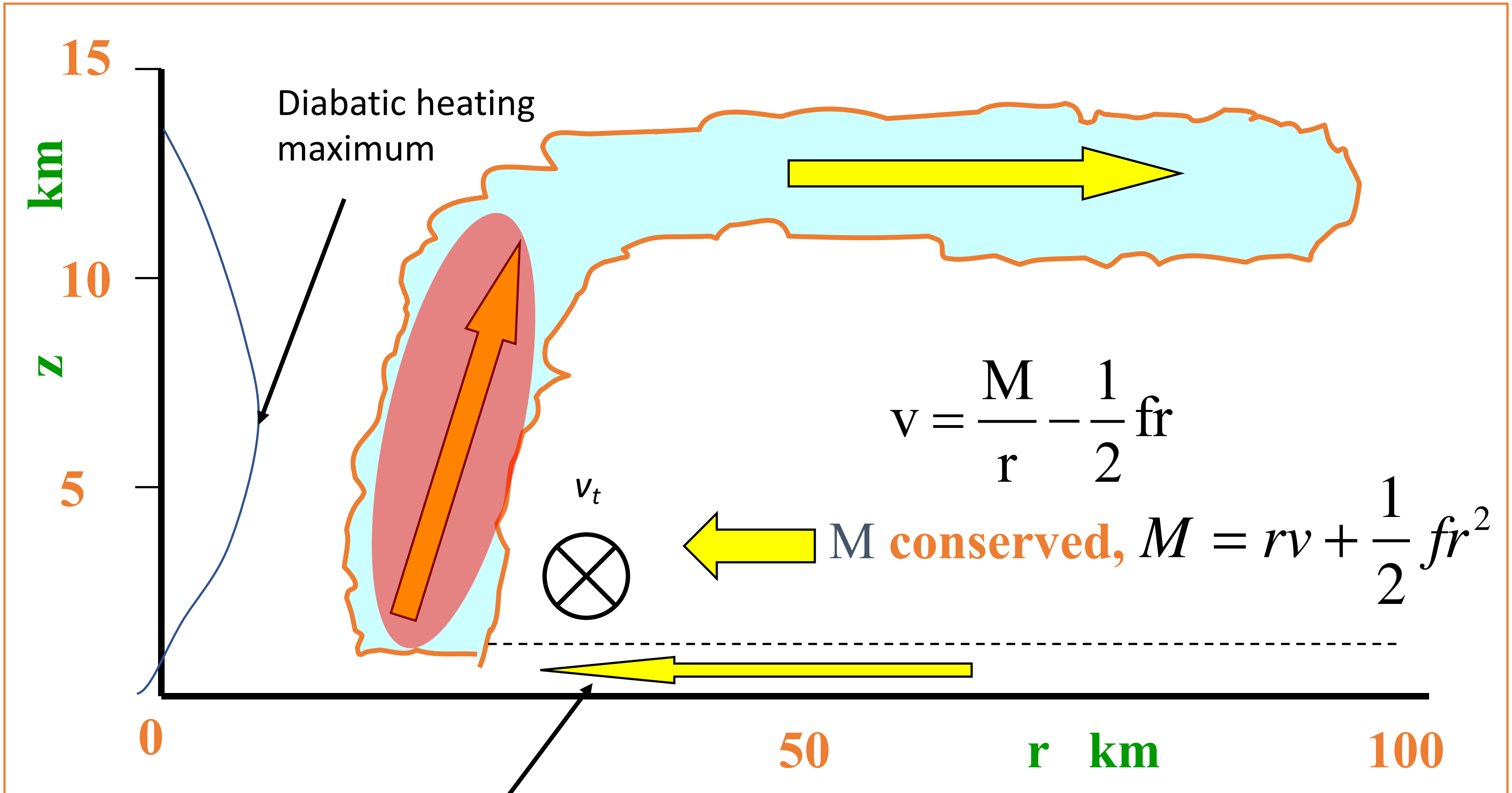

M not materially conserved,
boundary layer supplies clouds with moisture

Conventional view of intensification

(Charney & Eliassen (CISK), Ooyama, Carrier)

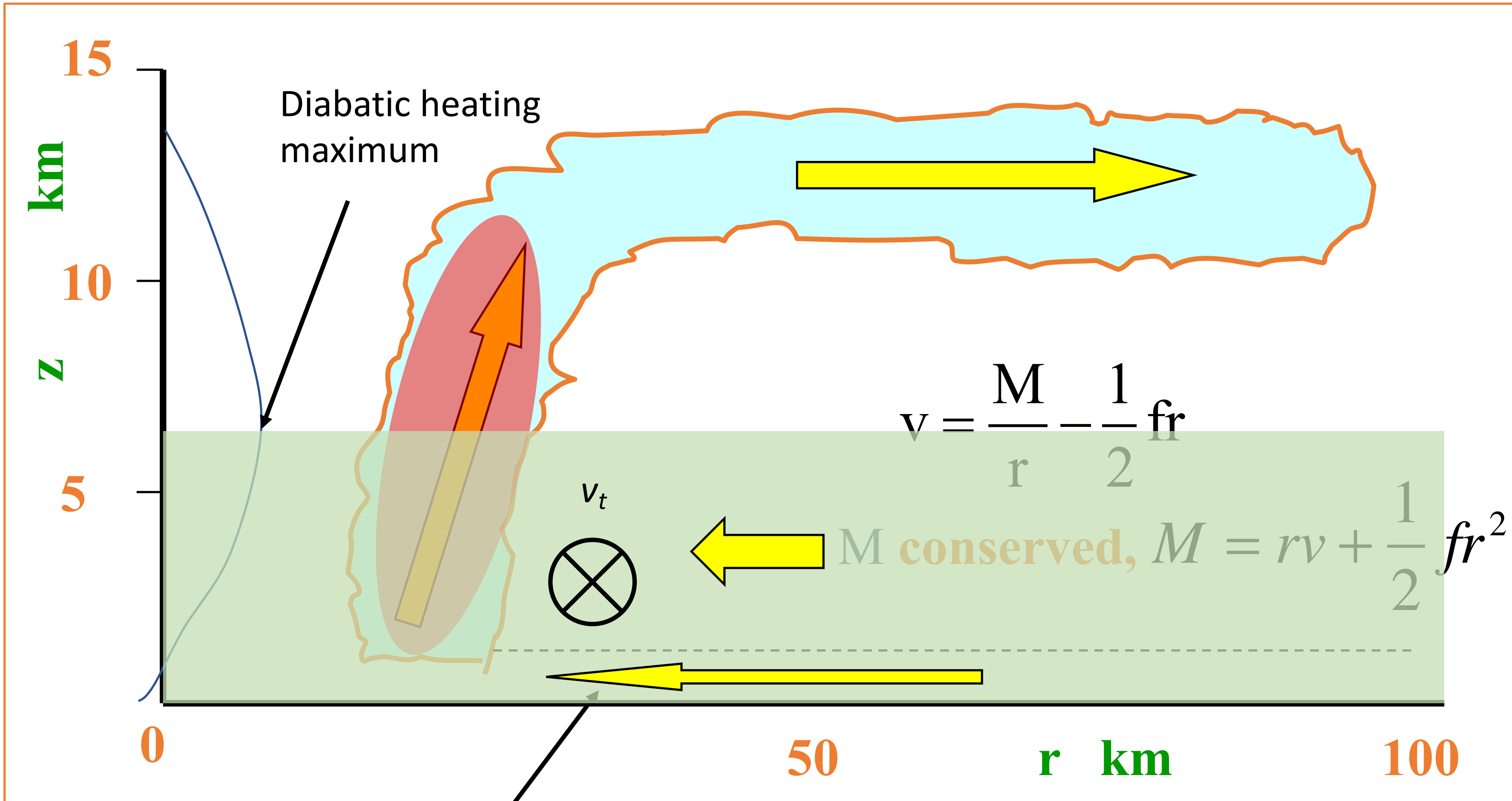

M **not materially conserved,**
boundary layer supplies clouds with moisture

Conventional view of intensification

(Charney & Eliassen (CISK), Ooyama, Carrier)

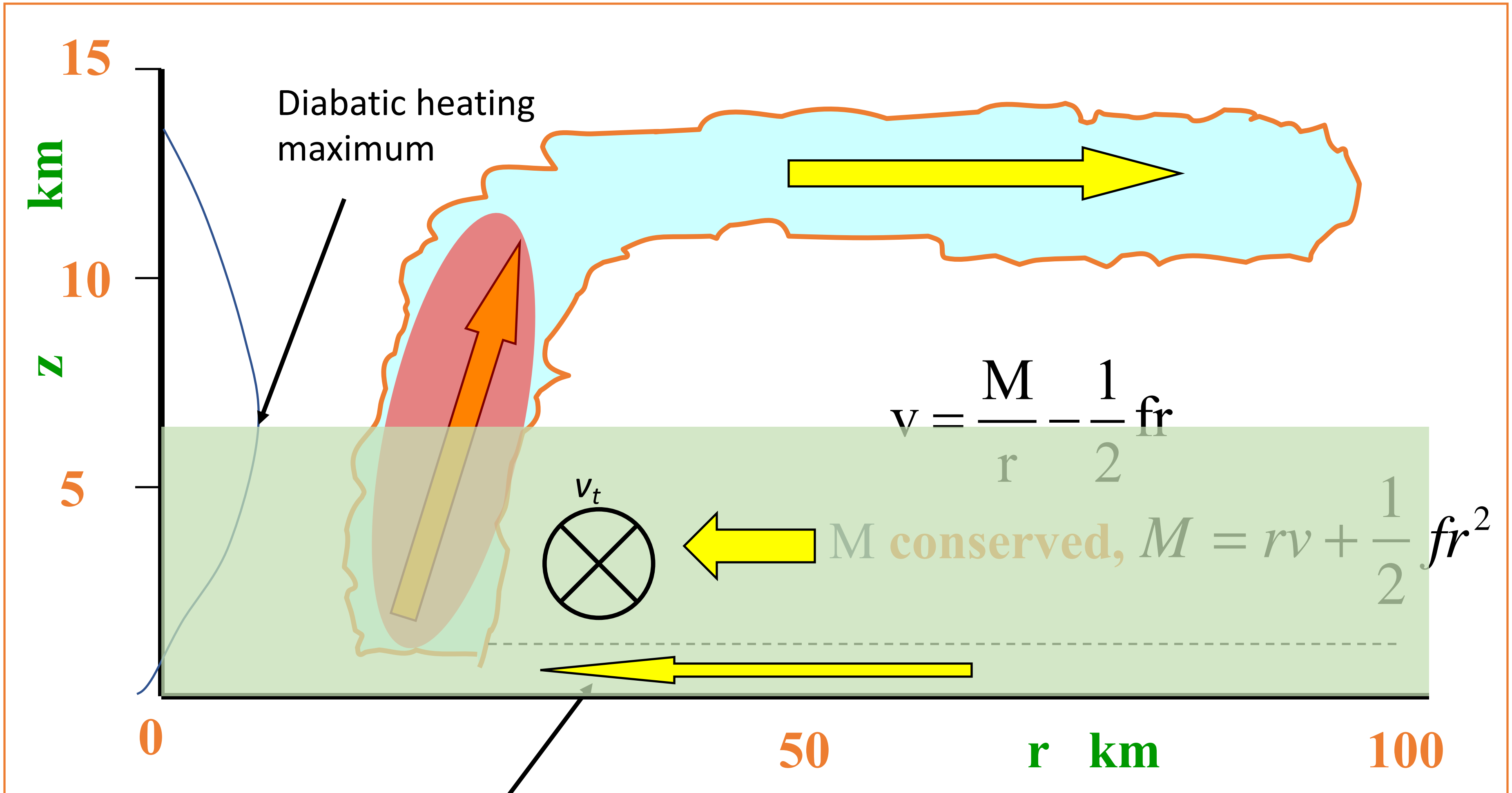

M **not materially conserved,**
boundary layer supplies clouds with moisture

Conventional view of intensification

(Charney & Eliassen (CISK), Ooyama, Carrier)

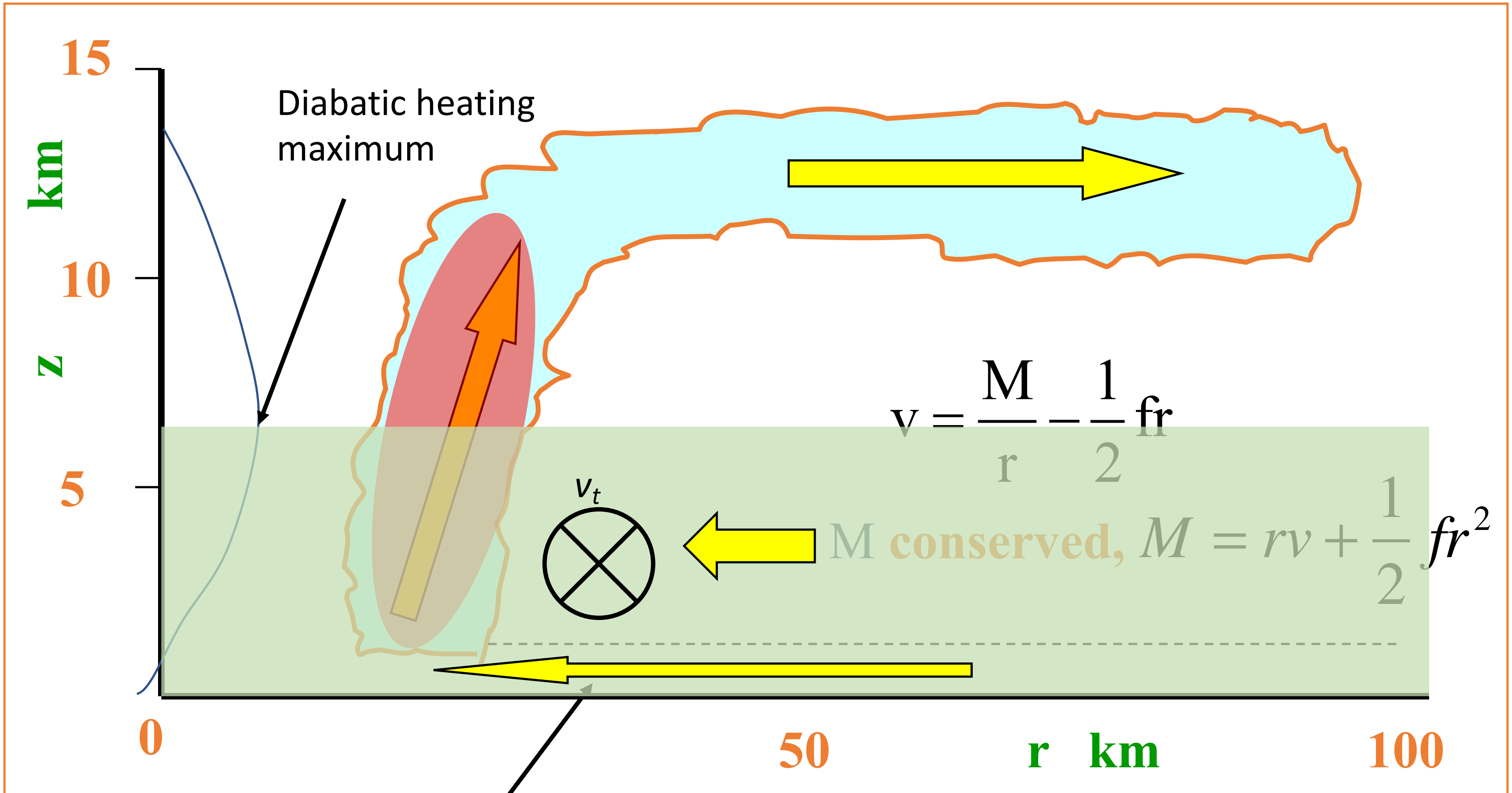

M **not materially conserved,**

boundary layer supplies clouds with moisture

CISK Steps (in a nutshell)

- Diabatic heating and its gradient largest in mid-troposphere.
- Inflow beneath dQ/dr maximum.
- Coriolis force acting on inflow in secondary circulation enhances tangential wind.
- Enhanced tangential wind increases frictional inflow in BL and increases moisture convergence.
- Implied increase in latent heating and dQ/dr, which increases strength of low-level inflow.

- **WISHE = Wind Induced Surface Heat Exchange**

- **Acronym used to link source of fluctuations in sub-cloud layer entropy or θ_e arising from fluctuations in wind speed (Yano & Emanuel 1991)**

- **Q: What is the WISHE mechanism of TC intensification?**

- **A:``… intensification proceeds through a feedback mechanism wherein increasing surface wind speeds produce increasing surface enthalpy flux ..., while the increased heat transfer leads to increasing storm winds.” (Emanuel 2003)**

Answer:

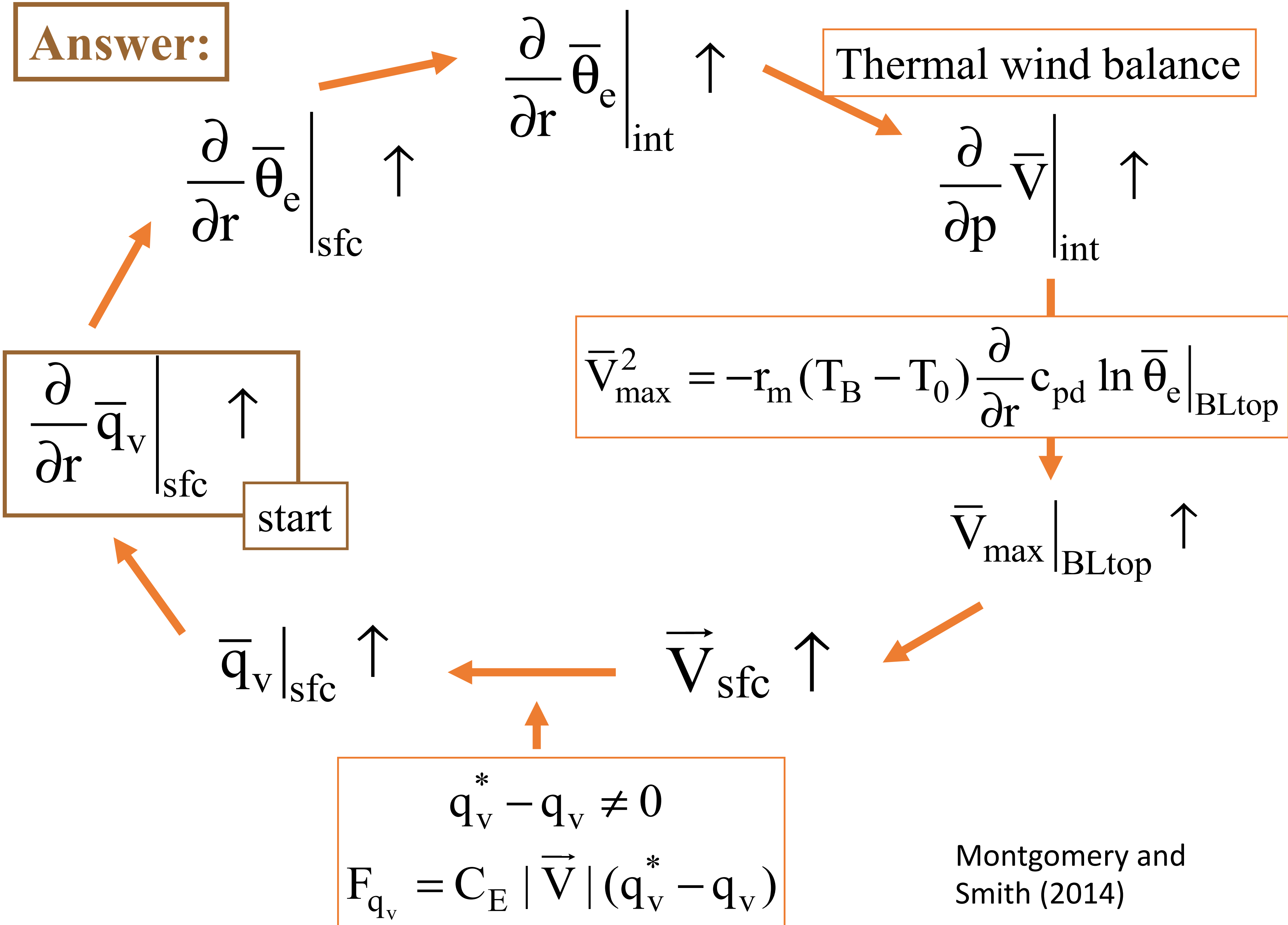

Montgomery and Smith (2014)

Surface Fluxes

Two types of surface fluxes: Latent and sensible heat fluxes

Latent heat flux: Heat flux between atmosphere and surface associated with phase change of water. For example, evaporation of ocean water into the atmosphere would be a positive flux of latent heat to the atmosphere.

Sensible heat flux: Conductive heat flux between surface and atmosphere. If the surface is warmer than the surface-layer of the atmosphere, then the sensible heat flux to the atmosphere will be positive.

$$L = \rho L_v C_q U(q_s - q)$$

$$S = \rho c_p C_h U(\theta_s - \theta)$$

The *C* variables are exchange coefficients that are dependent on conditions at the air-sea interface.

Both fluxes are functions of wind, and the subscript *s* indicates the conditions of the ocean. q_s is the saturation specific humidity associated with air with the same temperature as the sea surface.

Montgomery et al. (2015)

Red = normal fluxes

Green = Surface wind speed capped in flux equations at 10 m/s

Blue = … @ 5m/s

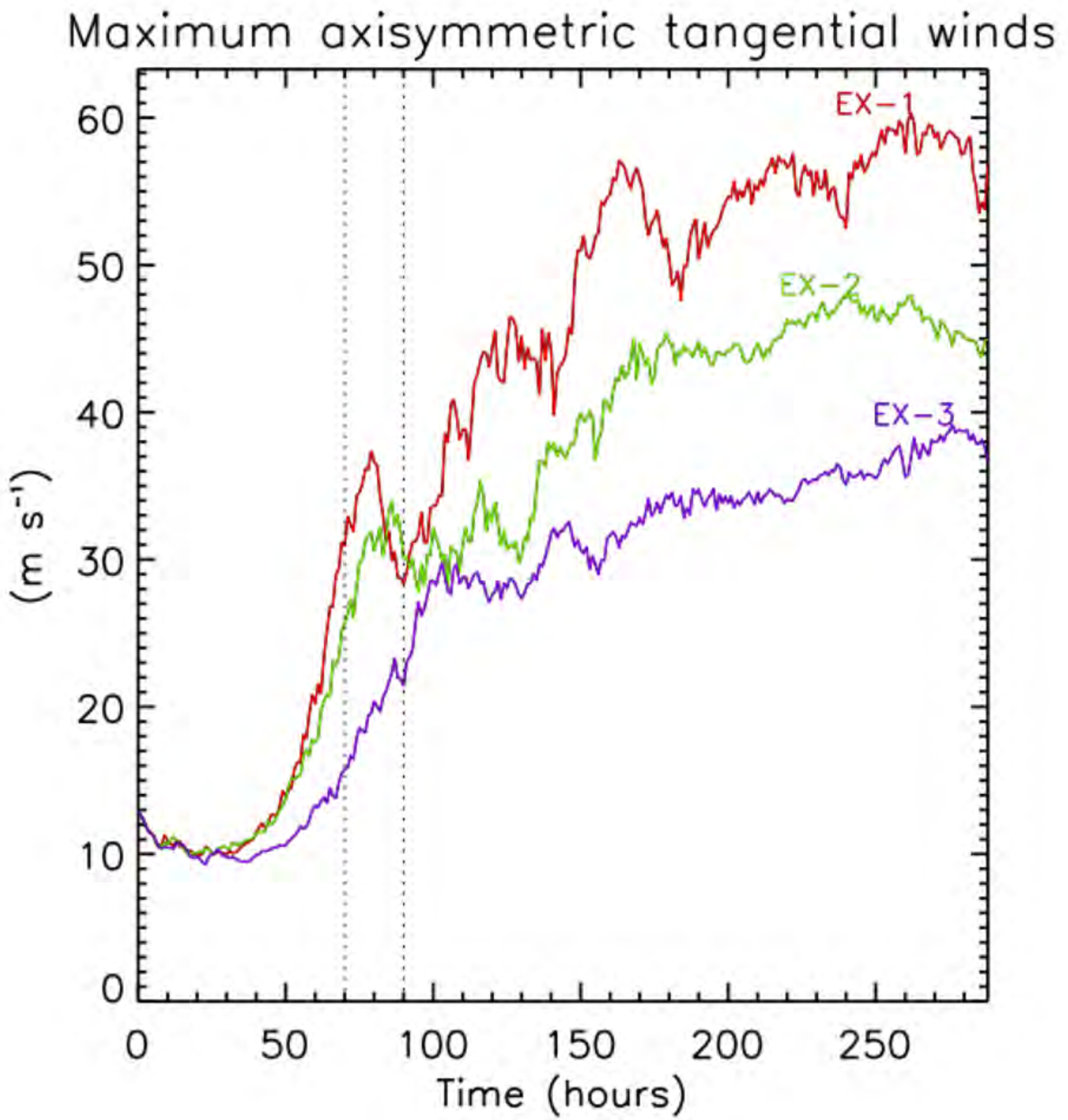

Figure 1. Time series of maximum tangential winds from the control "EX-1" and the capped flux experiments "EX-2" and "EX-3" (see text). Two vertical, dotted lines show times noted below to represent rapid intensification; 70 h for EX-1 and EX-2 and 90 h for EX-3.

Vortical Hot Towers

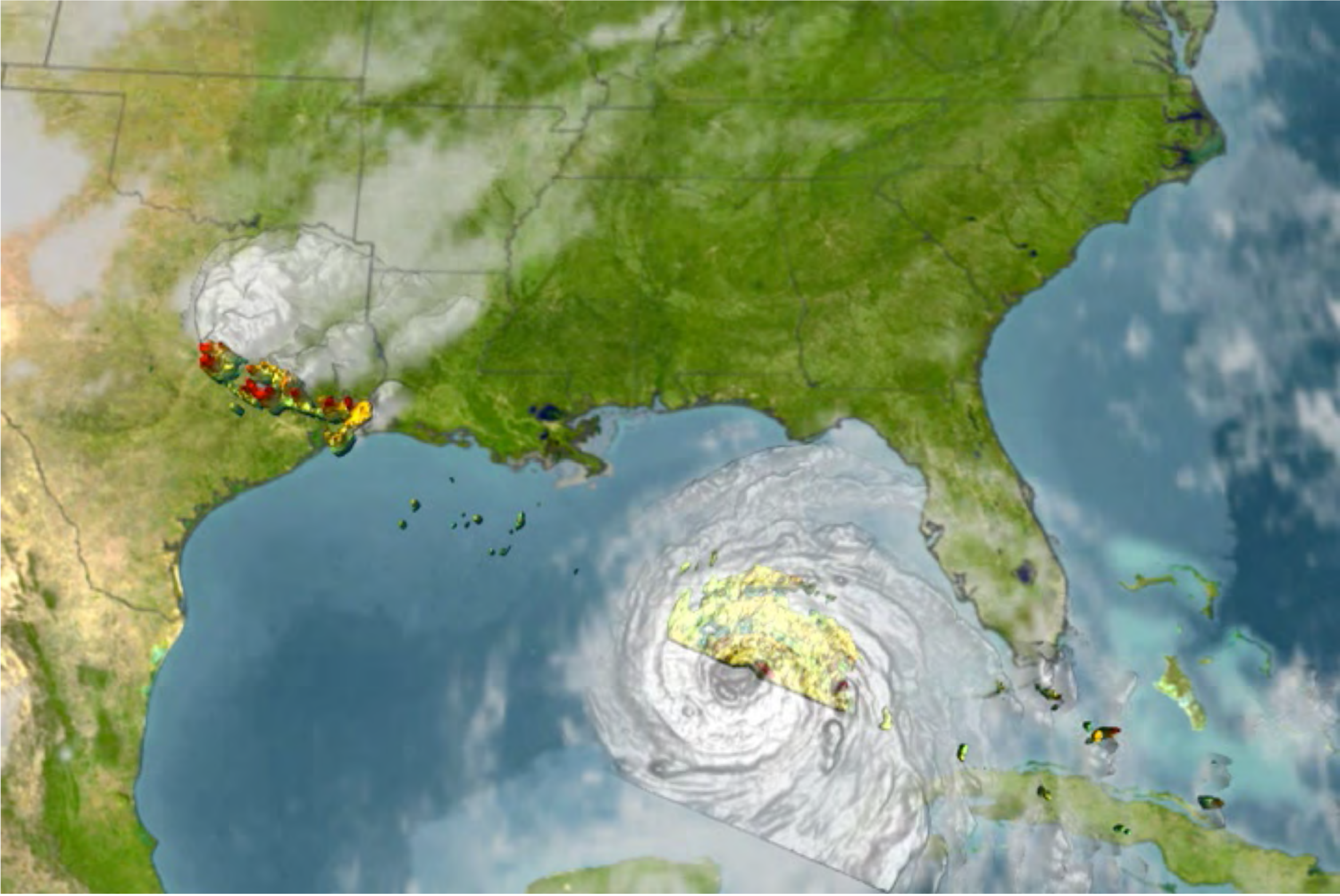

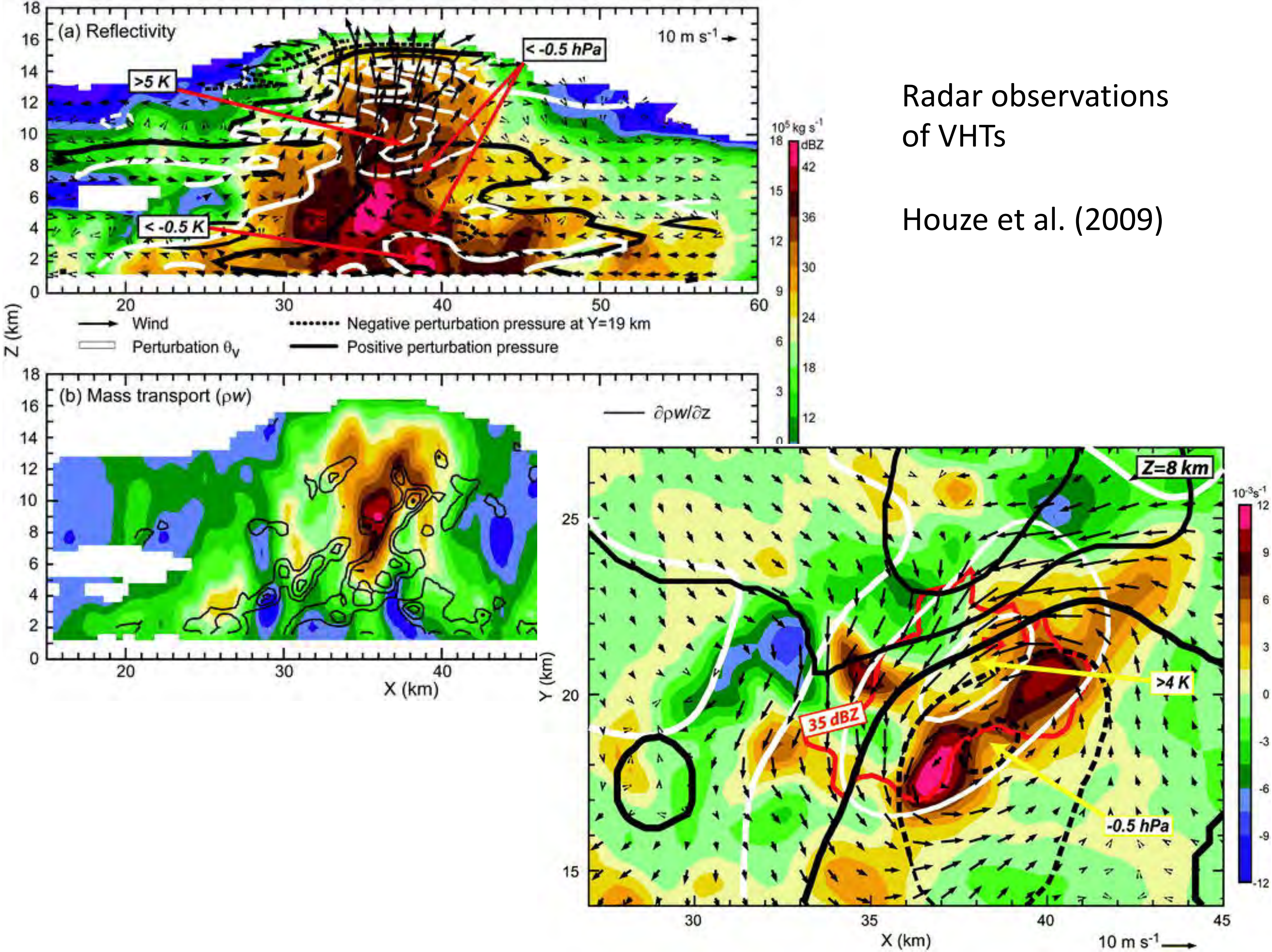

Radar observations of VHTs

Houze et al. (2009)

Maximum Potential Intensity Theory

What is the maximum intensity a TC can achieve?

- Emanuel (1988, 1995) developed a steady-state theory of the maximum intensity of axisymmetric tropical cyclones
- Based on Carnot Heat Engine
- Set energy production from ocean equal to energy lost by dissipation in eyewall region
- ${V_s^*}^2 = \frac{C_k}{C_d}(T_s - T_o)(k_s^* - k_a)$
    - C_k: enthalpy exchange coefficient
    - C_d: drag coefficient
    - T_s: sea surface temperature
    - T_0: outflow temperature
    - k_s*: saturation enthalpy at ocean surface
    - k_a: enthalpy of unsaturated air just above ocean surface

Ideal Carnot Cycle of Tropical Cyclone

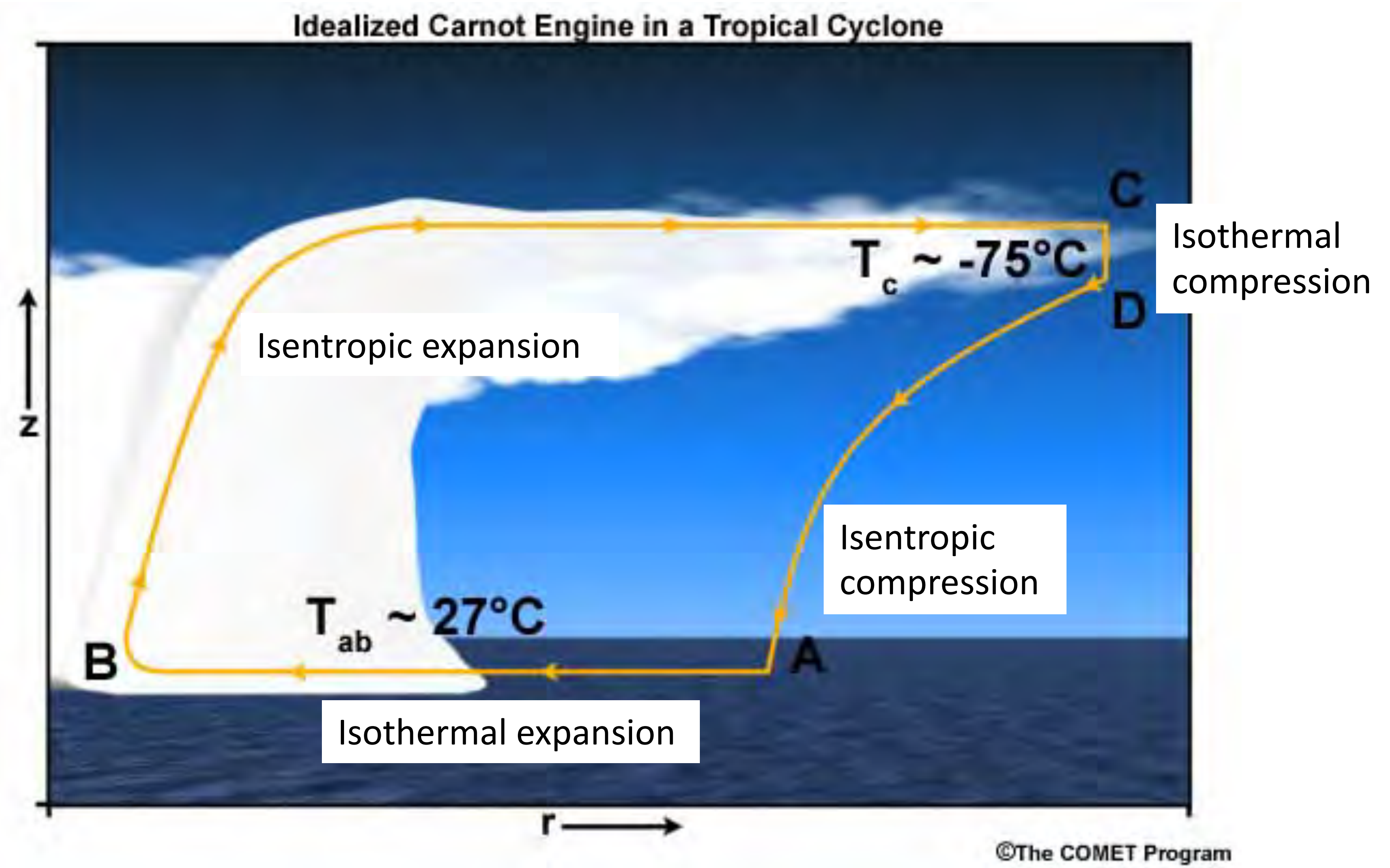

Maximum Potential Intensity Maps

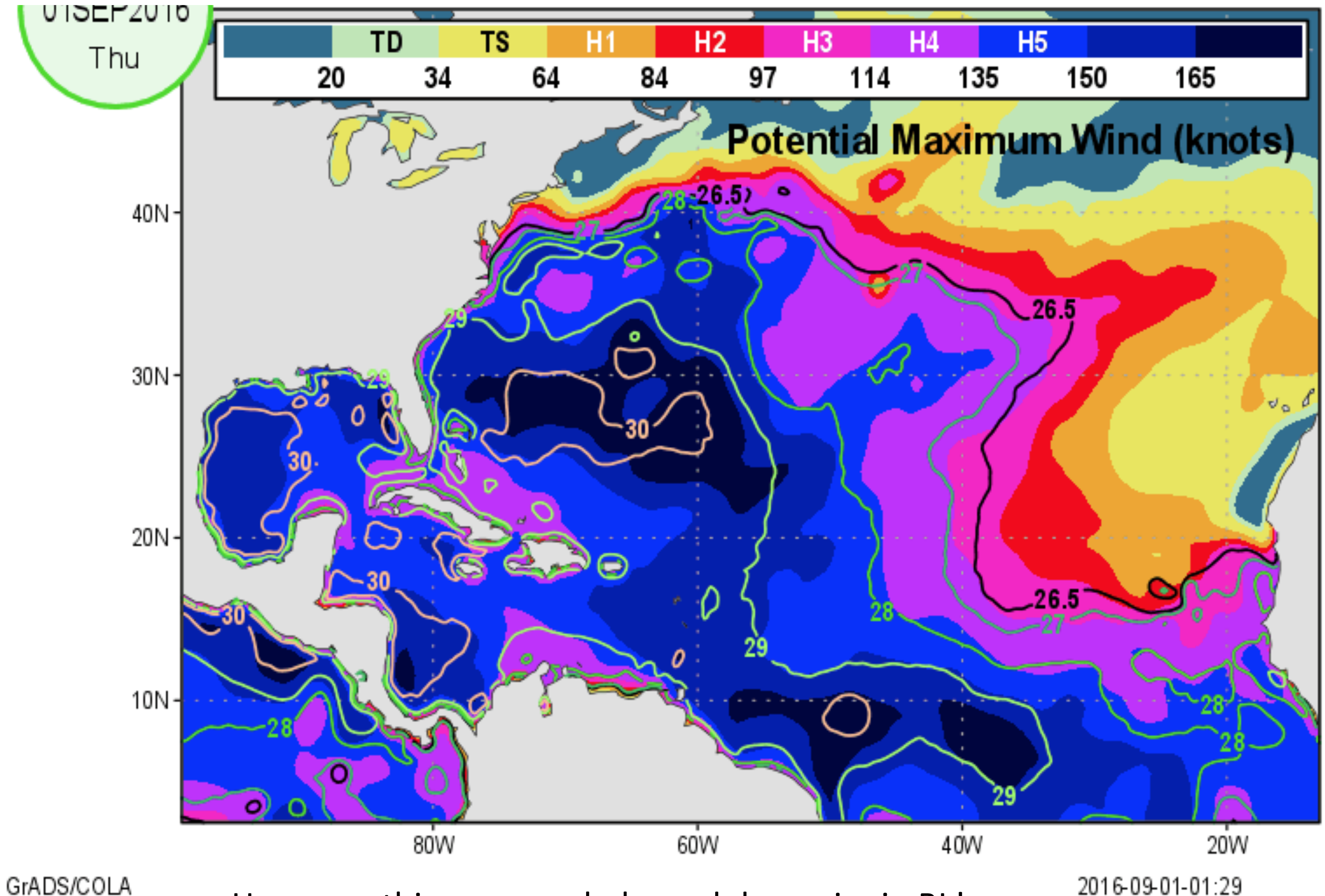

However, this assumes balanced dynamics in BL!

Hurricane max intensity in sea-surface temperature (Ts) and outflow temperature (To) space

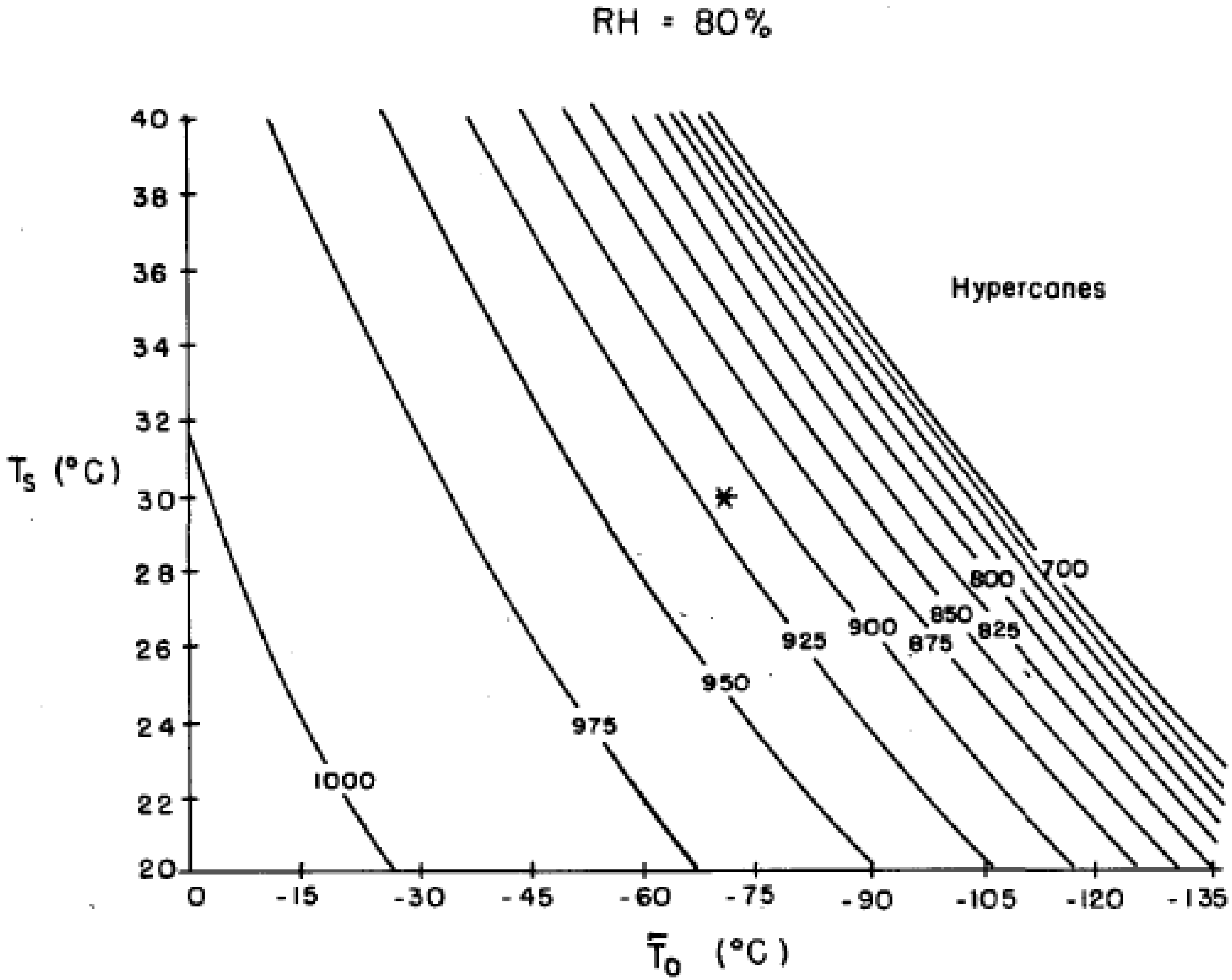

Smith et al. (2008)

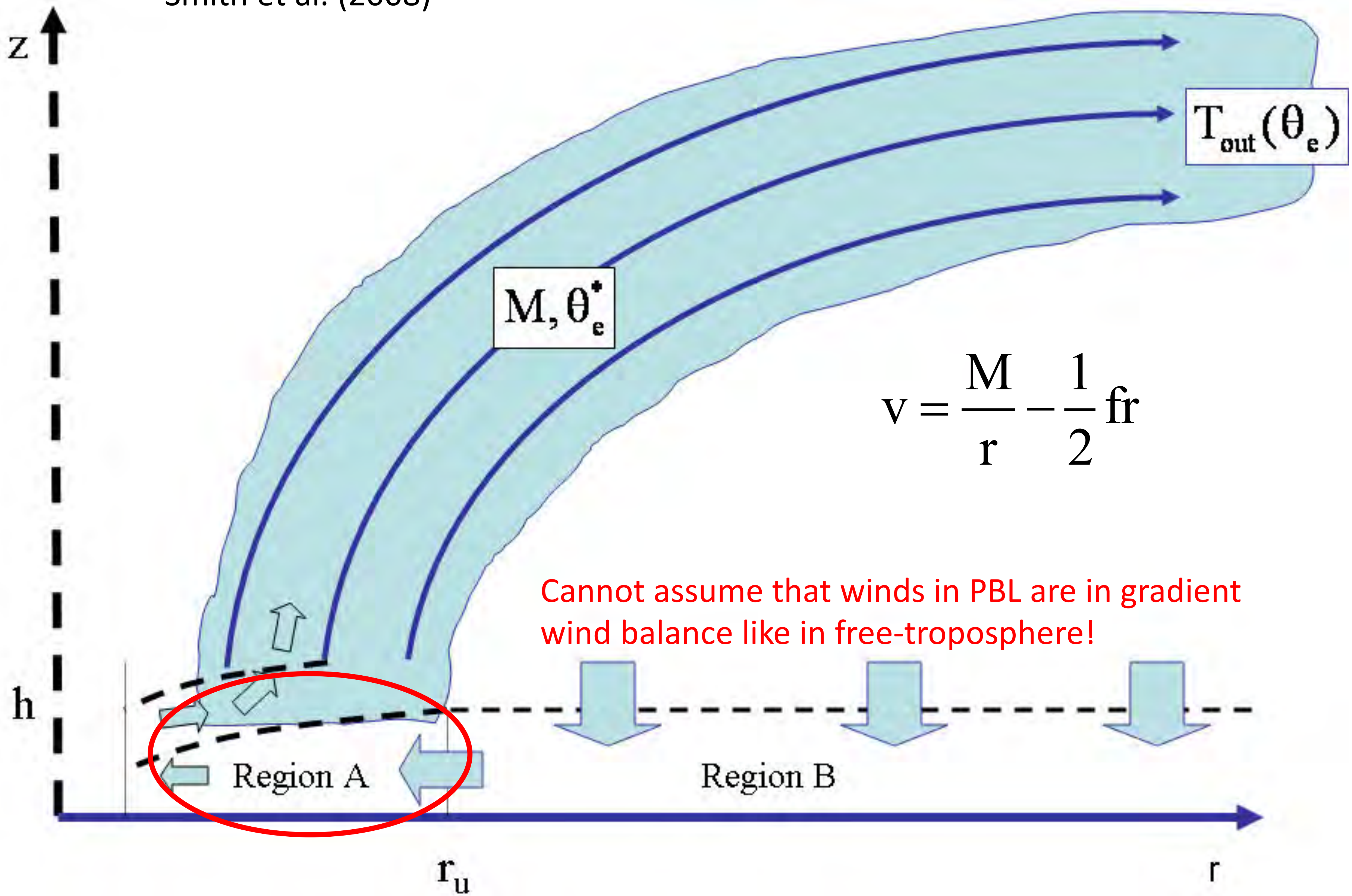

Cannot assume that winds in PBL are in gradient wind balance like in free-troposphere!

MR3252: Tropical Meteorology

Easterly Waves: Description and Locations

Figure: Alaka (2014)

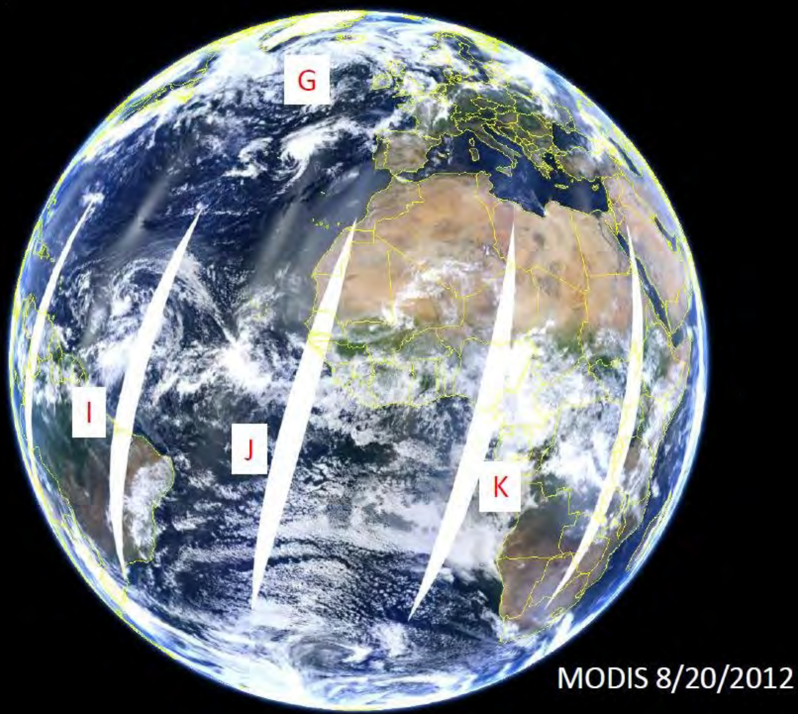

Main Topics:

- Easterly wave location
- Easterly wave structure
- African easterly waves
- African easterly jet

Module 3.6

2–6 day periodicity depending on zonal scale

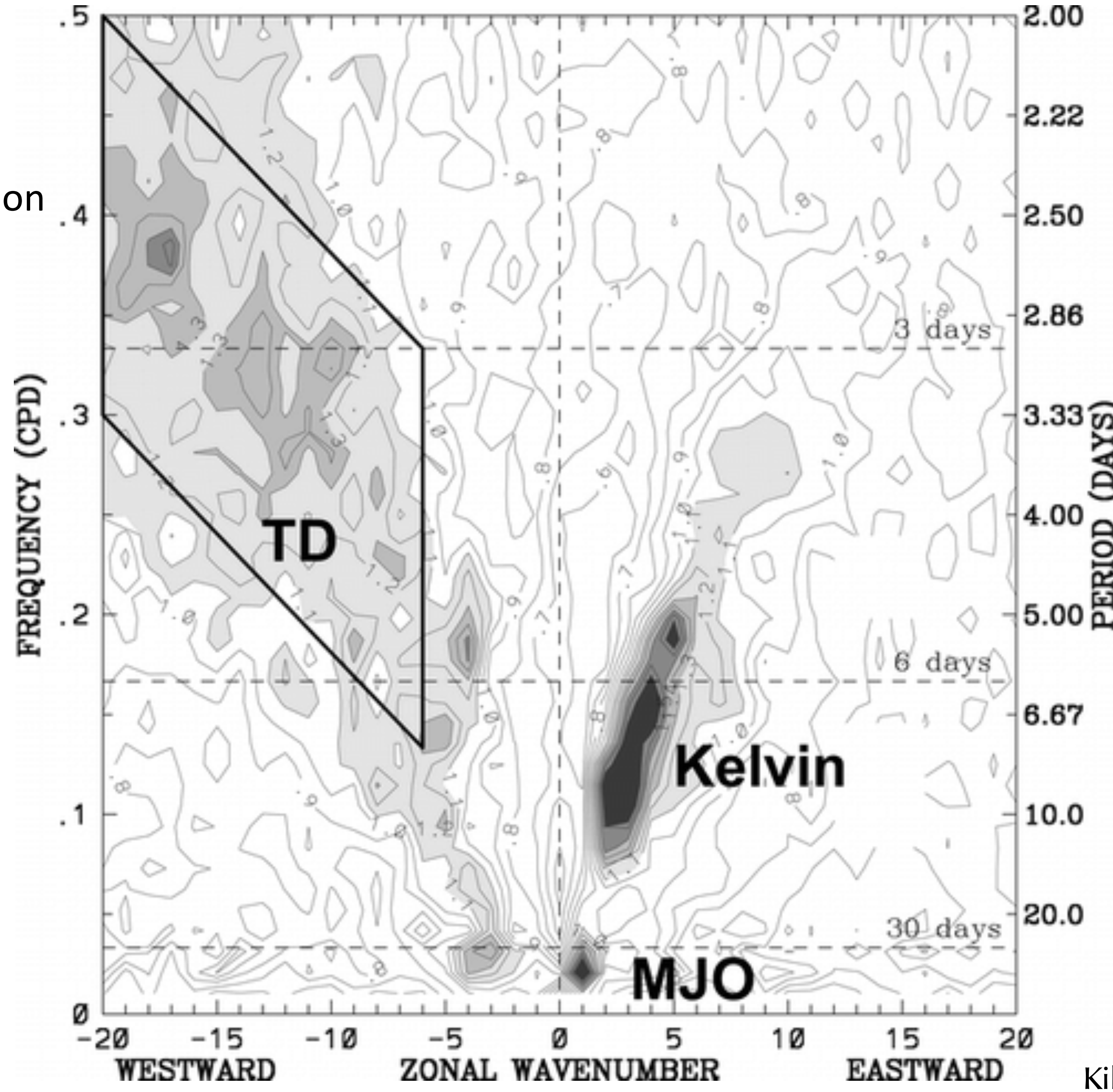

Kiladis et al. (2006)

East Pacific

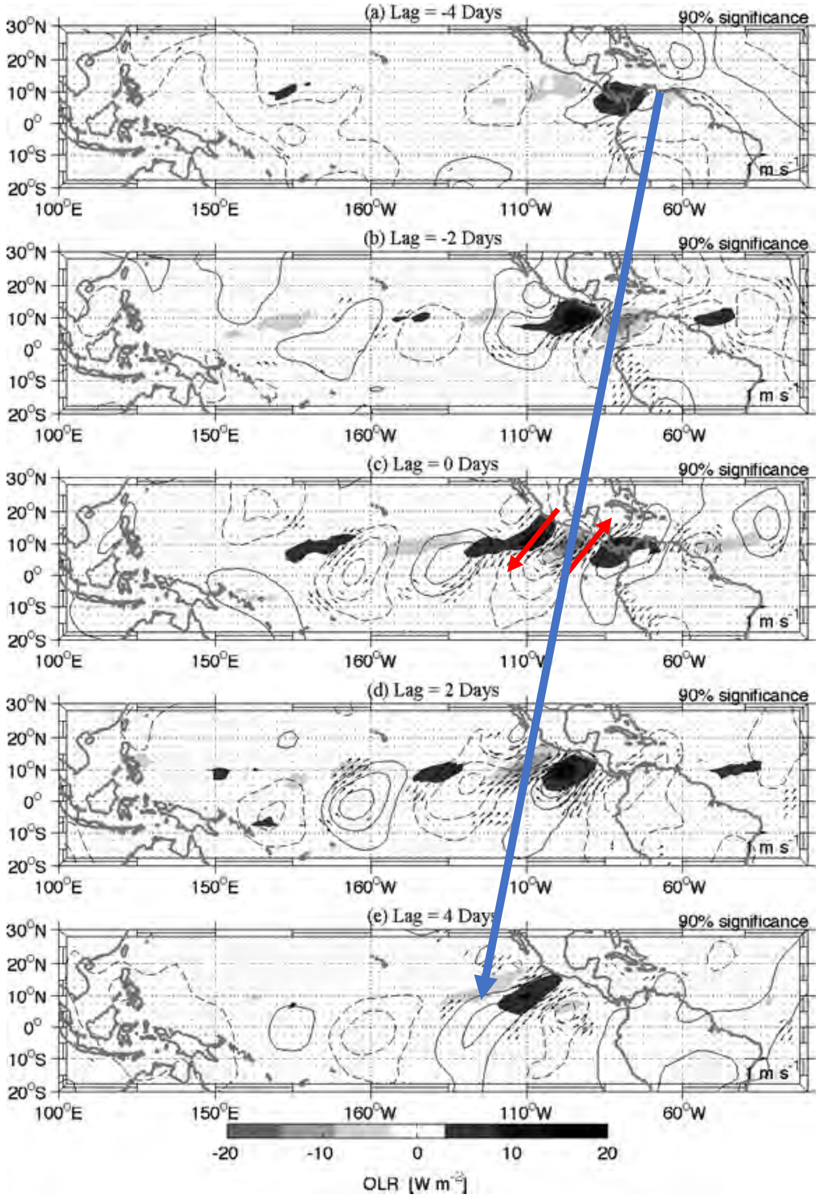

West Pacific

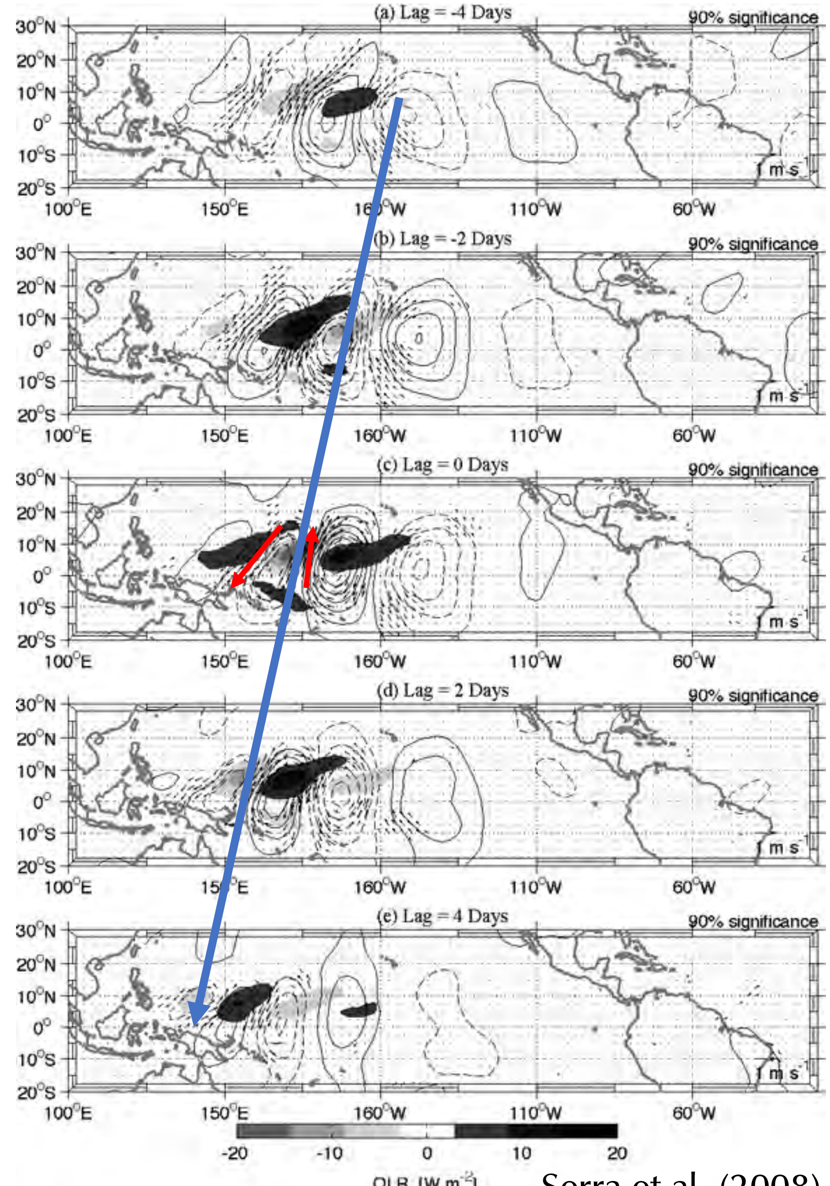

Serra et al. (2008)

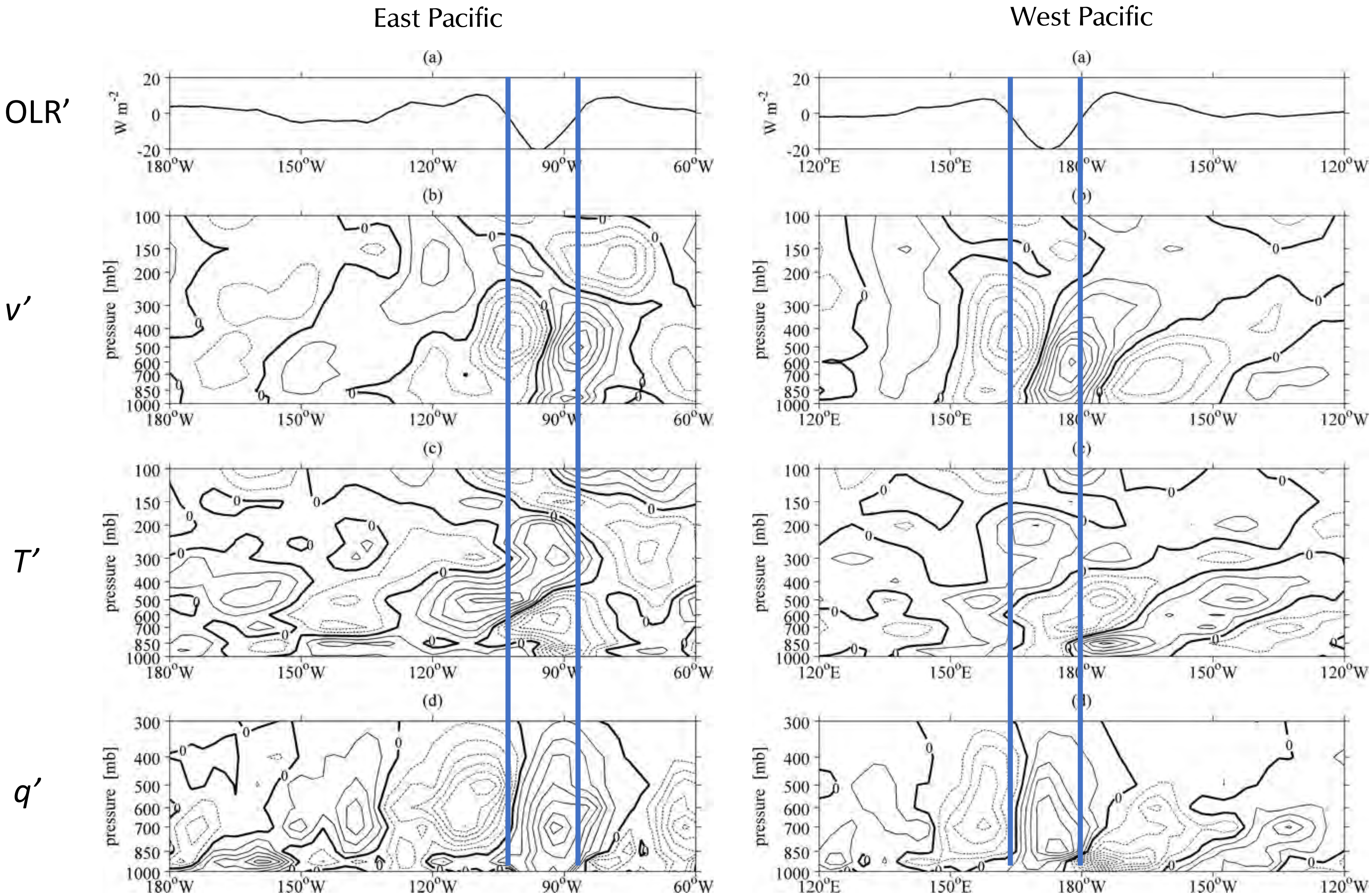

Serra et al. (2008)

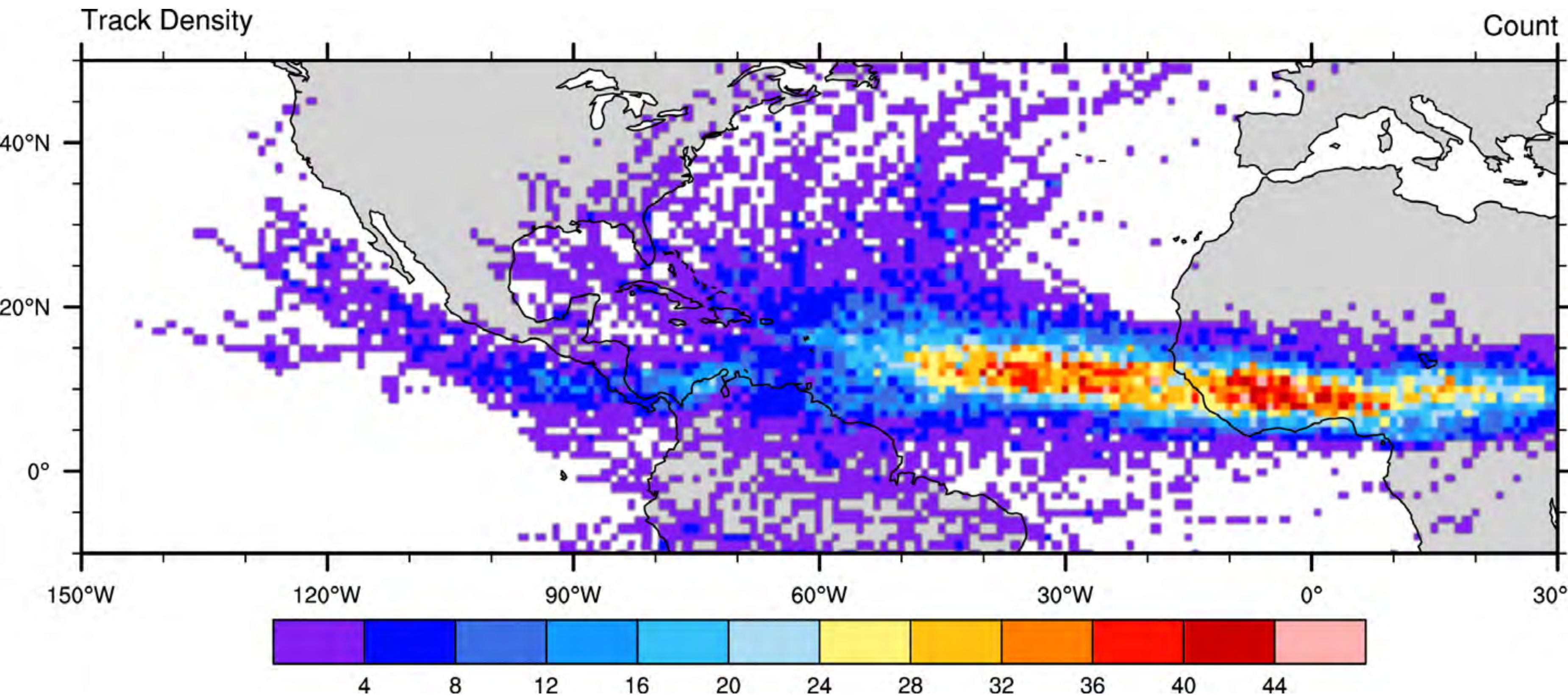

Brammer and
Thorncroft (2015)

Easterly Wave Genesis over East Pacific also!

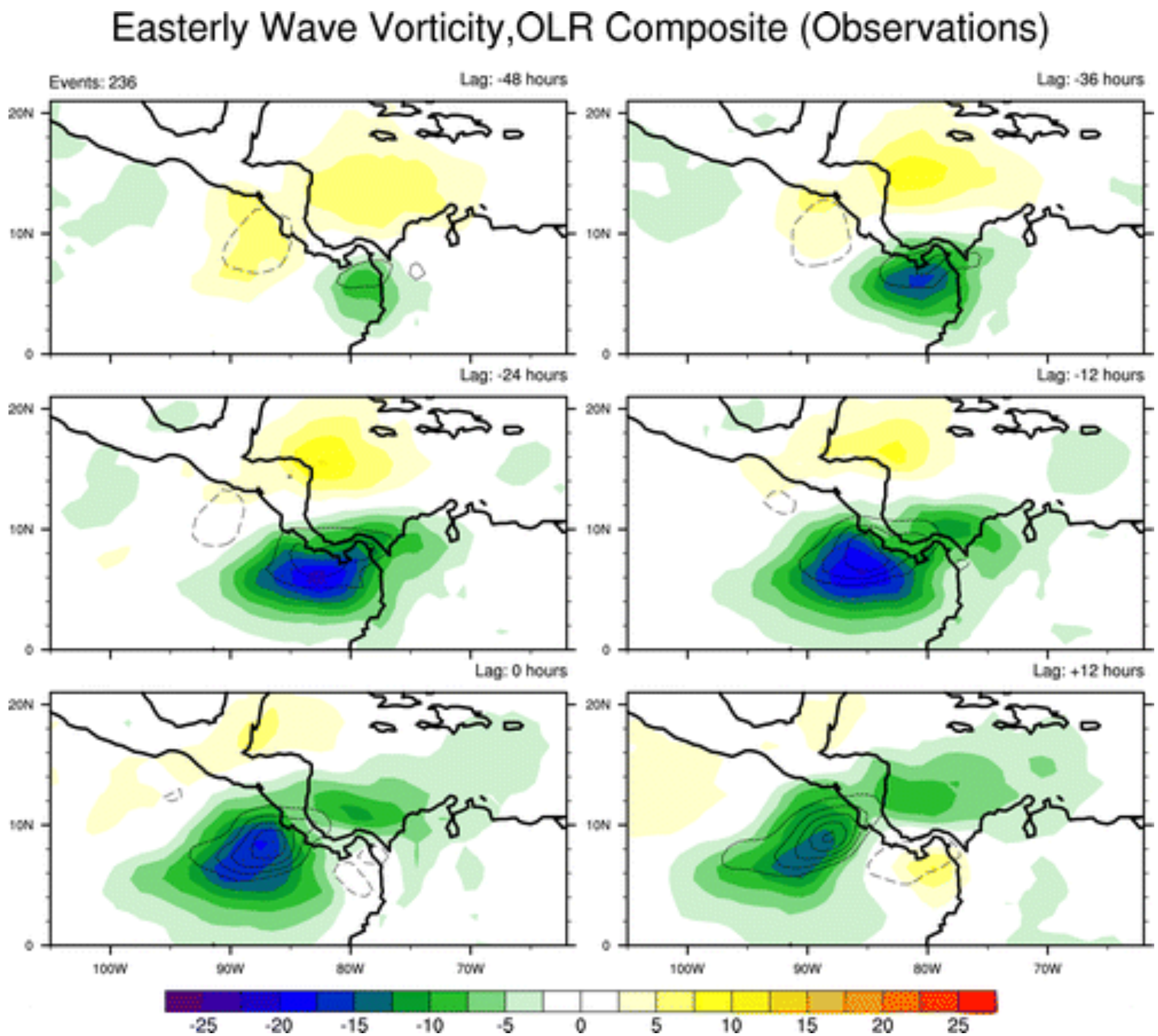

Rydbeck et al. (2017)

WV OLR with hypothetical 700 hPa streamfunction

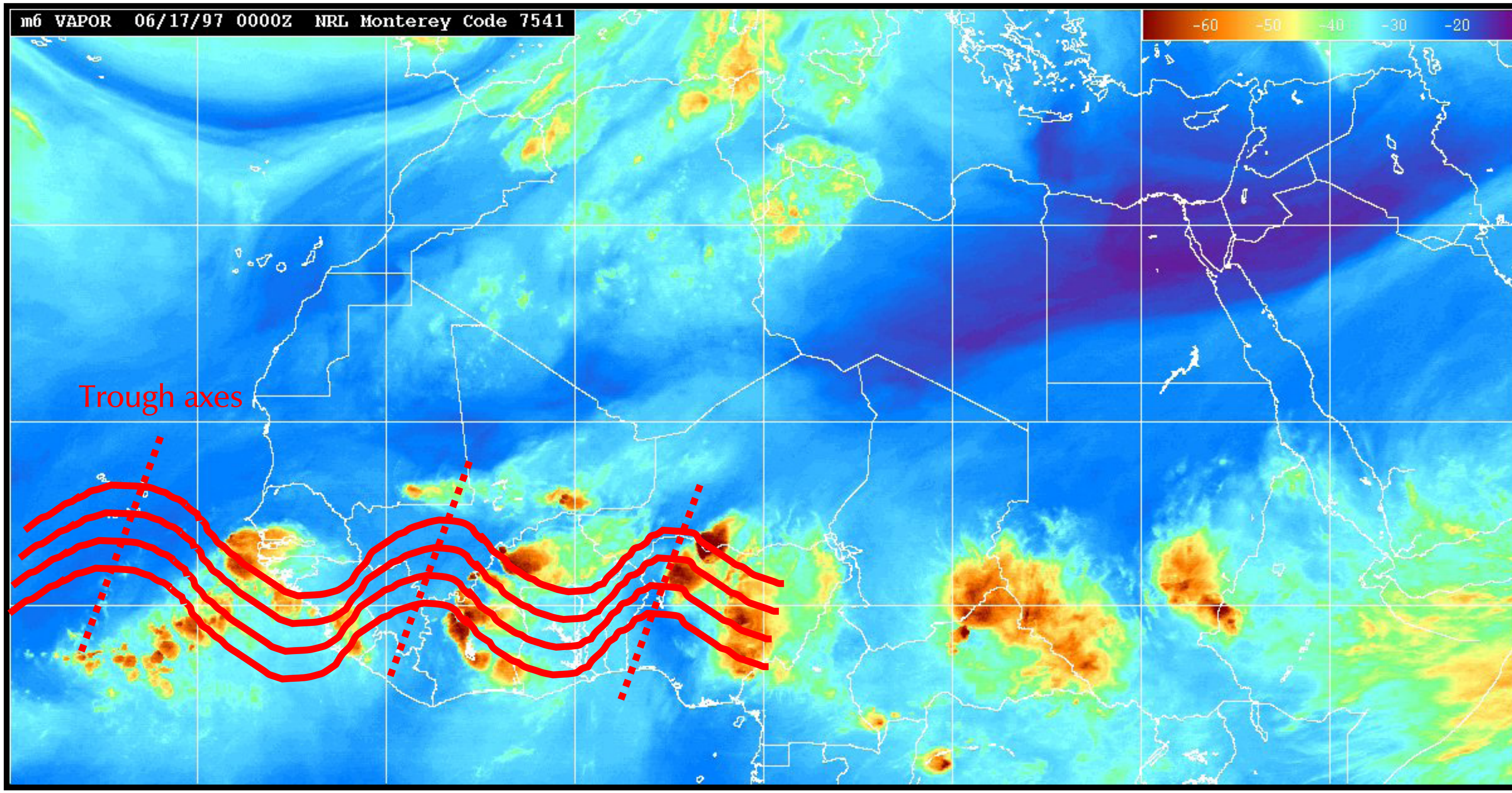

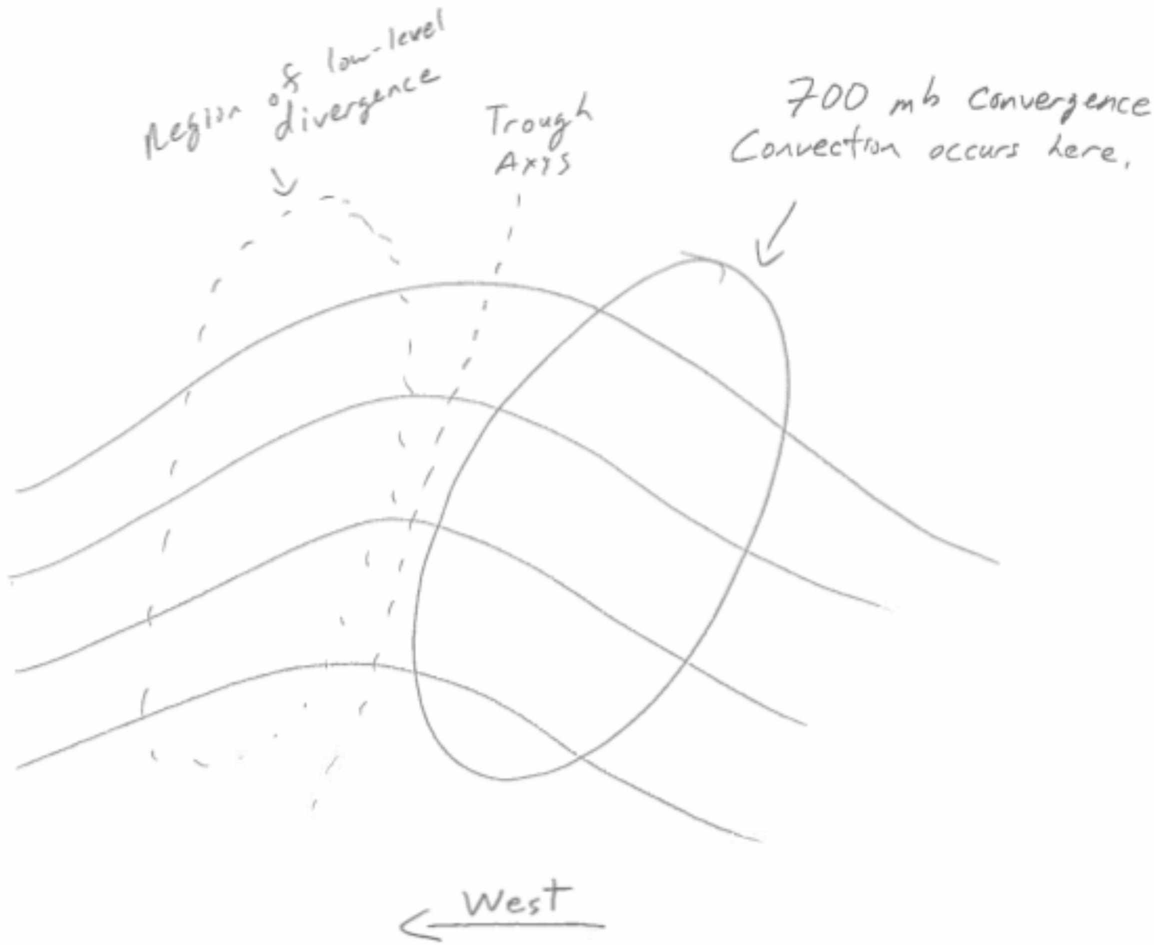
Region of low-level divergence
Trough Axis
700 mb convergence
Convection occurs here.
West

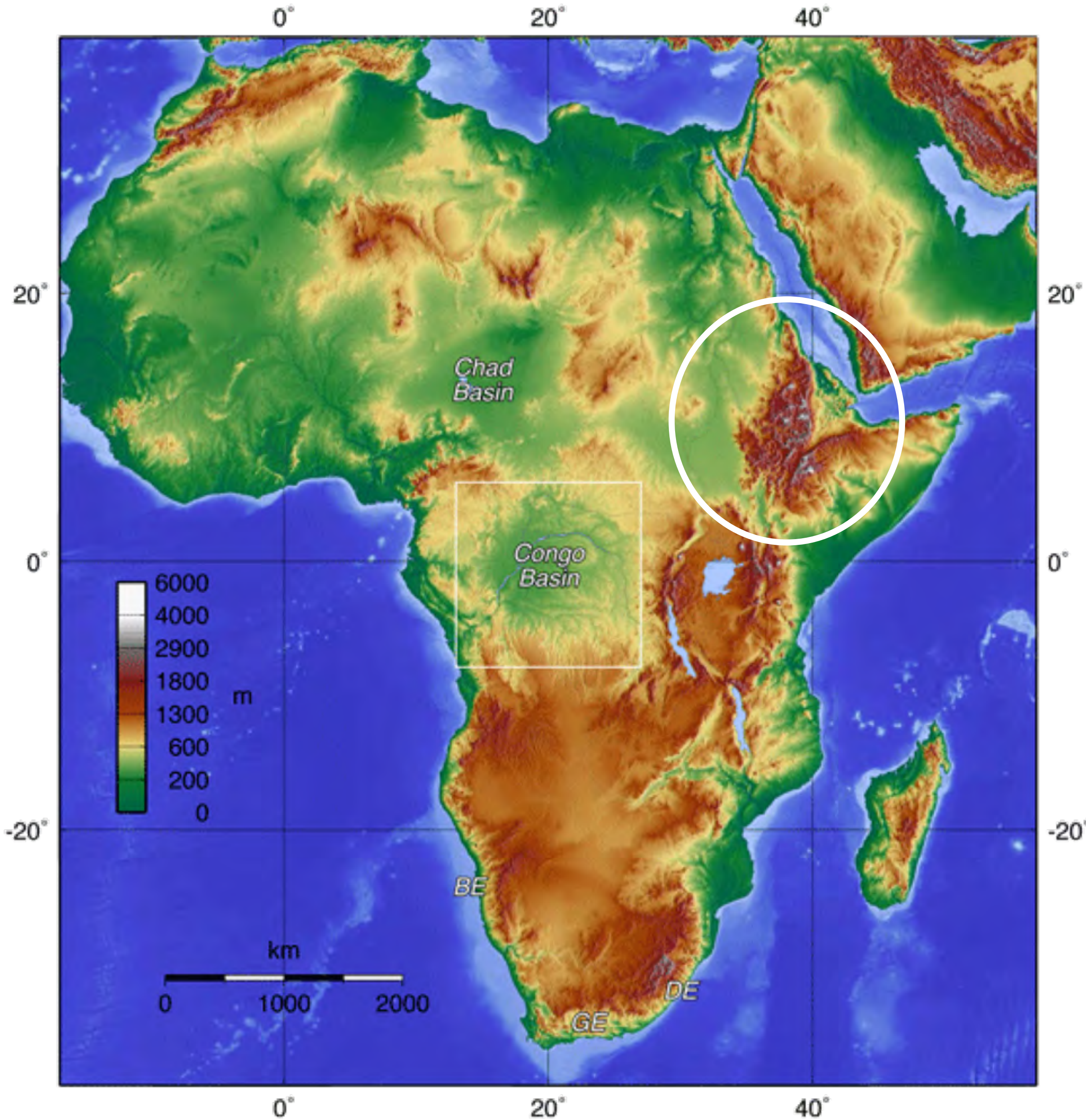

Image: Cal Tech

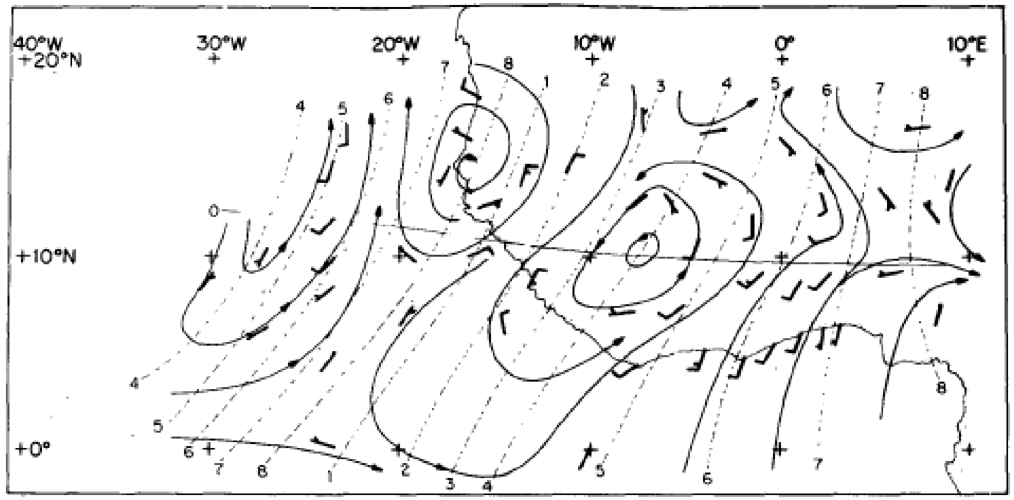

(a)

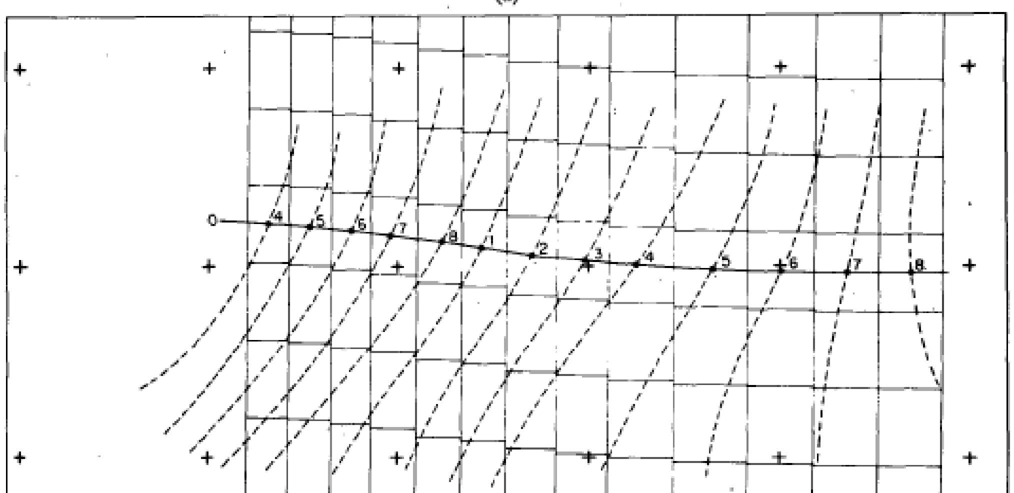

(b)

FIG. 1a. Streamline analysis with superimposed phase lines (dashed) and disturbance path (thin solid line) for 1200 GMT 7 September 1974. Band-pass filtered winds are plotted at station locations. Plotting convention: one full barb corresponds to 5 m s^{-1}, one-half barb to 2.5 m s^{-1} and no barb to 1m s^{-1}.

FIG. 1b. Boxes used in compositing.

Reed et al. (1977)

Surface

850 mb

700 mb

500 mb

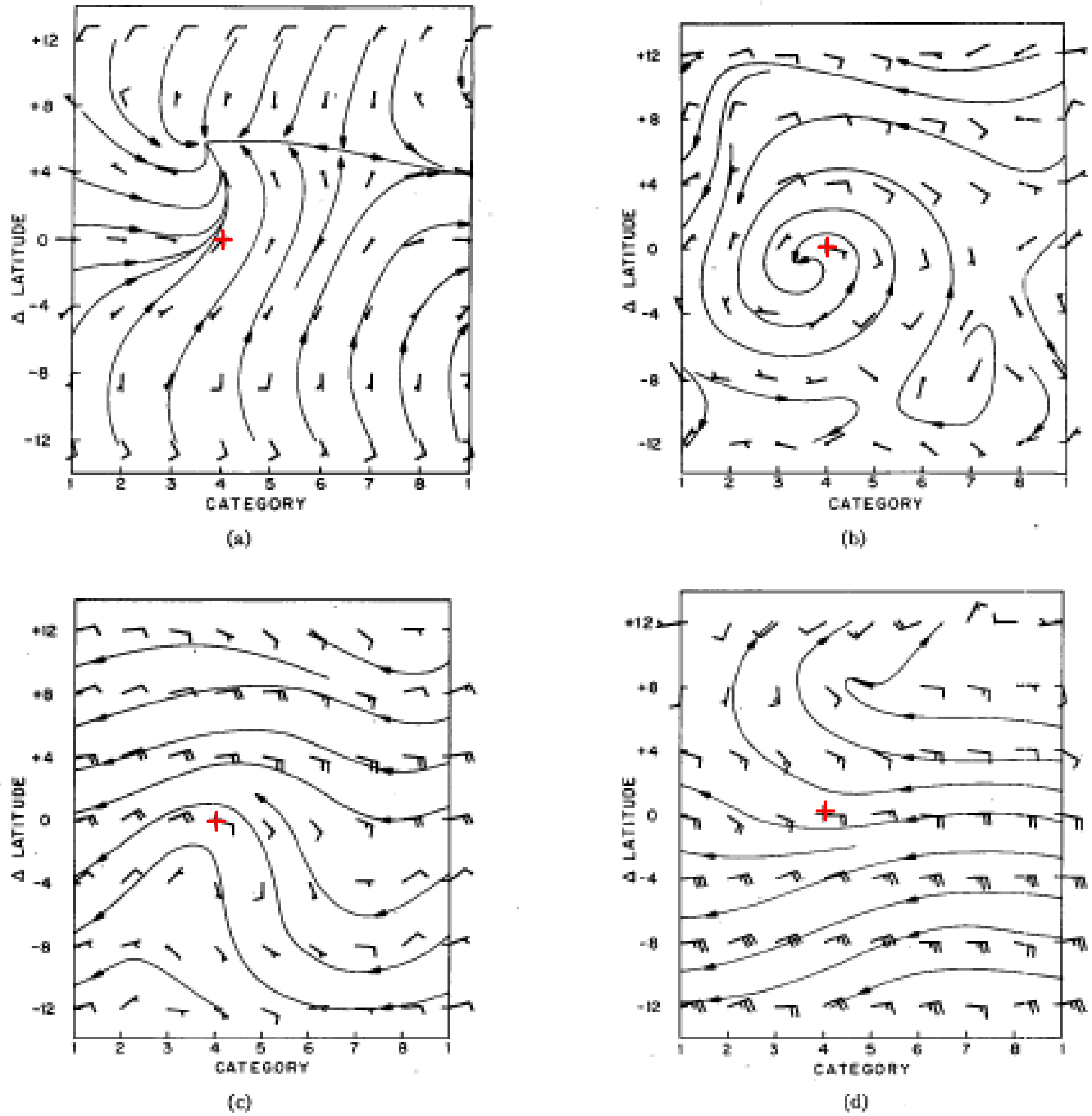

FIG. 3. Streamlines for the total wind field. Category separation is approximately 3° longitude. Cross denotes disturbance center at 700 mb. One full barb corresponds to 5 m s^{-1}, one-half barb to 2.5 m s^{-1} and no barb to 1 m s^{-1}. (a) Surface, (b) 850 mb, (c) 700 mb, (d) 200 mb.

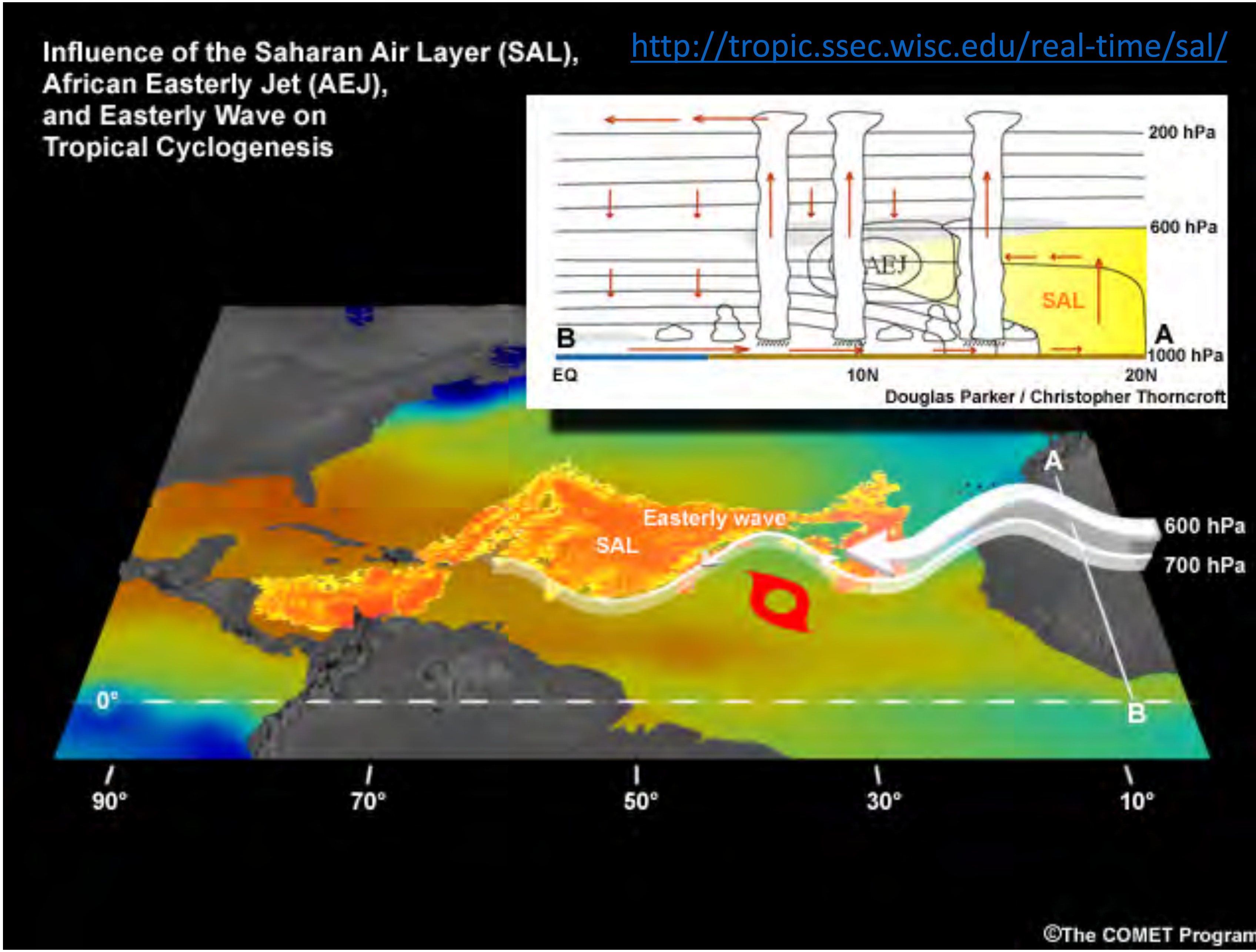
Influence of the Saharan Air Layer (SAL),
African Easterly Jet (AEJ),
and Easterly Wave on
Tropical Cyclogenesis
http://tropic.ssec.wisc.edu/real-time/sal/
200 hPa
600 hPa
AEJ
SAL
B
A
1000 hPa
EQ
10N
20N
Douglas Parker / Christopher Thorncroft
A
Easterly wave
SAL
600 hPa
700 hPa
0°
B
90°
70°
50°
30°
10°
©The COMET Program

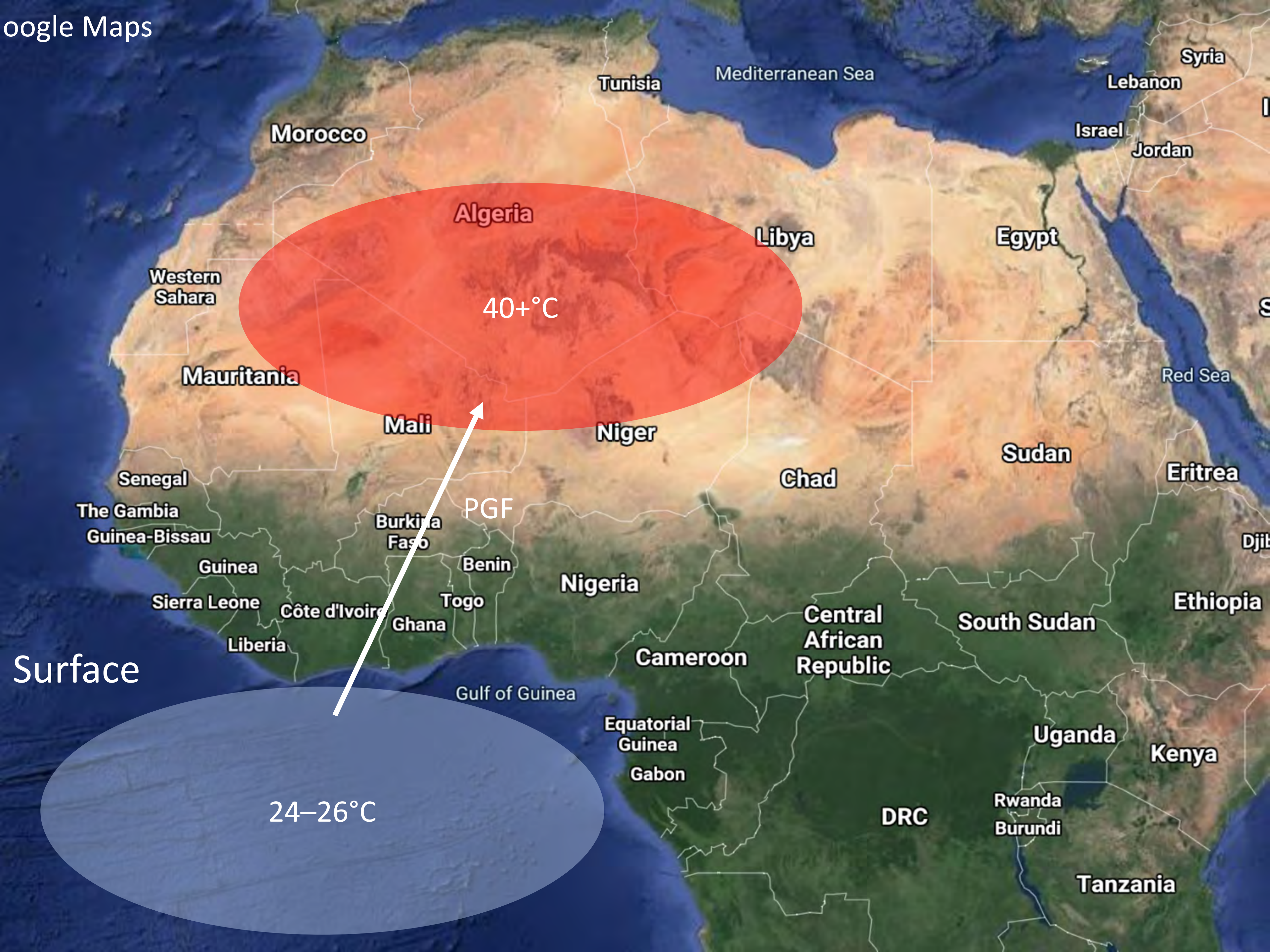
oogle Maps
Surface
40+°C
24–26°C
PGF
Mediterranean Sea
Tunisia
Morocco
Algeria
Libya
Egypt
Syria
Lebanon
Israel
Jordan
Western Sahara
Mauritania
Mali
Niger
Chad
Sudan
Eritrea
Red Sea
Senegal
The Gambia
Guinea-Bissau
Guinea
Sierra Leone
Liberia
Côte d'Ivoire
Burkina Faso
Ghana
Togo
Benin
Nigeria
Cameroon
Central African Republic
South Sudan
Ethiopia
Gulf of Guinea
Equatorial Guinea
Gabon
DRC
Uganda
Kenya
Rwanda
Burundi
Tanzania

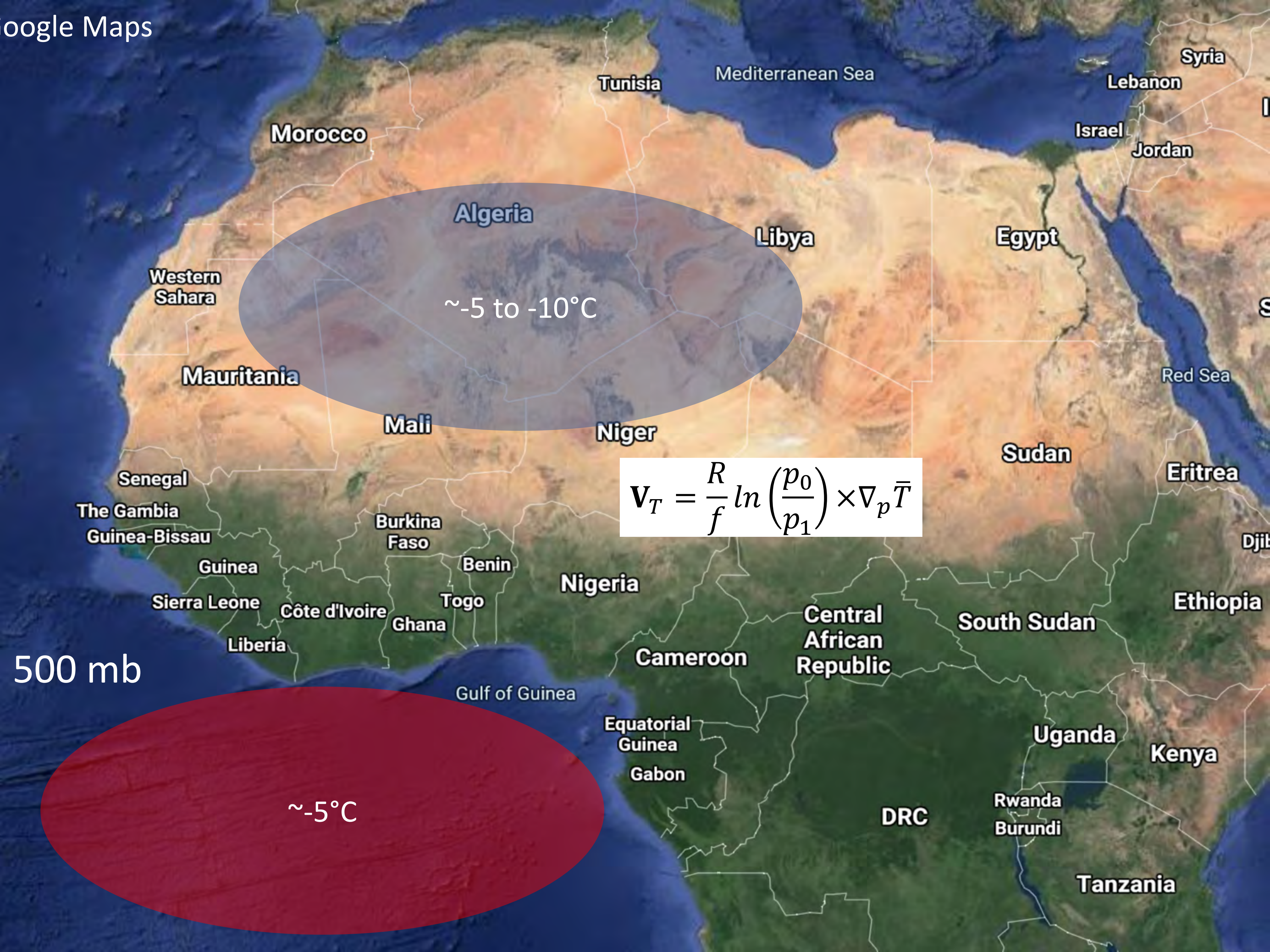

$$\mathbf{V}_T = \frac{R}{f} ln\left(\frac{p_0}{p_1}\right) \times \nabla_p \bar{T}$$

Reed et al. (1977)

Zonal mean winds

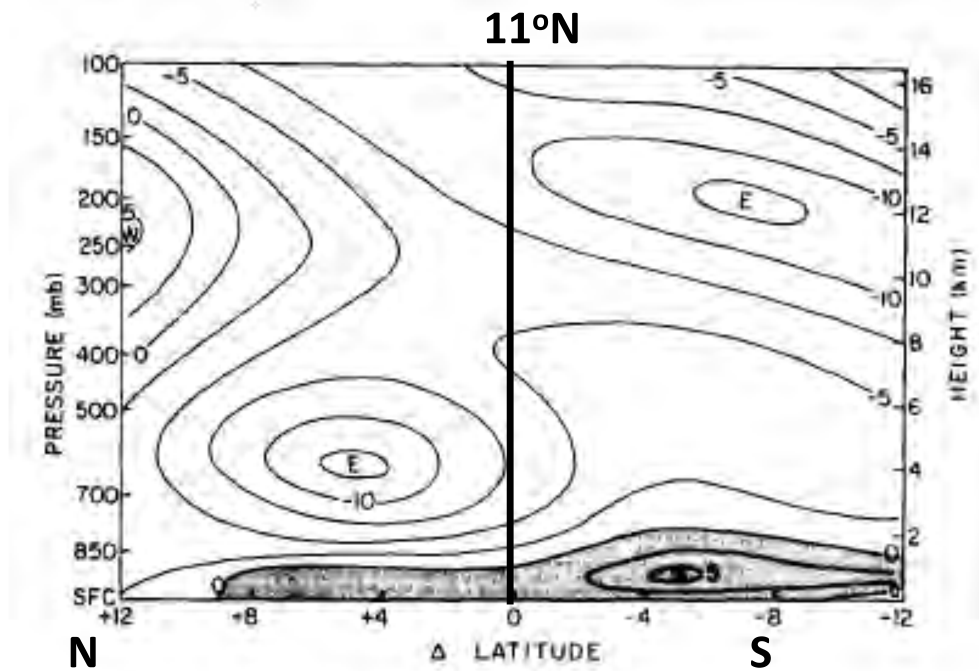

(a)

Temperature deviations

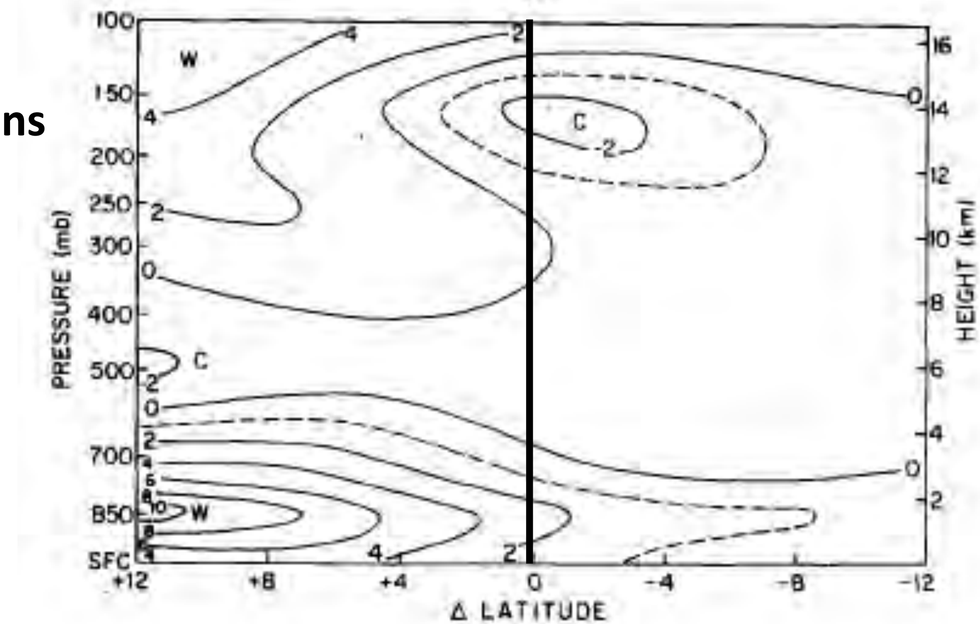

(c)

Reed et al. (1977)

Absolute Vorticity 10^{-5} s^{-1}

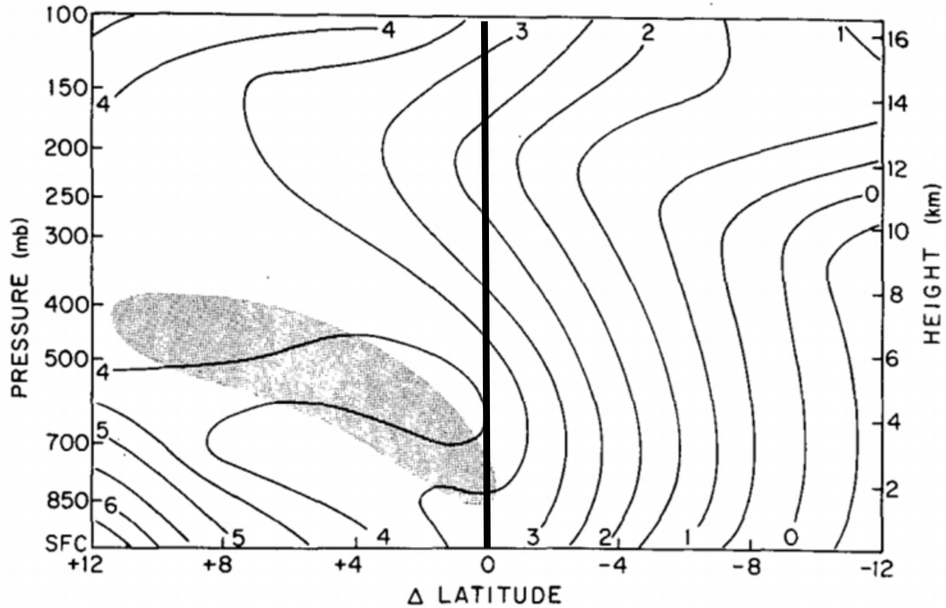

(b)

11°N

Relative Humidity (percent)

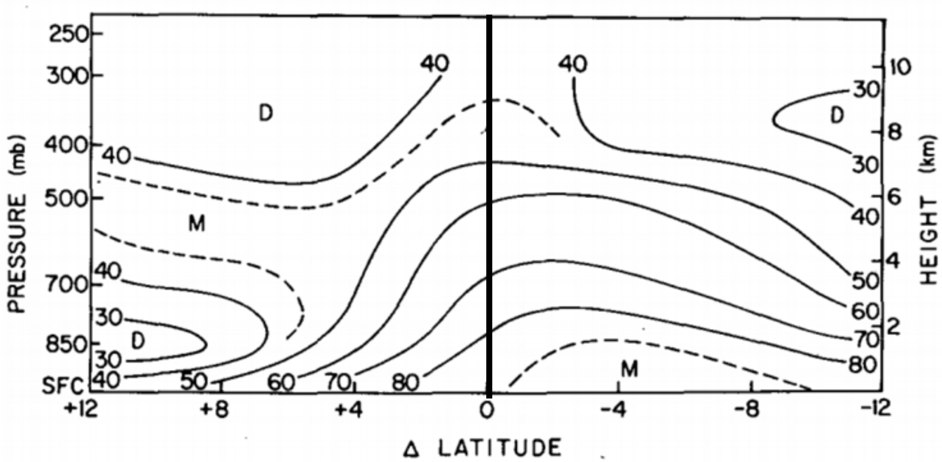

(d)

MR3252: Tropical Meteorology

Easterly Waves: Energetics and Growth Mechanisms

Figure: Alaka (2014)

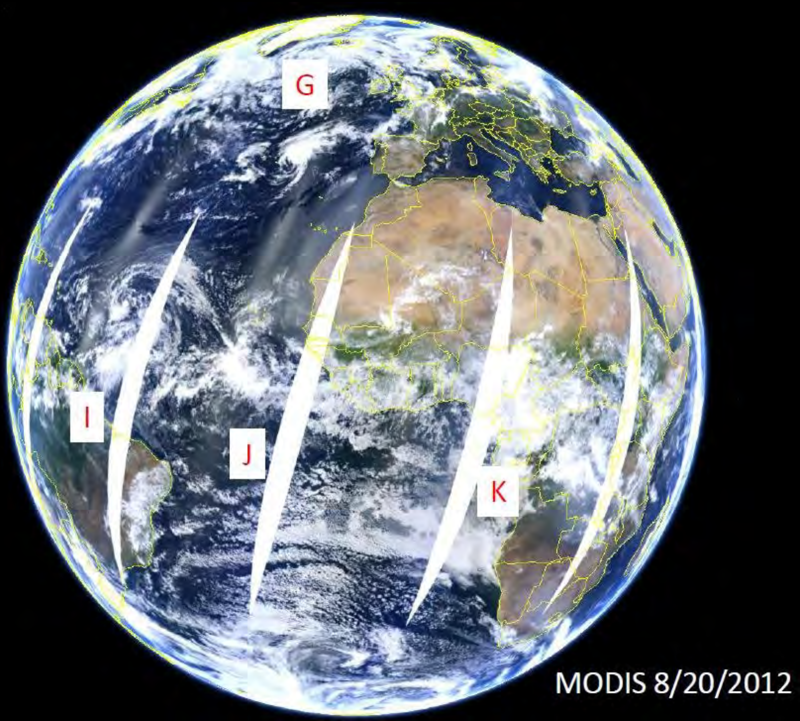

Main Topics:

- PV generation in the African Easterly jet
- Energy conversion in easterly waves

Module 3.7

$$\frac{\partial(\mathbf{PV})}{\partial y} \equiv \frac{\partial q}{\partial y} = \frac{\partial}{\partial y}\left[f + \nabla^2\psi + \frac{\partial}{\partial p}\left(\frac{pf_o^2}{RS_p}\frac{\partial\psi}{\partial p}\right)\right]$$

$$\frac{\partial\overline{q}}{\partial y} = \beta - \frac{\partial^2\overline{u}}{\partial y^2} - \frac{\partial}{\partial p}\left(\frac{pf_0{}^2}{RS_p}\frac{\partial\overline{u}}{\partial p}\right) < 0$$ ← Requirement for instability

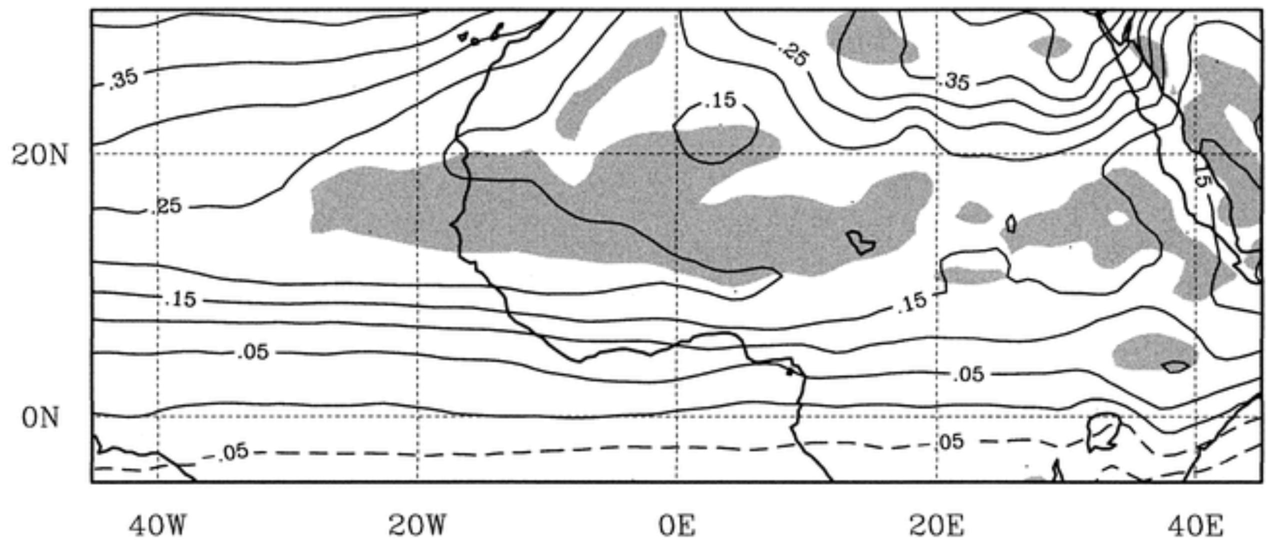

The 10-yr summertime (1 Jul–31 Oct) mean PV (in PVU, 1 PVU = 10^{-6} K m^2 kg^{-1} s^{-1}; contoured) and region of meridional PV gradient less than zero (shaded) on the 320-K surface. Contour interval for PV is 0.05 PVU.

Dickinson and Molinari (2000)

$$\frac{\partial(\mathbf{PV})}{\partial y} \equiv \frac{\partial q}{\partial y} = \frac{\partial}{\partial y}\left[f + \nabla^2\psi + \frac{\partial}{\partial p}\left(\frac{pf_o^2}{RS_p}\frac{\partial\psi}{\partial p}\right)\right]$$

$$\frac{\partial\overline{q}}{\partial y} = \beta - \frac{\partial^2\overline{u}}{\partial y^2} - \frac{\partial}{\partial p}\left(\frac{pf_0{}^2}{RS_p}\frac{\partial\overline{u}}{\partial p}\right) < 0$$

← Requirement for instability

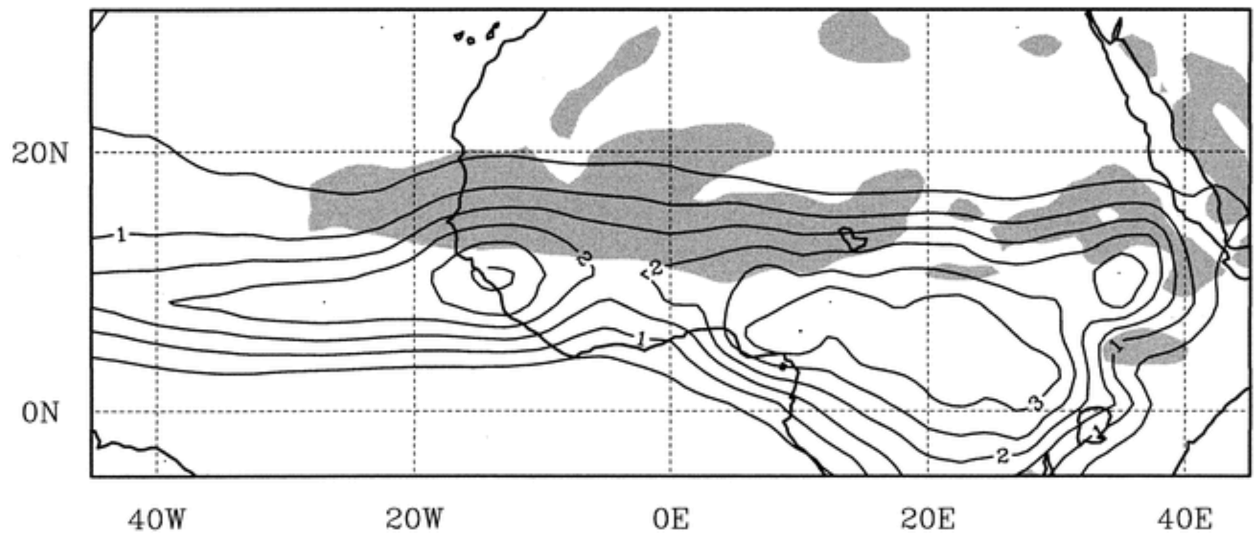

As in Fig. 1 but for vertically integrated diabatic heating from Eq. (3) (contoured). Contour interval is 0.5°C day^{-1}.

Dickinson and Molinari (2000)

Latitudinal Distribution of PV over Africa and Northern Australia

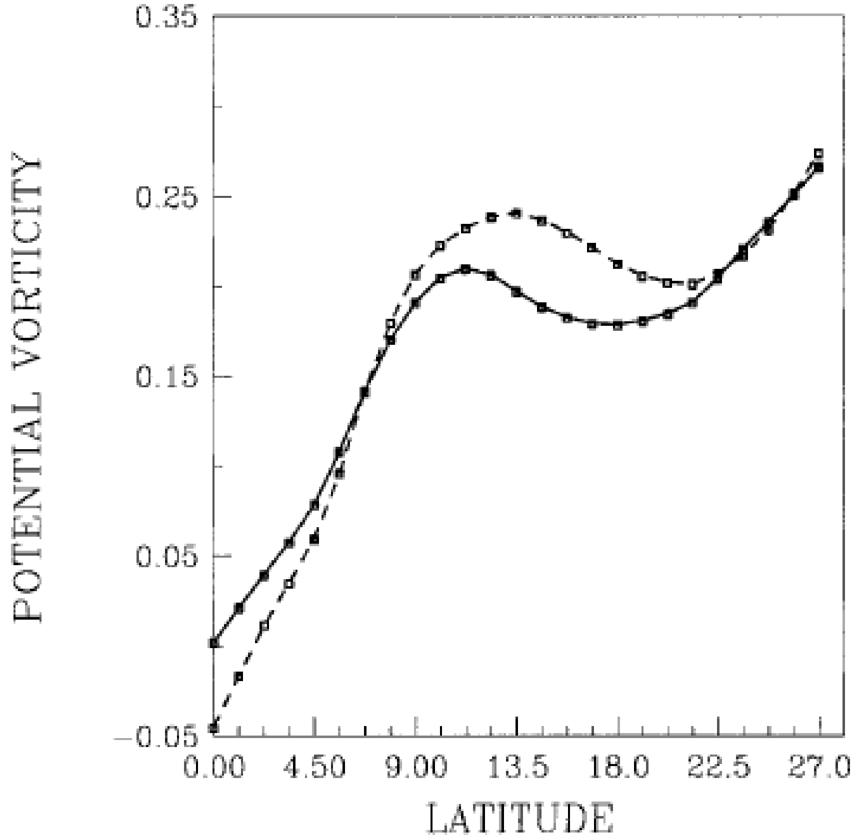

FIG. 15. The 10-yr summertime mean PV (in PVU) distribution with latitude, averaged along the sign reversal, for the African (solid) and Australian (dashed) regions. PV in Australia is multiplied by −1.

Dickinson and Molinari (2000)

Barotropic conversion of KE to eddy (or perturbation) KE

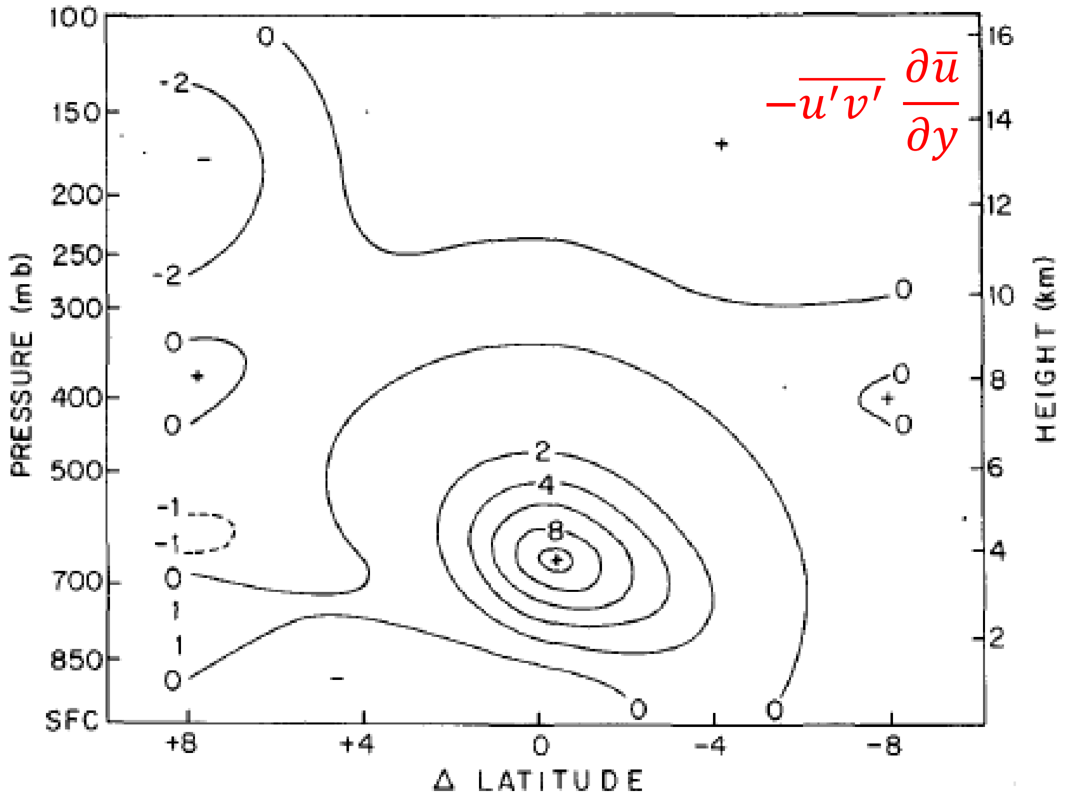

FIG. 2. Meridional distribution of $-[u'v']\partial[u]/\partial y$ for the combined region. Units are 10^{-5} m^2 s^{-3} (or W kg^{-1}).

Norquist et al. (1977)

Baroclinic conversion of PE to eddy (or perturbation) PE

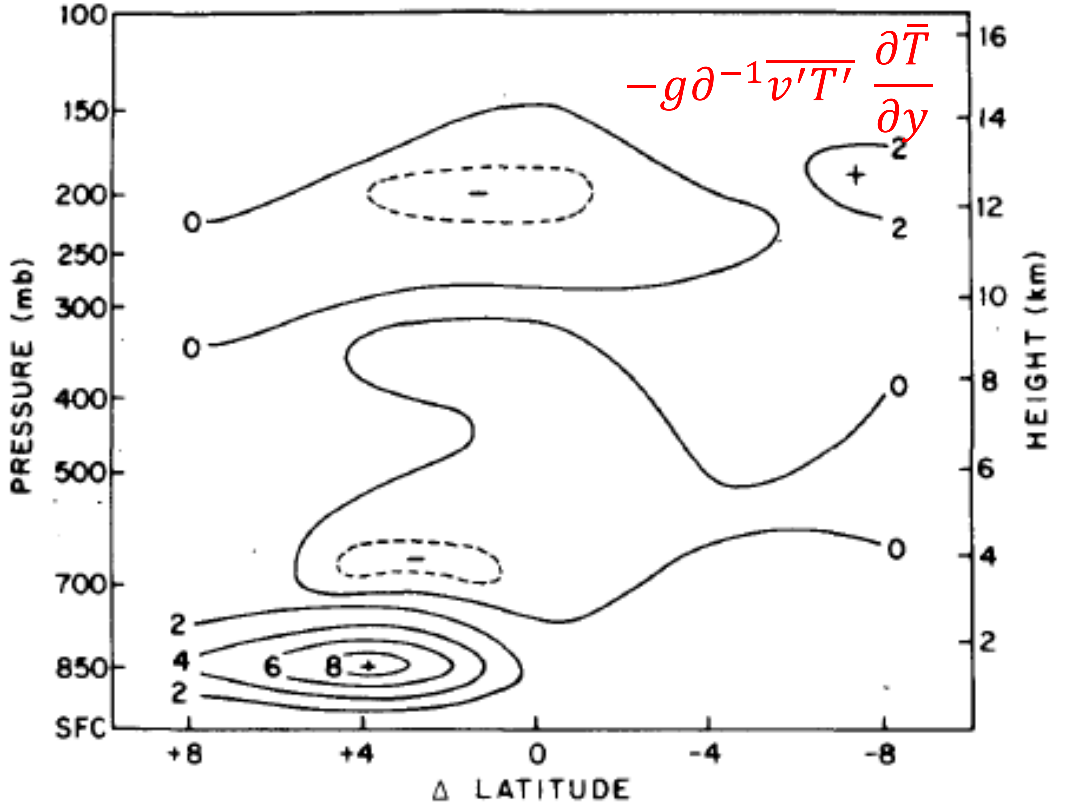

FIG. 4. Meridional distribution of $-g\partial^{-1}[v'T']\partial[T]/\partial y$ for the combined region. Units are 10^{-5} m^2 s^{-3}.

Norquist et al. (1977)

Conversion of eddy APE to eddy KE

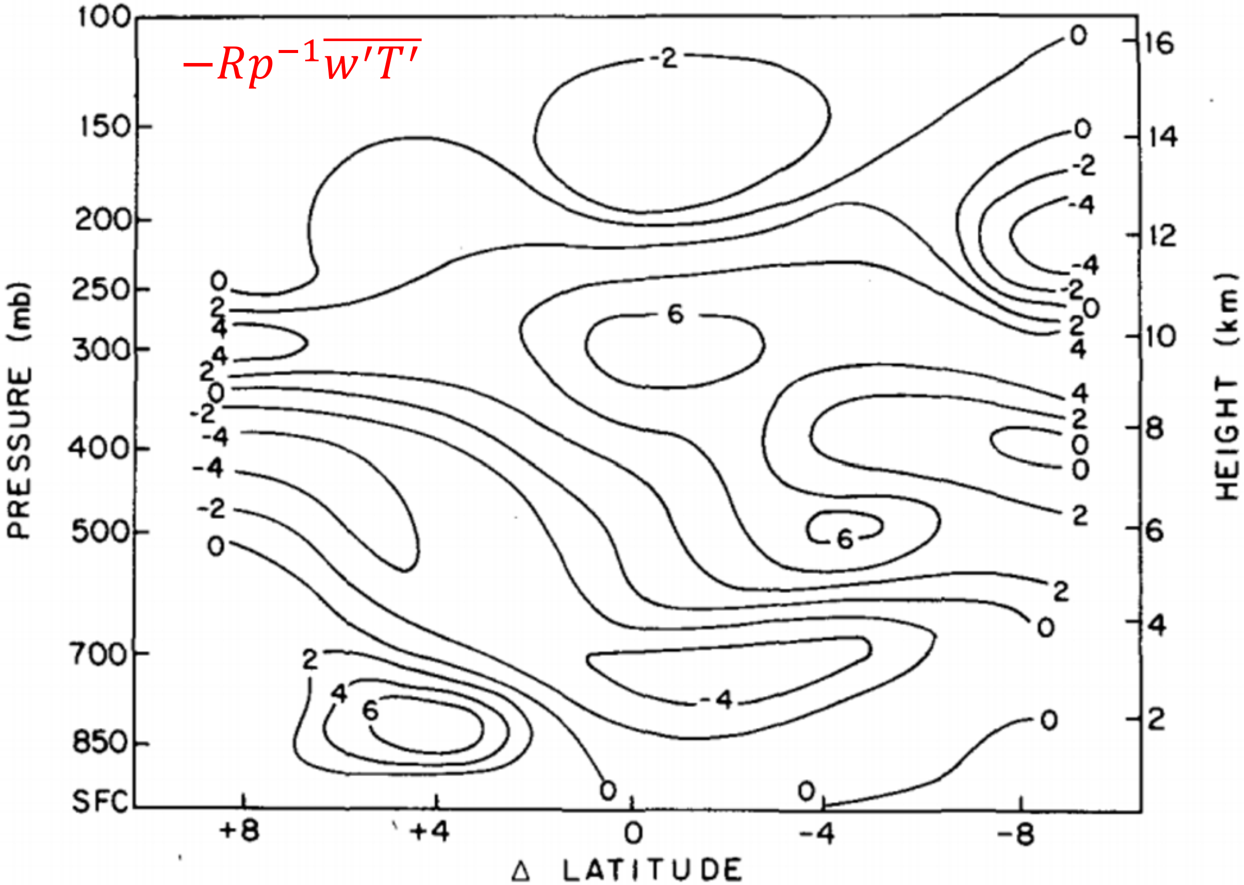

Norquist et al. (1977)

600 mb

Thorncroft and Hodges (2001)

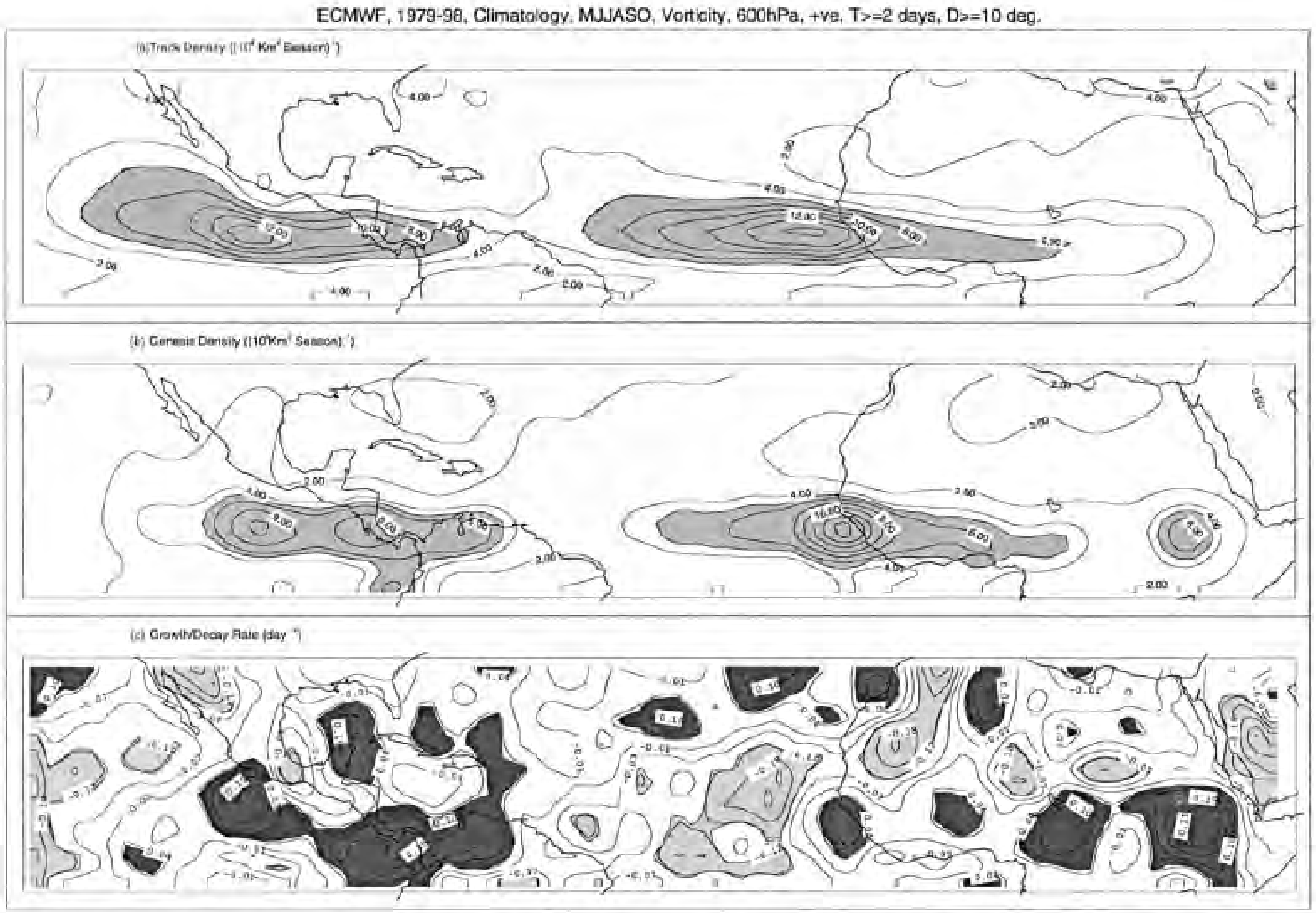

FIG. 5. Climatological tracking statistics at 600 mb based on the ERA data (1979–93) and the ECMWF analyses (1994–98). (a) Track density scaled to number density per unit area ($\sim 10^6$ km^2) per season (MJJASO), shading for values greater than 6. (b) Genesis density per unit area ($\sim 10^6$ km^2) per season (MJJASO), shading for values greater than 5. (c) Growth and decay rates in units of per day, shading for values greater than 0.05 and less than -0.1.

$$\frac{\partial A'}{\partial T} \approx \gamma(\overline{Q_1' T'})/\overline{T} + R(\overline{\omega' T'})/p - c_p \gamma(\overline{V_h' T' \cdot \nabla_h \overline{T}})/\overline{T}, \tag{1}$$

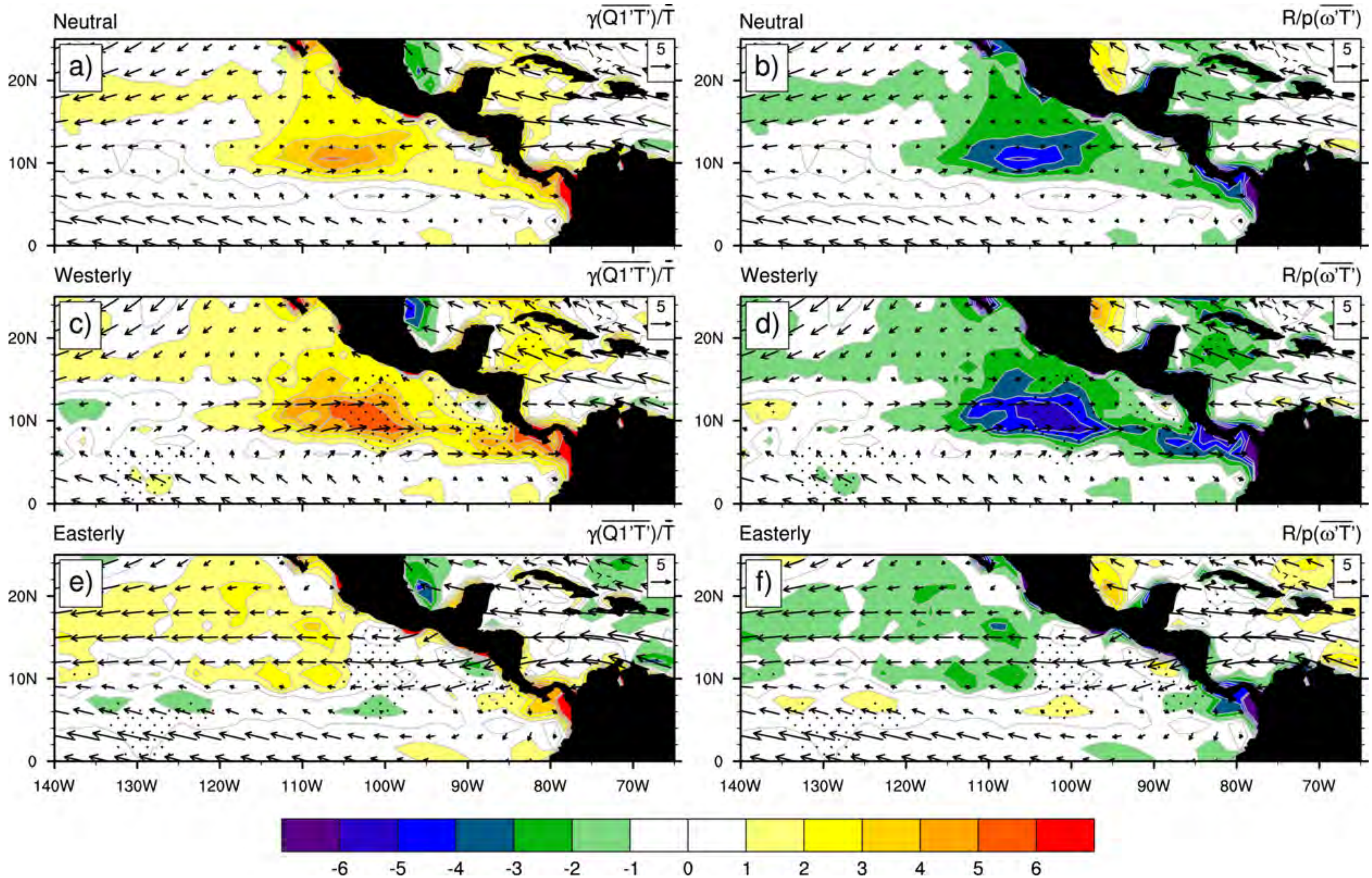

Rydbeck and Maloney (2014)

Rydbeck and Maloney (2014)

$$\frac{\partial K'}{\partial T} = -\overline{V_h'(V' \cdot \nabla)\overline{V}_h} - \overline{V} \cdot \nabla K' - \overline{V' \cdot \nabla K'} - R(\overline{\omega' T'})/p - \nabla \cdot (\overline{V' \Phi'}) + D, \qquad (2)$$